THE
PHYSICAL REVIEW
A Journal of Experimental and Theoretical Physics Established by E. L. Nichols in 1893

VOL. 53, NO. 4 FEBRUARY 15, 1938 SECOND SERIES

Long Period Activity of Indium Produced by Slow Neutrons

ALLAN C. G. MITCHELL
Physics Department, New York University, University Heights, New York, N. Y.
(Received December 28, 1937)

Indium was irradiated with slow neutrons from a radium-beryllium source for a period of several months. A period of 45 ± 3 days was produced quite strongly. It is shown that this period is produced when In^{113} captures a neutron to form In^{114}. The ratio of the activity of the long period to that of 54 minutes, due to In^{116}, is approximately the same as the isotope ratio In^{113}/In^{115}. The capture cross sections for the two processes are given by the relation $\sigma_{113}=0.56\sigma_{115}$.

SINCE this laboratory had available a neutron source, consisting of 200 milligrams of radium and beryllium, it was thought worth while to see if long period radioactivities could be produced by slow neutron bombardment. The strength of a radium-beryllium source does not decrease appreciably with time, as does the activity of a radon beryllium source. It therefore provides an ideal tool for long period irradiations. Accordingly, a number of substances were placed in a large box suitably filled with paraffin, in the center of which was placed the neutron source. The irradiation commenced July 1, 1937 and has continued up to the present, except for short but rather frequent intervals, in which the neutron source was removed for other purposes. Of the substances so far investigated, the most active is indium, which shows a long period of 45 ± 3 days in addition to the well-known period of 54 minutes. While this work was in progress Lawson and Cork[1] reported the discovery of an activity of 50-day period in indium which they ascribed to In^{114}. The relation between this work and the present paper will be discussed in more detail below.

[1] J. L. Lawson and J. M. Cork, Phys. Rev. **52**, 531 (1937).

IRRADIATION AND MEASUREMENT OF PERIODS

The box used for irradiating the samples was 26 cm high, 24 cm long, and 12 cm wide. The radium-beryllium source was placed in a small lead container in the center of the box. Two indium sheets 6×10 cm^2 and of a thickness of 0.109 g/cm^2 were placed about 5 cm from the neutron source, the rest of the box being filled with paraffin.

The first indium sample was removed after 80 days intermittent irradiation. Its activity was measured by wrapping it around a Geiger-Müller tube counter attached to an amplifier and a thyratron recording mechanism. The sensitivity of the counter system was measured before each measurement of the activity of the indium with the help of a standard uranium sample. The activity of the indium was then corrected for slight changes in counter sensitivity. Measurements on the activity of the sample did not commence until 5 minutes after it had been removed from the neutron source, so that the 13-sec. period was not measured. The scale of two recording instruments used to measure the first sample would not follow at counting rates above 1000 per minute so that the early part of

the run could not be followed accurately. This defect was rectified when the second sample was measured, and the results will be discussed below.

The activity of the sample was followed for 62 days. It was found to decay with a period of 42 days. The initial activity was 142 counts/min. above a background of 35 counts/min. so that it was easily measurable. The long period activity subtracted from the total, gave the short period activity a period of 50±5 min., with an extrapolated initial rate of about 10,000/min. In this calculation only those points were considered for which the counting rate was less than 1000/min. The short period could be followed for seven hours after the end of irradiation and there was no evidence indicating the existence of any intermediate periods.

A second indium sample, identical with the first, was removed after 155 days irradiation. The activity of the sample was measured in the same manner as before, except that the recording mechanism was a "scale-of-eight" counter fed by an amplifier of short time constant. The system was reliable for counting rates of 5000 per min., and probably missed only a small fraction of the counts at counting rates of 10,000 per min. Measurements were taken at half-hour intervals for a period of twenty hours. After the twelfth hour the activity was relatively constant at about 370 counts/min. above the background. This activity, measured from time to time over a long period was shown to decay with a period of 47 days. Subtracting the activity of the long period from the total activity only the 54-min. period was found.[2] The 54-min. period was observable for 10 hours. No indication of an intermediate period was found. The initial activity of the 54-min. period was 1.75×10^4 counts/min. while that of the long period was 3.72×10^2 counts/min.

Beta- and Gamma-Rays

In order to see whether the radioactive indium of long period emitted positive or negative electrons, an active sample, several weeks old, was placed in a cloud chamber. The curvature of the tracks in a magnetic field showed that the emitted particles were negative electrons. Lawson and Cork performed a similar experiment in which they were able to show that the upper limit of the electron energy is 2.15 Mev.

To test for gamma-rays a counter surrounded by lead of thickness 1.44 grams/cm² was used. Two days after the end of the irradiation the more active indium sample was examined with the gamma-ray counter. The counting rate (background) with no sample present was 23±2 per minute, while that with the sample wrapped around the counter was also 23±2. If there had been as many as 10 counts per min. due to gamma-rays these would have been detected. The count due to beta-rays from the sample at the time of measurement was 370 per min. Thus the gamma-ray effect is certainly less than 1/40 the beta-ray effect.

It is interesting to compare the above result with results of a similar experiment by Mitchell and Langer[3] on the relative number of counts due to beta- and gamma-rays associated with the 54-min. period of indium. Using the same apparatus as was used in the present experiment, these investigators found that the total count (beta-rays+gamma-rays) was 3700 per minute, while that for the gamma-rays alone was 700 per minute, both for the 54-min. period. Hence the ratio

$$\frac{I_0(\gamma)}{I_0(\gamma+\beta)}=\frac{700}{3700}=0.189. \qquad (1)$$

Now the gamma-rays from the 54-min. period have an energy of 1.40 Mev.[4] If the 45-day activity had emitted γ-rays of like energy and in a corresponding amount, one should have obtained a count of 70 per min. with the gamma-ray counter. Since there was no observed count due to gamma-rays, one must conclude either that there are no gamma-rays associated with the long period or that their energy is quite small. The first assumption appears to be the more plausible.

The Origin of the 50-Day Activity

In order to show that the long indium period is not due to a fast neutron reaction with In^{115} the following experiments were tried. A silver

[2] Measurements were commenced too late to observe the 13-sec. period.

[3] A. C. G. Mitchell and L. M. Langer, to appear shortly.

[4] A. C. G. Mitchell and L. M. Langer, Phys. Rev. **52**, 137 (1937).

foil, the same size as the indium foil was given the same length of irradiation as the indium. Aside from a weak activity of very long period (probably about 3 months), the only other periods found were the well-known ones of 22 sec. and 2.3 min. There was no trace of the 26-min. period known to be produced in silver by fast neutrons.

A second experiment was performed in which an Ag detector was placed in the box in the same position as the indium foil and was irradiated for 1 hour. On measurement, this detector likewise showed only the 22-sec. and 2.3-min. periods. The latter period was followed until it disappeared into the background at the end of 35 min., there being no trace of the 26-min. period. Finally, the radium was removed from the paraffin and was allowed to irradiate for 1 hour an Ag foil, bent into the form of a cylinder around the source. In this case the 26-min. period was present and began to show its influence as early as the tenth minute of counting. Since there was no observable activity due to the 26-min. period of Ag, when this substance was irradiated in the box containing paraffin, we estimate that the contribution to the activity due to fast neutrons, under these conditions of irradiation, is less than 0.1 percent. The long period activity of the indium must therefore be due to slow neutrons.

In view of the above experiments it seems certain that the activity of 45-day period is due to In^{114} produced through the capture of a slow neutron by In^{113} according to the reaction.

$$In^{113}+n^1=In^{114},$$
$$In^{114}=Sn^{114}+e^-. \qquad (2)$$

The two normal indium isotopes occur in the following percentages: In^{113}, 4.5 percent; In^{115}, 95.5 percent. Since the activational process has been shown to be due to the capture of slow neutrons, one can get some information as to the nature of the process by comparing the initial rates of decay for the 54-min. period and the 42-day period.

The 54-min. activity needs no correction for time of irradiation since it was radiated for a period very long compared to the half-life. In comparing the activities one should use only the beta-activity of the short period, since the long period gave no gamma-activity. The correction for gamma-rays is, however, negligible since a thin walled glass counter was used in which the gamma-rays would not produce many secondaries.

The initial activity of the long period radioactivity must be corrected for irradiation time. The time of irradiation is somewhat indefinite but lies between 2 and 3 half-lives. The observed initial activity of 3.72×10^2 counts per min. becomes 4.9×10^2 or 4.2×10^2 counts per min. when corrections are made for irradiation time of 2 or 3 half-lives, respectively. Now, the 54-min. period is certainly due to In^{116} produced from In^{115} by neutron capture. Assuming that the capture cross sections are the same for the two isotopes we can calculate the percentage abundance of the two isotopes. Taking the data given above we have for the abundance ratio

$$\frac{N_{113}}{N_{113}+N_{115}}=\frac{4.6\times10^2}{175+4.6}\times10^2$$
$$=\frac{I_0\,(45\text{ d.})}{I_0\,(45\text{ d.})+I_0\,(54\text{ min.})}=2.6\text{ percent.}$$

In view of the uncertainties involved, the figure is in satisfactory agreement with the value 4.5 percent for In^{113} obtained from mass spectra data. It, therefore, appears certain that the 45-day activity is due to In^{114}. Conversely if one assumes that activities are in the ratio of the relative abundance N_{113}/N_{115} one can calculate the relative cross section for the activation of In^{113} to In^{115} by neutrons. By use of the above figures one obtains $\sigma_{113}=0.56\sigma_{115}$.

Lawson and Cork[1] have found a number of periods due to indium when this element was bombarded by deuterons, neutrons (fast or slow), and when cadmium was bombarded by deuterons. The indium periods produced by deuterons on cadmium are: 2.3 hours (In^{117}); 20 minutes (In^{111}); and 4.1 hours ascribed to In^{114}. With fast neutrons on indium they found the periods 72 sec. (In^{112}), 4.1 hours (In^{114}), 50 days In^{114} and the well-known 13-sec. and 54-min. periods ascribed to In^{116}. With slow neutrons they obtained the 13-sec. and 54-min. periods and the 4.1-hour period, which apparently appeared only weakly.

The present work substantiates the conclusion of Lawson and Cork that the 45–50-day period is to be attributed to In^{114}, since it has been shown here to go with slow neutrons on indium. Furthermore, the relative activity of the 50-day period compared with the 54-min. period, produced by slow neutrons, is about what one would expect from the relative abundances of In^{113} and In^{115}.

From the evidence presented by Lawson and Cork it seems very probable that the 4.1-hour period is due to In^{114} since it was obtained with deuterons on Cd and quite strongly with fast neutrons on In. It is isomeric with the 50-day period. In the present investigation no 4.1-hour period was observed when slow neutrons bombarded indium. Lawson and Cork found this period to be produced only weakly with slow neutrons. It is not impossible that the weak activity observed by them was due to residual fast neutrons not slowed down by the paraffin. From the above, it appears that the 4.1-hour period is due to In^{114}, that it is produced by fast neutrons on In^{115}, but that it is not readily produced by slow neutrons on In^{113}. Since the two periods 4.1 hours and 50 days are isomeric, one must conclude, from the nonappearance of the 4.1-hour period with slow neutrons that the formation of this state is forbidden due to energy considerations or to the action of a selection rule.

The author is indebted to Dr. R. N. Varney and Mr. C. G. Shull for helping him with some of the readings. The work has been made possible by a grant from the Penrose Fund of the American Philosophical Society.

FEBRUARY 15, 1938 PHYSICAL REVIEW VOLUME 53

Note on *K* Electron Capture and Isomerism in Radiosilver

M. L. Pool and Edward C. Campbell
Mendenhall Laboratory of Physics, Ohio State University, Columbus, Ohio

(Received December 27, 1937)

From radioactivity data a tentative energy-level diagram is constructed for the isomeric nucleus Ag^{106}. These data indicate that, for the 8.2-day period, the relative probabilities of *K* electron capture: negative β-emission: positive β-emission = 640 : 40 : 1. The 24.5-min. Ag^{106} level is metastable and 0.3 Mev above the 8.2-day Ag^{106} ground state. Theory requires that the difference in angular momentum associated with these two levels be at least 5 nuclear units.

Introduction

THE capture of orbital electrons as an alternative to positron emission by radioactive nuclei has been considered theoretically by several investigators.[1] For heavy radioactive nuclei the probability for *K* electron capture has been calculated to be comparable to, or even a thousand times greater than that of the corresponding positron emission. It is also probable that some radioactive nuclei which are stable with respect to positron emission may be unstable with respect to *K* electron capture.[2]

The x-rays following *K* electron capture have been found by Alvarez[3] in the comparatively light element V^{48}, which emits positrons and has a half-life of 16 days. The possibility of *K* electron capture in potassium has been discussed by Weizsäcker[4] and Bramley.[5] Various observations on radiosilver Ag^{106} have been made which suggest that *K* electron capture plays an important role in the radioactive transformation of this nucleus.[6]

Recapitulation of Data

The 8.2-day period in silver was determined by the γ as well as by the $\beta+\gamma$ activity; 447

[1] Möller, Physik. Zeits. Sowjetunion **11**, 9 (1937); Uhlenbeck and Kuiper, Physica **4**, 601 (1937); Yukawa and Sakata, Phys. Rev. **51**, 677 (1937); Hoyle, Nature **140**, 235 (1937).
[2] Sizoo, Physica **4**, 467 (1937).
[3] Alvarez, Phys. Rev. **52**, 134 (1937).
[4] Weizsäcker, Physik. Zeits. **38**, 623 (1937).
[5] Bramley, Science **86**, 424 (1937).
[6] Pool, Phys. Rev. **53**, 116 (1938).

β-tracks were measured and gave by inspection an upper limit of 1.3 Mev. The number of γ-quanta per β-ray was about 35. The γ-ray spectrum was complex but probably consisted of at least lines at 0.3, 0.7 and 1.0 Mev. Out of 600 negative β-tracks, 15 positron tracks were measured; the maximum energy observed was 0.41 Mev.

The 24.5-min. period was also measured by the γ and $\gamma+\beta$ activity; 847 positron tracks gave by inspection an upper limit of 1.9 Mev. The number of γ-quanta per positron was about 2.

Both periods were best obtained by fast neutron bombardment of silver. The branching ratio of the 8.2-day to the 24.5-min. period is about 20.

K Electron Capture

Uhlenbeck and Kuiper[1] have calculated a set of curves which show the dependence of the ratio of capture probability to that of positive β-emission as a function of atomic number and of the energy W_0 available for the transition. The above data give the relative probability of K electron capture: negative β-emission: positive β-emission = 640 : 40 : 1. Using the ratio 640/1 one obtains from the curves a value of $W_0 = 2.2\,mc^2$ which corresponds to 0.6 Mev for the upper limit of the positron spectrum. Since 0.41 Mev was the maximum energy observed from such a limited number of tracks, 0.6 Mev or even more might easily be expected for the upper limit. To obtain more positron tracks a very much stronger source is necessary. The sample of silver used was irradiated six hours with neutrons from Li bombarded with 7μA of 6.3 Mev deuterons.

These data with interpretations are presented in Fig. 1. Since the 8.2-day period is determined by the probabilities of three processes, the total decay constant $\lambda = \lambda_k + \lambda_- + \lambda_+$. It appears from the Sargent diagram, when the intrinsic decay constants λ_- and λ_+ are used, that the negative β-emission is doubly forbidden while the positron emission is approximately singly forbidden.

Metastable States

The subject of metastable states in nuclei has been reviewed by Bethe.[7] He gives an expression

[7] Bethe, Rev. Mod. Phys. **9**, 226 (1937).

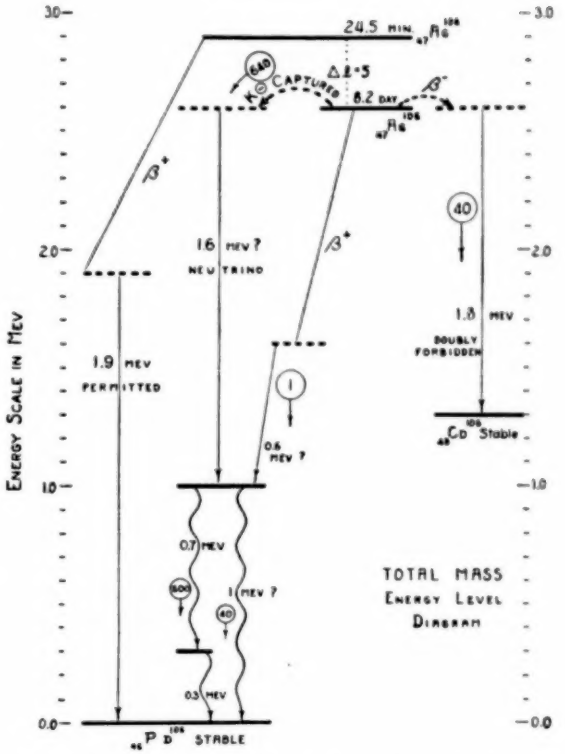

FIG. 1. Tentative energy-level diagram for the isomeric nucleus Ag^{106}. The relative transition probabilities are inscribed in circles. Total mass includes the rest mass of the orbital electrons.

for the lifetime of a state with respect to γ-emission and shows that the lifetime may be of the order of ordinary β-ray periods (seconds or days) provided that a large change Δl of the angular momentum is involved in the transition or that the levels between which the transition occurs lie very close together. Since the upper limit of the 24.5-min. positron spectrum is known to be 1.9 Mev, the difference in energy between the 24.5-min. level and the 8.2-day level is calculated to be 0.3 Mev as is shown in Fig. 1. One may then calculate that the condition $\Delta l \geqslant 5$ is necessary in order that the upper level should have a lifetime with respect to γ-emission long compared to 24.5 min. Since the 24.5-min. positron period is a permitted transition and since the nuclear spin of stable Pd^{106} is probably zero (even Z, even A) one would expect the 24.5-min. level of silver also to have zero angular momentum and the 8.2-day level to have an angular momentum of 5. This very high angular momentum should not be too disconcerting insofar as several stable

nuclei are known whose angular momentum is 9/2 in the ground state.

Discussion

In order to avoid the large Δl calculated above, the 8.2-day period might be assigned to Ag^{105}. If this new assignment be made, a n-$3n$ reaction would be involved instead of the n-$2n$ process. Since neutrons of 6 to 10 Mev are more abundant in the Li+d source than those of higher energies, the number of n-$2n$ reactions should in general, on purely energetic grounds, exceed the number of n-$3n$ reactions.[8] But the observations show that the 8.2-day silver is formed at a much greater rate than the 24.5-min. silver. Therefore the assignment to Ag^{105} seems unlikely. The most serious obstacle of all to this assignment is that the negative β-spectrum, which shows a normal energy distribution, would have to be attributed to Compton recoil electrons or that a new stable isotope Cd^{105} would have to be postulated.

Instead, the 24.5-min. period might be assigned to Ag^{105}. This period, however, has been obtained with neutron bombardment at energies as low as 10 Mev and the n-$3n$ reaction necessary in this case would be quite unlikely. Furthermore, one must assume that the 24.5-min. period is obtained from the reactions Cd-n-d and Rh-α-$2n$ instead of the suggested reactions Cd-n-p and Rh-α-n. Reactions of the types α-$2n$ and n-d have not so far been experimentally established.

Consequently, the data at present suggest more strongly that both the 24.5-min. and the 8.2-day periods should be assigned to Ag^{106}. If a very much stronger source were available, the 8.2-day γ-ray and positron spectra could be more accurately measured. The branching ratio of 20, obtained from the reactions Ag-n-$2n$, could then be checked by the following reactions: Cd-n-p, Pd-d-p and Rh-α-n. In the latter three reactions the 24.5-min. period and a long period (presumably the 8.2-day period) have been found but the intensity of the long period was too small to permit a reliable estimate of the branching ratio. However, the experiments are not in disagreement with the hypothesis that the branching ratio is about the same in all three reactions as would perhaps be required for the two periods to be isomeric.

The authors wish to thank Professor L. H. Thomas and Professor H. A. Bethe for helpful discussions regarding the theoretical aspects of this work.

[8] Pool, Cork and Thornton, Phys. Rev. **52**, 41 (1937); Walke, Phys. Rev. **52**, 669 (1937).

FEBRUARY 15, 1938 PHYSICAL REVIEW VOLUME 53

X-Ray Spectroscopic Data in Regard to the Electronic Energy Bands in Potassium and Sodium Chlorides

Joseph Valasek
University of Minnesota, Minneapolis, Minnesota

(Received December 23, 1937)

The wave-lengths of several lines in the $K\beta$ group of Cl in NaCl and KCl, and of K in KCl, have been measured in the secondary radiation from pressed blocks of the salts. The results are discussed in terms of the electronic energy bands in these crystals. It is shown that certain of the weaker lines arise from transitions of valence electrons belonging to one of the ions into a K shell vacancy in the other ion. Some of the residual nondiagram lines seem to be related to the excited levels in irradiated crystals.

RECENT discussions of the electronic energy bands in crystals, of which NaCl has been treated in greatest detail,[1] make it of interest to examine the x-ray spectrum of compounds more closely in the light of these results. One obtains in this way supplementary information on the locations of the principal energy bands and the transitions which take place. There are, however,

[1] Pauling, Phys. Rev. **34**, 954 (1929); Slater and Shockley, Phys. Rev. **50**, 707 (1936).

more lines than can be accounted for by the use of the energy diagram which has been given, and these indicate a needed extension of the theory.

Some time ago the writer measured the $K\beta_1$ lines of a series of alkali halides[2] using a secondary radiation method for producing the radiation. An application of Pauling's theory of the energy bands in solids left no doubt as to the origin of these lines. The present work is principally concerned with the weaker satellites which accompany the $K\beta_1$ line. The source of the radiation was improved somewhat by the use of a water-cooled clamp to hold the pressed pellet of salt just back of the focal spot on a water-cooled target. A tungsten screen in front of the target prevented direct x-rays from the focal spot from entering the spectrograph.

The exposures usually amounted to 100 hours at 5–10 ma and 15 kv which resulted in good intensity of the two satellites on the immediate short wave side of $K\beta_1$. In addition a number of very weak lines were observed. The locations of the three strongest lines $K\beta_1$, β_x, and β_5, were measured with respect to tungsten $L\alpha_1$ in the third order. In this way a redetermination of $K\beta_1$ was obtained as well as the new values for the other two lines. The results now given for $K\beta_1$ differ somewhat from those previously reported.[2] The present values are based on more measurements and on better exposed plates and were obtained by the use of two different calcite crystals.

Many weak lines were observed in addition to the three principal lines referred to above. These were difficult to measure accurately because they usually disappeared into the granular background when observed under the measuring microscope even when the lowest available magnification was used. Chemical intensification of the plates was attempted but did not prove to be satisfactory. It seemed best to locate these lines under a hand lens and to indicate their position by marking on the plate with a sharp pencil. These marks were carefully examined with the hand lens and only those which were apparently on the line were then measured with the micrometer microscope. The wave-lengths of these lines are probably correct to within 1 x.u. and they agree as well as can be expected with the values given by Tazaki[3] for the corresponding lines obtained by direct impact on a thin layer of the salt on an aluminum target. It was found that direct impact of electrons on powdered NaCl on Al gave a wave-length for Cl $K\beta_1$ which was less by about 0.5 x.u. than the values obtained from the secondary radiation. However, when lines other than β_x, β'', and β_5 were measured relative to $K\beta_1$ any shift with respect to this line due to the method of excitation was less than the experimental error in measuring these weak lines. Hence in order to obtain better values for these lines some plates were exposed to the direct radiation produced by direct electron impact on a salt coating over an aluminum target. These wave-lengths were then measured relative to the value for $K\beta_1$ as given by the secondary radiation method. The best plates were obtained when the current was reduced to one-half of a milliampere, the salt being changed after each two hours of exposure time. The total exposure was about forty hours.

TABLE I. *Wave-lengths of Kβ lines of Cl in NaCl.*

LINE	EXC.	WAVE-LENGTH x.u.	Δλ x.u.	ΔV ev
η	*b*	4437	53	34
β'	*b*	4421	37	24
β_1	*a*	4394.90	11.0	7.1
β_x	*a*	4391.34	7.4	4.7
β_5	*a*	4385.6	1.7	1.1
β_1'''	*b*	4336.5		
β_{II}'''	*c*	4332		
β_1''''	*c*	4325		
β_{II}''''	*c*	4320		

The wave-lengths are given in Table I with the designations of lines following Siegbahn[4] and Tazaki.[3] The letters in the second column refer to the nature of the source used. The letter *a* indicates that the wave-lengths of the lines so marked were determined solely by measuring spectrograms of the secondary radiation from pressed blocks of the salt. Those marked *b* are averages derived from the former type of exposure supplemented by others in which direct electron bombardment of a salt film over an aluminum target was also used. The lines marked *c* were found only in the spectrum of the radiation from the latter type of source. Accord-

[2] Valasek, Phys. Rev. **47**, 896 (1935).

[3] Tazaki, Hiroshima J. Sci. **6**, 299 (1936).

[4] Siegbahn, *Spektroskopie der Roentgenstrahlen*, second edition (1931), p. 169.

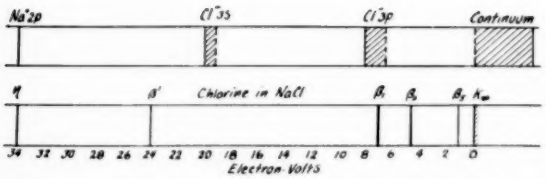

FIG. 1. Upper: electron energy bands of NaCl. Lower: K series emission lines of chlorine in NaCl on energy scale relative to the K absorption edge.

ingly these c values are repetitions of Tazaki's measurements and will be found to agree with them to better than one x.u., the estimated error. However, because of the nature of the source it is not certain that some of these lines may not be due to reaction products of the salt with the aluminum target. The chlorine $K\beta'$ line is so near tungsten $L\alpha_1$ in the third order (corresponding to $\lambda=4420.08$) that it is no doubt shifted due to the slight amount of overlapping tungsten radiation. This line appears to be a bona fide chlorine line as measurements in the spectra of chlorine in both NaCl and KCl indicate characteristic differences.

The probable errors of the wave-lengths of the $K\beta_1$ lines are 0.07 x.u. for $K\beta_1$ of K, and of Cl in NaCl, and 0.14 for $K\beta_1$ of Cl in KCl. The wave-lengths given to tenths of x.u. are probably correct to 0.3 x.u. and the other weak lines are estimated to be within one x.u. of the correct value.

The column of differences $\Delta\lambda$ gives the distances of the lines from the K absorption edges of the elements considered. These differences were obtained by using Stelling's values:[5] 4383.9 for the K edge of Cl in NaCl, 4385.1 for Cl in KCl, and 3427.9 for K in KCl. The final column gives these differences in electron volts which is of convenience in discussing the energy levels.

Since the location of the K absorption edge is just beyond the $K\beta_5$ line, β''' and β'''' must be spark lines. These are most probably of the $KL-ML$ type analogous to those which are prominent as satellites of the $K\alpha$ lines of these elements. However, there is at present no satisfactory theory for these $K\beta$ satellites comparable to that which has been given by Wolfe[6] for the $K\alpha$ satellites. On the experimental side, Tazaki has shown that they fit the same semi-Moseley curves as the similar lines measured by Ford[7] and others in the spectra of the heavier elements.

The remaining lines are plotted on an electron-volt energy scale in Fig. 1 with the absorption edge as origin, from the values of ΔV of Tables I–III. In the case of those lines which arise from transitions in an atom originally lacking only a K electron, the locations of the lines on such a plot indicate the energy levels from which the radiating electrons come. These levels can then be compared with the calculated energy bands for the crystal. Accordingly, the x-ray emission spectrum is accompanied by an energy band spectrum for NaCl similar to that given by Slater and Shockley.[1] It is evident that the Cl $K\beta_1$ line must result from a $Cl^- 1s-Cl^- 3p$ transition so that the two spectra are made arbitrarily to coincide at this point. A very rough estimate of the width of the Cl $K\beta_1$ line is only one electron-volt, which is much less than the width of the $Cl^- 3p$ level indicated by Slater and Shockley. The width shown in Fig. 1 agrees better with experiment. In addition to Cl $K\beta_1$ there is only one other possible diagram line, Cl $K\eta$, a very weak line, which is apparently due to the transition $Cl^- 1s-Na^+ 2p$, i.e., due to a sodium $2p$ electron falling into a vacancy in the chlorine K shell. This improbable occurrence may be understood by consideration of the quantum-mechanical picture of the energy bands of the valence electrons as extending continuously through the lattice though naturally the wave-function has much higher values in the vicinity of ions of the class to which it belongs.

TABLE II. *Wave-lengths of $K\beta$ lines of Cl in KCl.*

LINE	EXC.	WAVE-LENGTH x.u.	$\Delta\lambda$ x.u.	ΔV ev
η	b	4437	52	33
β_{II}'	b	4424	39	25
β_I'	b	4418	33	21
β_1	a	4394.91	9.8	6.2
β_x	a	4391.16	6.1	3.9
β_5	a	4385.3	0.2	0.1
β_7	c	4375		
β_6	b	4368		
β_8	c	4359		
β_I'''	b	4438		
β_{II}'''	c	4333		
β_I''''	c	4326		

[5] Lindh, *Roentgenspektroskopie* (1930), pp. 298–9, 302.
[6] Wolfe, Phys. Rev. **43**, 221 (1933).
[7] Ford, Phys. Rev. **41**, 577 (1932).

An examination of the K^+ and Cl^- spectra of KCl shows lines which support this conclusion. In Fig. 2 it is noted that the Cl $K\beta_1'$ line results from a $Cl^- 1s - K^+ 3p$ transition and that the K $K\beta_5$ line is due to a $K^+ 1s - Cl^- 3p$ transition. The superposition of corresponding lines in the two spectra is not exact. This seems to be principally due to the fact that they are plotted relative to Stelling's values for the respective absorption edges and that one of these, at least, should be revised. This is most probably that of Cl in KCl for which Stelling gives a wave-length of 4385.1 x.u. This value is out of line with those for Cl in the chlorides of the lighter and the heavier alkalis. An older measurement by Lindh[5] is 4382.9 which is correspondingly too low. An average of these two determinations gives very good agreement between the two spectra of Fig. 2.

The line in the spectrum of Na in NaCl which corresponds to K $K\beta_5$ is in a very different part of the x-ray spectrum but has been observed by Wetterblad.[8] Backlin[9] designated this line Na $K\beta_1$ and considered it to be of "semi-optical" origin, due to a combination between some excited optical level of Na^+ with its K level. He pointed out that normally Na^+ ($1s^2\ 2s^2\ 2p^6$) has no occupied M level which is needed for the emission of the ordinary $K\beta_1$ line. The fact that this line appears was taken to indicate that transitions occur from a virtual or optical state. The marked deviation of the frequencies of this line from Moseley's law at Na, and also Mg, supports the anomalous origin of this x-ray line. The writer considers that the "optical state" postulated by Backlin is to be identified with the $Cl^- 3p$ electron energy band of the NaCl crystal and that Na $K\beta_1$ is a $Na^+ 1s - Cl^- 3p$ transition analogous to the $K\beta_5$ line of potassium in KCl. Since the sodium ion has no M shell, this line becomes the principal line in the $K\beta$ group of Na in NaCl.

TABLE III. *Wave-lengths of Kβ lines of K in KCl.*

LINE	EXC.	WAVE-LENGTH x.u.	Δλ x.u.	ΔV ev
η	c	3490	61	63
β'	b	3476	49	51
β_1	a	3447.00	19.1	19.9
β''	a	3442.95	15.0	15.6
β_5	a	3434.97	7.1	7.4
β_6	c	3416		
β_1'''	b	3404.5		
β_{II}'''	b	3396.4		
β''''	c	3375		

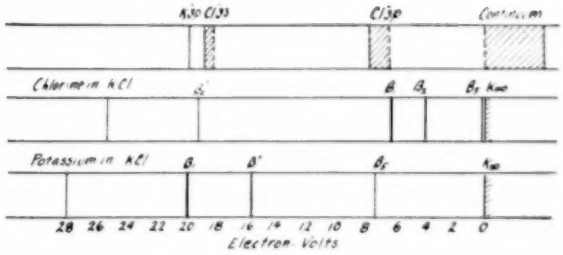

FIG. 2. Top: electron energy bands of KCl. Center: K series emission lines of chlorine in KCl on energy scale relative to the K absorption edge. Bottom: ditto, potassium in KCl.

The remaining lines belong to the general class of "nondiagram" lines. They are not necessarily due to double ionization, though this is needed to account for the lines at shorter wave-lengths than $K\beta_5$. Optical absorption studies[10] support the conclusion that the transparent, perfect crystal has no other levels than the present theory indicates. However, by the action of radiation or other ionizing agents, it is possible to produce coloration[11] which indicates that new discrete energy bands arise from the neutralization of the charges on some of the ions in the crystal. Such bands may be involved in the emission of the $K\beta_x$ line of Cl and K, and of the $K\beta_5$ line of Cl. Since selection rules will permit only the combination of P and S states, the x-ray lines cannot be identified in Figs. 1 and 2, with the ground states for the F and U absorptions which must be S-like levels, though they may originate in the same general process. This interpretation requires further investigation.

The writer expresses his thanks to the Graduate School of the University of Minnesota for its generosity in supporting this investigation, and to Mr. Rolf Landshoff for his assistance with a considerable part of the laboratory work.

[8] Wetterblad, Zeits. f. Physik **42**, 603 (1927).
[9] Backlin, Siegbahn and Thoraeus, Phil. Mag. **49**, 1320 (1925).
[10] Schneider and O'Bryan, Phys. Rev. **51**, 293 (1937).
[11] Hilsch and Pohl, Zeits. f. Physik **59**, 812 (1930); **64**, 606 (1930). Hughes, Rev. Mod. Phys. **8**, 294 (1936).

The Effect of Temperature on the Atomic Distribution in Liquid Sodium

FRANK H. TRIMBLE
Northeast Missouri State Teachers College, Kirksville, Missouri

AND

NEWELL S. GINGRICH
University of Missouri, Columbia, Missouri

(Received November 24, 1937)

X-ray diffraction patterns of liquid sodium at eight temperatures ranging from 100°C to 400°C have been obtained with monochromatic Mo $K\alpha$ radiation. Fourier analyses of the 100°C and the 400°C intensity curves were made in order to obtain the atomic distribution functions. The distribution function at 400°C shows that at this temperature, the first concentration of atoms about any atom occurs at a distance of 3.90A and the second concentration of atoms occurs at about 7.2A. The peaks in this curve are broader, and the curve approaches the average density more rapidly, than in the 100°C case. For sodium at 100°C, the distance of closest approach of the atoms is 3.83A.

INTRODUCTION

THE atomic distribution functions for liquid mercury[1] and for liquid sodium[2] have been obtained for the liquids at one temperature, but no consistent attempt has been made to investigate the atomic distribution function in a liquid element at different temperatures. It is of interest to investigate this effect for the information it may give concerning interatomic forces or for the data it may supply in support of existing theories of the liquid state.

Analysis of x-ray diffraction patterns offers a direct means of obtaining the atomic distribution functions. In this method it is necessary to diffract monochromatic x-rays from the substance under investigation and obtain reliable values of the relative intensity *vs.* diffraction angle to as large values of the angle as possible. This relative intensity must be corrected for absorption in the sample, for polarization and for incoherent radiation. It is placed on an absolute basis in electron units by assuming that at sufficiently large angles of scattering so that interferences are completely washed out, the total radiation is the sum of the incoherent and the independent coherent radiations. From this fully corrected intensity curve in electron units, straightforward calculations on the basis of the theories of Zernike and Prins[3] and Debye and Menke[1] lead to the atomic distribution function Such analysis has been made not only in the case of liquids but also in the case of "amorphous" solids[4] and crystalline solids.[5]

A number of studies of the temperature effect upon the x-ray diffraction pattern of liquids have been made, but most of these studies have been made upon polyatomic liquids.[6] Liquid sulphur[7] has been investigated at a number of temperatures and some interesting conclusions were reached, but no determination of the atomic distribution function was made.

EXPERIMENTAL

In the present work, Mo $K\alpha$ radiation monochromatized by reflection from rocksalt was diffracted by liquid sodium contained in a very thin-walled Pyrex glass capillary of 2.8 mm diameter. Although the method described by Randall[8] for filling the capillary with sodium was first used, a simpler method was finally adopted. In this, freshly cut sodium was placed in one end of a glass tube with a series of about ten con-

[1] Debye and Menke, Erg. d. Tech. Rontgenkunde, II.
[2] Tarasov and Warren, J. Chem. Phys. **4**, 236 (1937).
[3] Zernike and Prins, Zeits. f. Physik **41**, 184 (1927).
[4] Hultgren, Gingrich and Warren, J. Chem. Phys. **3**, 351 (1935).
[5] Warren and Gingrich, Phys. Rev. **46**, 368 (1934).
[6] Stewart and Morrow, Phys. Rev. **30**, 232 (1927). Zachariasen, J. Chem. Phys. **3**, 158 (1935). Harvey, Phys. Rev. **51**, 998 (1937). Katzoff, J. Chem. Phys. **2**, 841 (1934). Pierce, J. Chem. Phys. **3**, 252 (1935).
[7] Blatchford, Proc. Phys. Soc. London **45**, 493 (1933).
[8] Randall, *The Diffraction of X-Rays and Electrons by Amorphous Solids, Liquids and Gases.* (John Wiley & Sons, 1934) p. 129.

strictions and the capillary was sealed to the other end of the tube. After prolonged pumping and gentle heating, the sodium was melted and forced through the constrictions and into the capillary by means of helium at low pressure. This procedure in which the sodium has been subjected only to the removal of surface impurities has been justified in other work.[9] The sealed-off capillary filled with sodium and mounted in plaster of paris was encased in a heavy brass cylinder with entrance and exit holes for the x-rays. The brass cylinder was heated by means of a soldering iron element and the temperature of the capillary tube just above the point where the x-rays passed through was measured with a fine iron-advance thermocouple. The capillary was centralized in a cylindrical camera of 8.85 cm radius, which was measured mechanically and by a calibration run with rocksalt. The photographic film had suitable blackening after an exposure of 36 hours with the x-ray tube operated at 30 kv and 18 ma. Microphotometering the film and converting to intensities in the usual manner resulted in the experimental intensity curve.

Application of the Fourier Method

In applying the Fourier method, it is necessary to have the experimental intensity on an absolute basis, in electron units, and this is obtained by using the fully corrected intensity curve at so large a value of sin θ/λ that all the radiation may be considered as independent. For this point, the ratio of coherent radiation to total radiation is calculated, the incoherent is subtracted from the total, and this serves to place the experimental curve on the same scale as the coherent, which is given in tables[10] in electron units per atom. The experimental intensity curve was corrected for absorption (practically negligible in this case), for polarization, and for incoherent radiation. Fully corrected intensity curves for sodium at 100°C and 400°C are shown in Fig. 1, together with a dashed curve representing the total independent scattering per atom (for the 400°C case only) and a dotted curve representing the incoherent scattering.

For a liquid element, the average density of surrounding atoms is given by the relation[5]

$$4\pi r^2\rho(r)=4\pi r^2\rho_0+(2r/\pi)\left(\int_0^\infty si(s)\sin rs\,ds\right), \quad (1)$$

where $4\pi r^2\rho(r)dr$ is the number of atoms between distances r and $r+dr$.

ρ_0 = average density of sample in atoms per unit volume.
$s=4\pi \sin\theta/\lambda$.
$i(s)=(I/N-f^2)/f^2$.
I/N = unmodified intensity per atom in electron units.
f = atomic scattering factor.

The product $si(s)$ is plotted against ks where k is a constant so chosen as to give convenient points in the final distribution curve. Curves of this type are shown in Fig. 2 for the 100°C and the 400°C cases. The integral of Eq. (1) was evaluated with the help of a Coradi analyzer,[11]

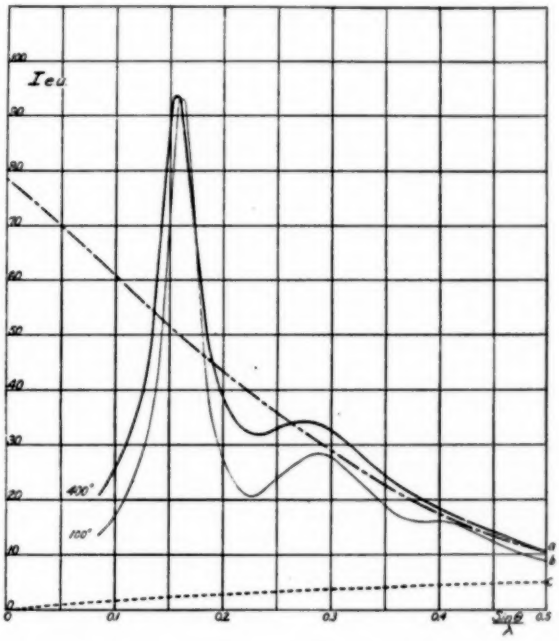

FIG. 1. Experimental intensity curves for x-ray diffraction from liquid sodium at 100°C and 400°C together with curves representing the incoherent radiation and the independent coherent radiation for the 400°C case.

[9] Bent and Forziati, J. Am. Chem. Soc. **58**, 2220 (1936).
[10] From tables of f and Σf^2, Compton and Allison, *X-Rays in Theory and Experiment*. (D. Van Nostrand 1935) p. 781.
[11] We are indebted to Professor B. E. Warren for the use of the Coradi analyzer at Massachusetts Institute of Technology.

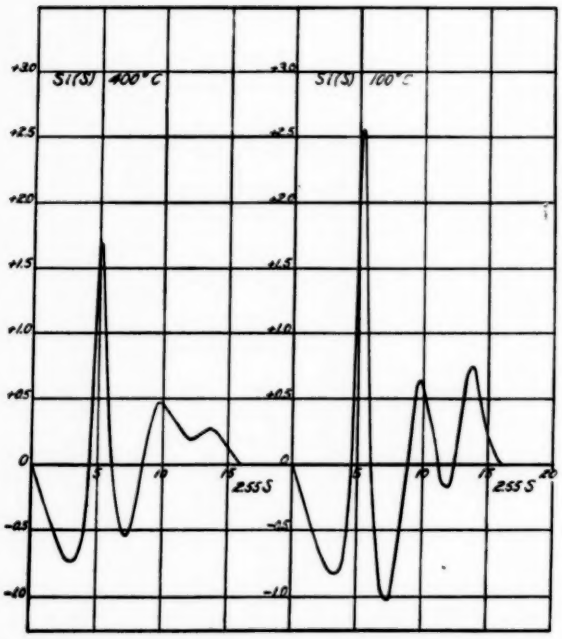

FIG. 2. Curves showing the $si(s)$ function for liquid sodium at 100°C and 400°C.

and the values for certain points were checked by graphical computation. The analysis resulted in the curves shown in Fig. 3 and Fig. 4. These distribution curves are plotted together with the curves for constant density.

DISCUSSION OF RESULTS

The effect of temperature upon the diffraction pattern of a liquid is shown in Fig. 1. For the same intensity of the main peak, the scattering at large angles is higher for the higher temperature, the second peak is less prominent and the third peak is almost absent. There is, in addition, a slight shift of the positions of the maxima in the high temperature case to smaller angles than in the low temperature case. Perhaps the most effective graphical representation of the temperature effect is shown in Fig. 2. In this the oscillations of the $si(s)$ function are highly damped in the 400°C case. For temperatures between 100°C and 400°C, there was a consistent, gradual transition in the shape of the $si(s)$ function. Complete analyses of these intermediate cases were not made.

The radial density curve for liquid sodium at 100°C shown in Fig. 4 confirms that obtained by Tarasov and Warren[2] except for a consistent difference in the abscissa values. This shows up most prominently for the first peak, which in their work appeared at 3.96A and in the present work appears at 3.83A.[12] The interpretation of the curve of Fig. 4 is that an atom at $r=0$ is surrounded on the average, by an atomic population between distances r and $r+dr$ given by the area under the curve between r and $r+dr$. The distance from $r=0$ to the position of the maximum of the first peak is interpreted as being the most probable distance to the nearest neighbors. Beyond this distance, the distribution curve oscillates about the curve of constant density but never approaches zero. In similar curves for glass, however, the distribution curve does reach zero after the first peak. The significance of this has been pointed out by Warren,[13] for in vitreous SiO_2, a silicon atom, for example, has four definite and permanent neighbors, while in liquids, neighbors are temporary and any distances of approach above the minimum are possible, although the probability of finding a neighbor at the "contact distance" is higher than for other distances. Beyond the first peak there is a fairly well defined average concentration of atoms at about 7.0A.

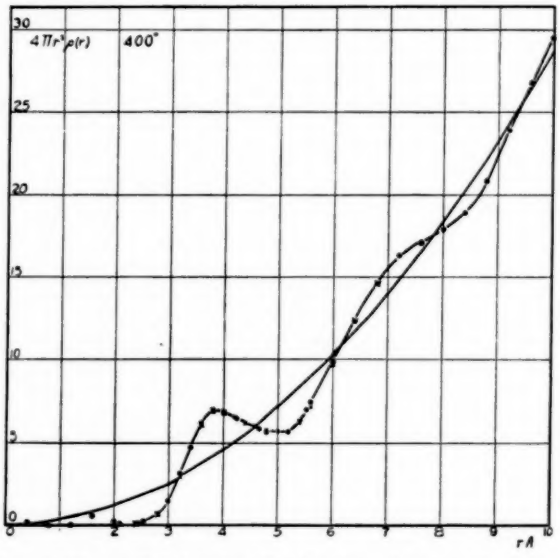

FIG. 3. The radial density distribution of atoms about any one atom in liquid sodium at 400°C.

[12] In a private communication, Professor Warren stated that there was an error of 2.6 percent in their microphotometer enlarging ratio. Correcting for this, their value becomes 3.86A, in essential agreement with the value obtained in the present work.

[13] Warren, J. App. Phys. **8**, 645 (1937).

The radial density curve for liquid sodium at 400°C shown in Fig. 3 shows much less pronounced concentrations of atoms. The first concentration has a peak value at 3.90A and the second at about 7.2 A, while the dip between these two peaks is less than that in the case of sodium at 100°C. In order to compare the distributions at 100°C and 400°C more conveniently and effectively, $\rho(r)$, the actual density, as a function of r is shown for the two temperatures in Fig. 5. The solid curve for 400°C, is shown oscillating about the straight line representing the average density at 400°C. The dotted curve is the $\rho(r)$ for 100°C with its ordinate scale shifted since it would normally oscillate about the average density of sodium at 100°C. The concentrations and deficiencies of atoms are less pronounced in the 400°C case than in the 100°C case. Furthermore, at 400°C, the curve has positive values at values of r less than that for the 100°C case. The reality of this slight difference depends upon the accuracy with which the diffraction patterns in the two cases are known. Some support is given to this effect, however, from the fact that all the patterns obtained at various temperatures showed a consistent trend in such a manner as to indicate the reality of this effect.

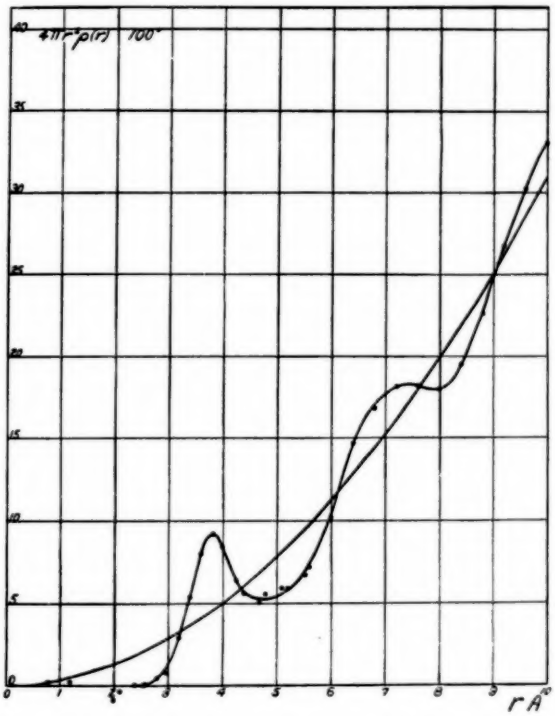

FIG. 4. The radial density distribution of atoms about any one atom in liquid sodium at 100°C.

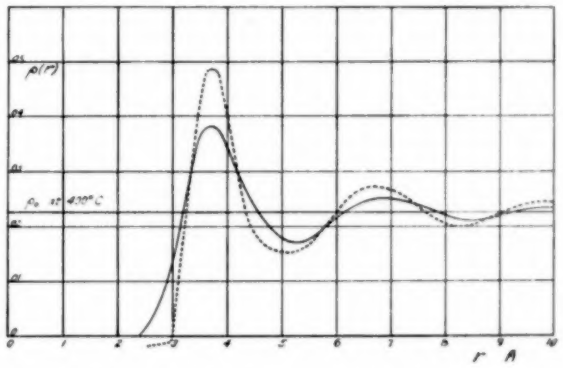

FIG. 5. The actual density in atoms per unit volume as a function of distance from any one atom in liquid sodium at 400°C. The dotted curve (with slightly shifted ordinate) shows that for liquid sodium at 100°C.

The impossibility of interpenetration of sodium atoms and the existence of interatomic binding requires that certain arrangements of these atoms with respect to their neighbors are more probable than others. These results show that the arrangement of sodium atoms is not wholly random, and they indicate the extent to which the atoms assume temporary arrangements due to their packing together. They show further, that the tendency to assume these temporary arrangements is less when the temperature is high than when it is low, and the curves shown in Fig. 3, Fig. 4 and Fig. 5 provide a measure of how much less this tendency is. They are in accord with the kinetic picture of a liquid, and on this picture, they may be given rough qualitative interpretation but it is possible that they may eventually lead to quantitative results concerning the interatomic binding forces or energies.

It is a pleasure to acknowledge grants-in-aid of-research made to one of us (N.S.G.) by the American Academy of Arts and Sciences from the Rumford Fund, and by the American Association for the Advancement of Science.

The Isotopic Constitution of Calcium, Titanium, Sulphur and Argon

ALFRED O. NIER*
Research Laboratory of Physics, Harvard University, Cambridge, Massachusetts
(Received December 23, 1937)

A mass-spectrographic study of the isotopic constitution of calcium, titanium, and sulphur has been made. Two new calcium isotopes, Ca^{46} and Ca^{45}, were found, present with abundances 1/29,000 and 1/520 that of Ca^{40}, respectively. No new titanium isotopes were found. A new sulphur isotope, S^{36}, was discovered, having an abundance 1/6,000 that of S^{32}. The proof for the existence of the new isotopes is presented. The relative abundances of the isotopes in these three elements were determined. A search for other possible rare isotopes was made in all mass number positions in the immediate neighborhood of the known isotopes. Upper limits for the existence of these hypothetical isotopes are given. A search was made for A^{42}.

THIS paper is one of a series dealing with the study of the isotopic constitution of the elements. A systematic research program was undertaken with the following objectives in mind: (1) To obtain accurate measurements of the relative abundances of isotopes (2) to establish the existence or nonexistence of questionable isotopes, and (3) to search in all mass number positions in the immediate neighborhood of the known isotopes for possible rare isotopes, and if none was found, to set upper limits for the existence of such hypothetical stable isotopes.

The elements which so far have been studied are A, K, Rb, Zn, and Cd;[1] Hg, Xe, Kr, Be, I, As, and Cs;[2] and Os.[3] A preliminary report has been given for Pb.[4] The present paper will show the results obtained for calcium, titanium and sulphur, together with an additional result for argon.

APPARATUS

The mass spectrometer used differed from that employed for the Hg, Xe, etc., study only insofar as a new tube was employed which enabled one to work with substances not volatile at ordinary temperatures. In the earlier work it was necessary that the substance to be studied should have a vapor pressure at least as great as 10^{-5} mm Hg at the temperature to which it is safe to heat the entire Pyrex tube. The new tube has a small furnace inside of it which now contains the substance to be studied. This small furnace may be heated to any desired temperature.

A diagram of a portion of the new tube is shown in Fig. 1. Its operation is quite similar to that of the previous tube. A ribbon of electrons, the cross section of which is indicated by the dashes between plates J and B, moves perpendicular to the figure. The small furnace G consists of a solid block of Nichrome V 6 mm $\times$6 mm$\times$10 mm long, heated by a one-half mm diameter tungsten spiral filament passing through the upper hole in the block. The substance to be studied is placed in the lower hole, which is closed at one end and has a threaded cap at the other. When the furnace is heated, molecules emerge through the slit below the lower hole and pass into the electron beam. Here positive ions are formed which are drawn through slits S_1 and S_2 into the 180° magnetic analyzer H. This molecular beam method of producing ions was employed with considerable success by Bleakney, Blewitt, Sherr and Smoluchowski[5] in their study of beryllium.

If one varies the energy of the ions and plots a curve of positive ion current collected beyond the exit slit of the analyzer, one obtains a mass spectrum having a peak for each isotope present. The magnetic field is, of course, held constant.

In the present apparatus one is limited to a furnace temperature of about 1200°C. In order to reach higher temperatures a furnace of tantalum will be employed.

RESULTS

Calcium

Calcium metal was placed in the furnace and the entire apparatus was baked out at a tem-

* National Research Fellow.
[1] Nier, Phys. Rev. **50**, 1041 (1936).
[2] Nier, Phys. Rev. **52**, 933 (1937).
[3] Nier, Phys. Rev. **52**, 885 (1937).
[4] Nier, Phys. Rev. **51**, 1007 (1937).
[5] Bleakney, Blewitt, Sherr and Smoluchowski, Phys. Rev. **50**, 545 (1936).

perature of 450°C until only small traces of impurities remained. For the study of calcium a furnace temperature of about 550°C gave positive ion peaks of sufficient magnitude without too great a rate of evaporation from the furnace. A typical mass spectrum is shown in Fig. 2. One sees here, in addition to the previously known isotopes, 40, 42, 43, and 44,[6] two new peaks, one at mass 48 and one at mass 46. That these newly found peaks really correspond to rare isotopes of calcium, and not to possible impurities present, may be concluded from the following:

(1) The abundance ratios Ca^{48}/Ca^{40} and Ca^{46}/Ca^{40} were studied as a function of furnace temperature, i.e., Ca vapor pressure, and were both found to remain constant within the experimental errors. The Ca^{48}/Ca^{40} ratio was studied over a 12-fold range and the Ca^{46}/Ca^{40} ratio over an 8-fold range of pressure.

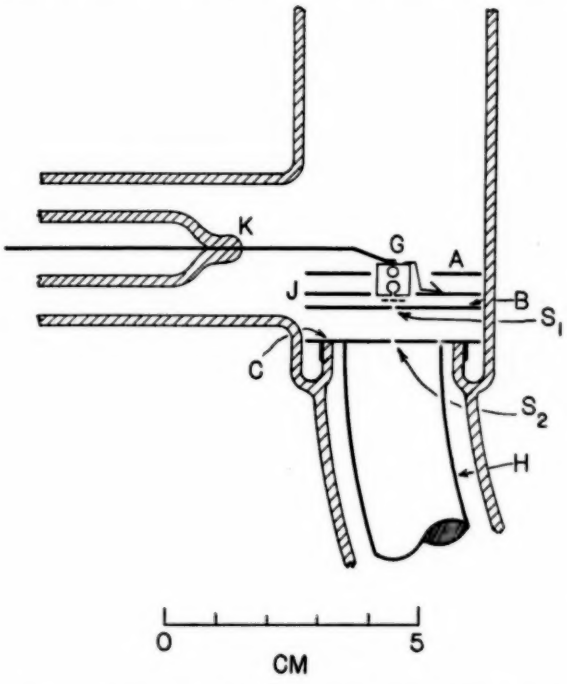

FIG. 1. Diagram of portion of mass spectrometer where ions are produced. The furnace G is supported by the glass stem K. Actually 4 electrical leads come through this stem. Two furnish the current to the furnace filament, one supports the furnace (this is the one shown in the diagram), and the fourth, together with the one supporting the furnace form a thermocouple junction for measuring the furnace temperature. If one cracks the reentry seal of which the stem K is a part, the stem and furnace may be removed without disturbing the rest of the apparatus. The function of the plate A is to support an electron gun and trap which are not shown in the figure. As in the earlier work no wax or grease joints are employed at any point in the apparatus. The entire tube may be thoroughly baked to remove impurities.

[6] Aston, Proc. Roy. Soc. **A149, 396** (1935).

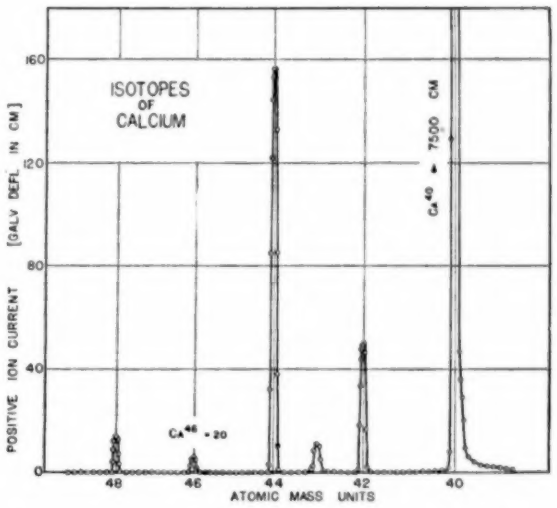

FIG. 2. Mass spectrum showing isotopes of calcium. Positive ion current expressed in terms of cm deflection of galvanometer at its highest sensitivity. One cm represents about 2.5×10^{-15} ampere.

(2) The results of a study of the number of ions of each isotope formed as a function of the energy of the electrons producing the ions is shown in Fig. 3. From this curve, one sees that not only do the three peaks, Ca^{40}, the peak at 46, and the peak at 48, all have the same form of efficiency curve, but they also have *the same appearance potential.* A detailed study of the form of the curves near the appearance potential showed that the appearance potential of the 48 peak was within at least 0.3 volts of that for Ca^{40}, while that for the 46 peak did not differ more than a volt from that for Ca^{40}.

(3) A study of the doubly charged ions showed that the 24 peak $(48)^{2+}$ had the same form of efficiency curve as did the $(Ca^{40})^{2+}$ peak. The appearance potentials were the same within the experimental error, two volts. The relative height of the two peaks agreed within a few percent of that found for the singly charged ions.

It should be mentioned that a trace of magnesium was present in the calcium. Mg^{24} contributed only about 10 percent of the total 24 peak at 70 volts, the point where the Ca^{2+} current versus electron energy curve has its maximum. As Mg has a much lower appearance potential than Ca^{2+}, and as its efficiency curve is

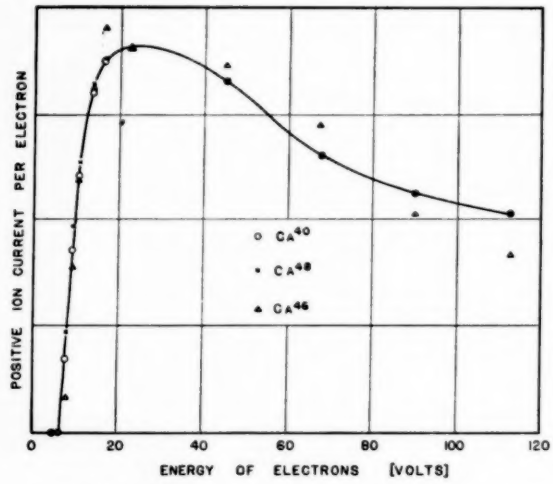

FIG. 3. Efficiency of ionization curve for Ca^{+}.

relatively flat for electron energies over the range where Ca^{2+} is formed, no difficulty was had in subtracting the Mg^{24} contribution from the total peak, and thus arriving at the conclusions of the previous paragraph.

It was not possible to examine the $(Ca^{46})^{2+}$ due to the fact that it was small as compared with a trace of sodium present in the calcium. The discovery of Ca^{46} confirms the result of Wigner,[7] who computed that Ca^{46} should be stable.

Table I shows a list of the stable isotopes of Ca, together with their respective abundances. Aston's values, converted from percentages to relative abundances, are also included.

All of the measured abundances, with the exception of that for Ca^{46}, are believed to be correct to 3 percent. The abundance for Ca^{46} may be in error by 15 percent. However, we have not taken account of the possible effect of free evaporation from the furnace. The mass of the heaviest Ca isotope differs by 20 percent from that of the lightest; only in hydrogen do the isotopes have a larger fractional spread in mass. In the case of *ideal* distillation of Ca from the furnace, the Ca^{48}/Ca^{40} ratio *as measured* would be only $(40/48)^{\frac{1}{2}}=0.895$ of what it should be. The other isotope ratios as measured would be in error by similar factors.

As the calcium atoms are evaporated from a solid surface and not from a liquid where mixing can take place, it does not seem likely that one would approach the ideal case. However, the effect should not be overlooked in this work.

The major problem of the present study of calcium was the establishment of the existence or nonexistence of rare isotopes. The relative abundances of the Ca isotopes will be examined in greater detail later.

With a packing fraction of -6 and a conversion factor of 1.000275 for going from the atomic to the chemical scale, one computes a chemical weight of 40.08 from both the writer's and Aston's values. The present chemical value is 40.08.

A search for other isotopes was also made. None was found, and it was possible to set the following upper limits for the abundances relative to Ca^{40}: Ca^{38}, 1/60,000; Ca^{39}, 1/40,000; Ca^{41}, 1/150,000; Ca^{45}, Ca^{47}, Ca^{49}, and Ca^{50}, 1/200,000. Aston had set an upper limit of 1/1000 for Ca^{41}.

Titanium

Titanium fluoride, TiF_3, was introduced into the furnace. It was found that the molecular ions were the most convenient to examine. A typical mass spectrum is shown in Fig. 4. The isotopes found were the same as those reported by Aston.[6]

Table II gives a list of the isotopes, together with their respective abundances. Aston's values are included for comparison. With a packing fraction of -7.2[8] and a conversion factor of 1.000275, the writer's values give a chemical weight of 47.88. Aston's figures yield the value 47.90. The present chemical value is 47.90. The writer believes that his abundances relative to Ti^{48} are all correct to 2 percent. The effect of free evaporation should be negligible here, as the spread in mass units between the heaviest and lightest ions is only 4 at mass 105.

The real reason for undertaking the study of

TABLE I. *Isotopes of calcium.*

	Mass Number					
	40	42	43	44	46	48
Abundance	100	0.66	0.150	2.13	0.0034	0.191
Aston's values	100	0.80	0.18	2.35	—	—

[7] Wigner, Phys. Rev. **51**, 947 (1937).

[8] Dempster, Bull. Am. Phys. Soc., Chicago Meeting, November, 1937.

titanium was to see if any other isotopes existed. None was found, and it was possible to set the following upper limits of abundance relative to Ti^{48}: Ti^{42}, 1/100,000; Ti^{43}, 1/10,000; Ti^{44} and Ti^{45}, 1/50,000; Ti^{51}, Ti^{52}, and Ti^{53}, 1/100,000; Ti^{54}, 1/25,000. Some difficulty with impurities was encountered in this search. However, it was possible to suppress the impurities in the several positions where they occurred below the limits given above.

Sulphur

Aston[9] found sulphur to consist of three isotopes, 32, 33, and 34, present in abundances roughly proportional to the numbers 96, 1, and 3, respectively. The present work on sulphur was undertaken in order to search for a possible S^{36} isotope, which Wigner[7] calculated should be stable.

After thoroughly outgassing the apparatus, SO_2 was allowed to flow into the tube through a capillary leak, the pressure being maintained below 10^{-4} mm mercury. No use was made of the small furnace in this case. Table III tabulates all of the ions observed in the SO_2^+, SO^+ and S^+ spectra and possible combinations of sulphur and oxygen isotopes which would produce ions of these masses. Combinations such as $SO^{17}O^{17}$ and $SO^{17}O^{18}$, which are very rare, are not included in the table.

Before proceeding to the proof that S^{36} exists it will be well to establish the abundances of the other sulphur isotopes. The relative abundances of S^{32}, S^{33}, and S^{34} were determined from the relative heights of the 64, 65, and 66 peaks in the SO_2^+ spectrum, and from the relative heights of the 48, 49, and 50 peaks in the SO^+ spectrum. As may be seen from the table, allowance has to be made for the rare oxygen isotope combinations in determining these abundances. Throughout this paper the isotopes of oxygen

TABLE II. *Isotopes of titanium.*

	Mass Number				
	46	47	48	49	50
Abundance	10.82	10.56	100	7.50	7.27
Aston's values	11.9	10.9	100	7.7	9.7

[9] Aston, *Mass Spectra and Isotopes*, p. 143.

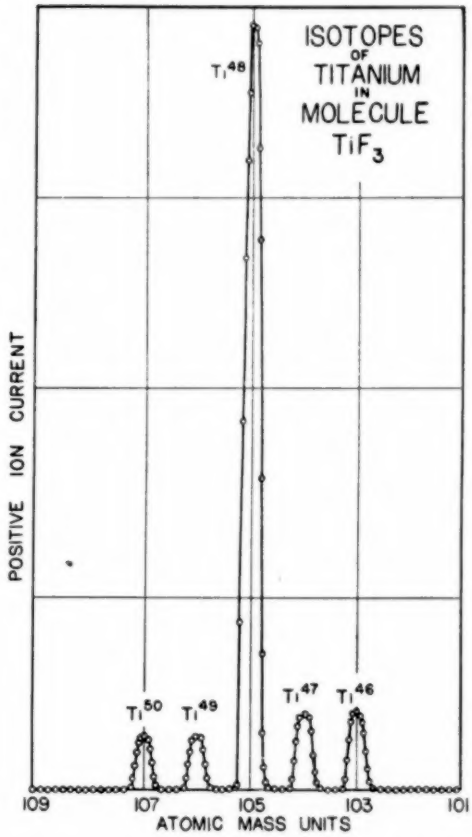

FIG. 4. Mass spectrum showing isotopes of titanium.

and their abundances are assumed to be: O^{16}, 100; O^{17}, 0.04; and O^{18}, 0.20. The results obtained for sulphur are then S^{32}, 100; S^{33}, 0.78; and S^{34}, 4.4. The values given are believed correct to two percent. It should be mentioned that these results are not greatly influenced by the exact abundances assumed for the oxygen isotopes.

That S^{36} exists may be concluded from the following:

(1) From a consideration of the relative heights of the 68 and the 64 peaks we find that only approximately one-half of the 68 peak can be attributed to the ions $(S^{34}O^{18}O^{16})^+$ and $(S^{32}O^{18}O^{18})^+$. We are thus forced to conclude that the remainder is due either to an impurity or to S^{36} in the ion $(S^{36}O^{16}O^{16})^+$ present to one part in 6000 ± 10 percent, compared with S^{32}. The excellent agreement between the efficiency curves shown in Fig. 5A makes the impurity possibility unlikely.

(2) From a comparison of the relative heights of the 52 and 48 peaks in the SO^+ spectrum we

find that only about $\frac{1}{3}$ of the height of the 52 peak can be attributed to $(S^{34}O^{18})^+$. The residue must thus again be due either to an impurity or to S^{36} in $(S^{36}O^{16})^+$. If one assumes the latter possibility, *the S^{36}/S^{32} ratio again turns out to be 1/6000±10 percent.* The excellent agreement between the efficiency curves shown in Fig. 5B also makes the impurity hypothesis unlikely.

(3) The relative heights of the 36 and 32 peaks are *also in the ratio 1/6000±10 percent.* Fig. 5C shows the efficiency curves for these two peaks, which also agree remarkably well when one considers the low probability of this ionization process.

The 67 peak observed in SO_2^+ was shown from a measurement of its abundance to be due entirely to $(S^{34}O^{17}O^{16})^+$ and $(S^{33}O^{18}O^{16})^+$. The 51 peak in SO^+ was found to be due entirely to $(S^{34}O^{17})^+$ and $(S^{33}O^{18})^+$. No peak was observed at mass 35 in the S^+ spectrum. In *each* of these three positions we are able to set an upper limit of 1/50,000 for the abundance of S^{35}.

A study of the other mass number positions enables us to set the following upper limits for the abundance of other possible isotopes relative to S^{32}: S^{37} and S^{38}, 1/200,000; S^{31}, 1/20,000; S^{30} 1/50,000.

With a packing fraction of −5.6 for sulphur and a conversion factor of 1.000275 in going from the atomic to the chemical scale, an atomic weight of 32.064 is computed for sulphur. The present chemical value is 32.06.

Argon

In the earlier work on argon[1] an upper limit of 1/20,000 of A^{40} was set for A^{42}. After discovering the new calcium and sulphur isotopes at this time it seemed worth while to look further for A^{42}. It is now possible to say that if it exists it must be less than 1/300,000 of A^{40}.

TABLE III. *Ions observed from SO_2.*

TYPE OF ION	MASS NUMBER	POSSIBLE COMBINATIONS PRODUCING IONS AT THESE MASS NUMBERS
SO_2^+	64	$(S^{32}O^{16}O^{16})^+$
	65	$(S^{33}O^{16}O^{16})^+$, $(S^{32}O^{17}O^{16})^+$
	66	$(S^{34}O^{16}O^{16})^+$, $(S^{32}O^{18}O^{16})^+$, $(S^{33}O^{17}O^{16})^+$
	67	$(S^{34}O^{17}O^{16})^+$, $(S^{33}O^{18}O^{16})^+$, possibly $(S^{32}O^{16}O^{16})^+$
	68	$(S^{36}O^{16}O^{16})^+$, $(S^{34}O^{18}O^{16})^+$, $(S^{33}O^{18}O^{18})^+$
SO^+	48	$(S^{32}O^{16})^+$
	49	$(S^{33}O^{16})^+$, $(S^{32}O^{17})^+$
	50	$(S^{34}O^{16})^+$, $(S^{32}O^{18})^+$, $(S^{33}O^{17})^+$
	51	$(S^{34}O^{17})^+$, $(S^{33}O^{18})^+$, possibly $(S^{36}O^{16})^+$
	52	$(S^{36}O^{16})^+$, $(S^{34}O^{18})^+$
S^+	32	$(S^{32})^+$
	33	$(S^{33})^+$
	34	$(S^{34})^+$
	36	$(S^{36})^+$

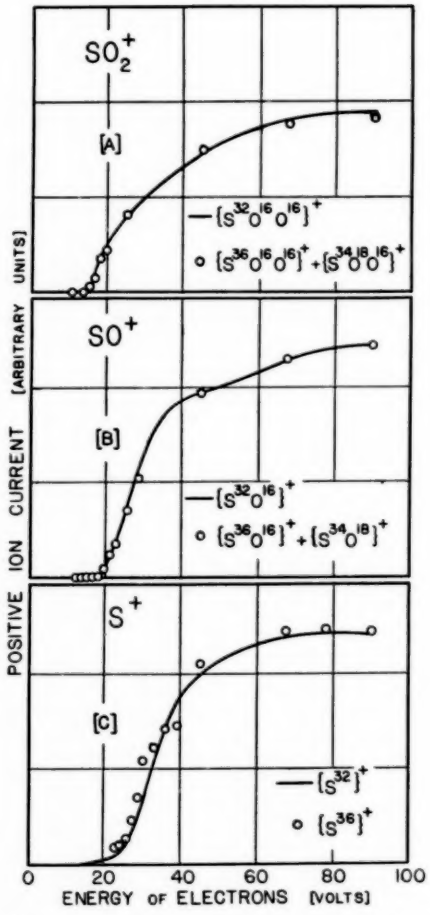

FIG. 5. Efficiency of ionization curves for SO_2^+, SO^+, S^+. The ion $(S^{32}O^{18}O^{18})^+$ is not listed in part *A* as a contribution to the 68 peak. It is quite negligible, contributing only approximately 1 percent to the peak. The curves in the three parts of the figure are the ones for the most abundant sulphur isotope, S^{32}. In order to avoid confusion the experimental points are not shown. The circles are the experimental points for the ions involving the isotope S^{36}. It is hardly necessary to state that there is a large scale factor between the data involving S^{36} and that involving S^{32}.

The writer wishes to express his appreciation to Professor Kenneth T. Bainbridge for his interest and encouragement in this work. Special thanks are due Dr. John Bardeen for numerous interesting discussions on the stability of the isotopes in the region studied. The search for S^{36} was undertaken as the result of one of these conversations. The glass housing for the new tube used in these experiments was constructed by Mr. H. L. Leighton.

The Photoelectric Sensitization of Aluminum*

LOUIS P. THEIN†
St. Louis University, St. Louis, Missouri
(Received November 26, 1937)

It is shown that the increase in photo-current from aluminum which had been subjected to hydrogen glow discharges, is dependent on the time of discharge and on the pressure of hydrogen. If the target is not outgassed a rapid decay is noted after sensitization, because of diffusion to the surface of gas contained in the body of the metal. Results indicate that this sensitization is due mainly to "clean-up" of the surface of the oxide coated aluminum. Glow discharges have little effect on the yield from freshly evaporated aluminum. Another type of sensitization is effected by exposing a freshly evaporated aluminum surface to minute quantities of dry air. The effect of the glow discharge upon a surface thus sensitized is one of desensitization. The current-voltage data from freshly distilled aluminum yield a curve which fits well upon the theoretical curve of the DuBridge theory. The curves from surfaces sensitized with air show no agreement with the theory. The threshold value obtained from a film of aluminum approaching bulk thickness is 2840A.

THE process of photoelectric sensitization of alkali metals by hydrogen glow discharges has been the object of a considerable amount of research. Data on this subject are relatively abundant and the theory of the factors involved has been advancing steadily. Meanwhile, investigation of the effect of glow discharges on metals outside the alkali group has been neglected to a great extent. The process has been used at times to sensitize metals in the latter class, but generally without much attention to the factors controlling sensitivity. The purpose of this paper is to report the results of preliminary experiments on the sensitization of aluminum by hydrogen glow discharges under various conditions. The experiments were undertaken with the hope of clarifying the uncertainties concerning the effect on the photoelectric emission of the duration for the discharge, its direction and the pressure of hydrogen. In the first set of trials the photoelectric emitter was un-outgassed aluminum and in the later experiments an evaporated aluminum surface sensitized by admission into the photocell of air in minute quantities.

The effect of the variation of film thickness upon the photo-current was observed, and also a test made of the DuBridge theory of the energy distribution of photoelectrons in pure aluminum.

Apparatus and Method of Procedure

The experimental photo-cell (Fig. 1) was a two-liter Pyrex flask with a quartz tubular window attached by means of a graded quartz-to-Pyrex seal. A thirty mil tungsten rod, led into the tube from the side opposite the window, carried the aluminum target 1.5 cm² in area. Freshly evaporated aluminum could be deposited on this target by passing heavy currents through three pairs of 60 mil tungsten leads, each supporting a 30 mil tungsten filament wound about a supply of aluminum from the same source as the target.[1] Hydrogen could be introduced into the system by flaming a palladium tube, and its pressure measured by ionization and McLeod gauges. Mercury vapors were trapped by means

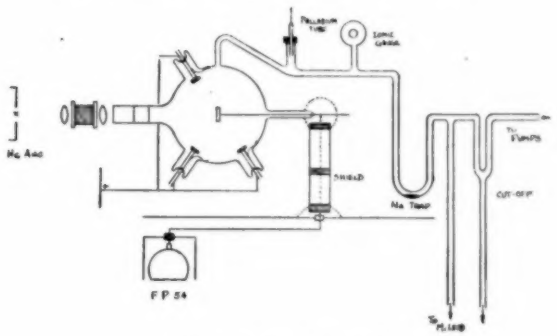

FIG. 1. The photo-cell.

* Paper presented at the Madison, Wisconsin Meeting of the Physical Society, June 20, 1937.

† Now located at St. Mary's University, San Antonio, Texas.

[1] The aluminum used was obtained from the Alcoa Laboratories through the courtesy of the chemistry department of St. Louis University. It was guaranteed to contain less than 0.1 percent impurities.

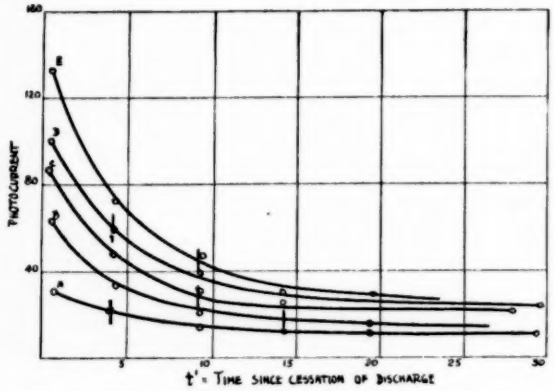

FIG. 2. Decay of sensitivity of un-outgassed aluminum.

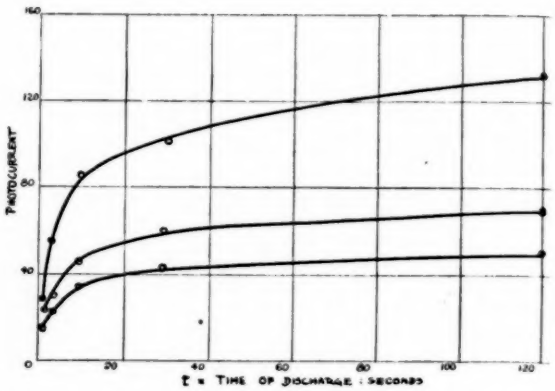

FIG. 3. Variation of sensitivity with time of discharge.

of triply-distilled sodium as described by Poindexter.[2] The photo-cell itself and the neighboring glass parts were outgassed by a seven-hour heating at a temperature averaging 350°C.

The circuit used for measuring the photo-electric current was that designed by Brown and DuBridge, using an FP-54 Pliotron.[3] With an input resistance of approximately 10^9 ohms, and a Leeds and Northrup high sensitivity galvanometer in the plate circuit currents smaller than 10^{-13} amp. were measurable. Light aluminum tubing was used in the shielding of leads. In the sensitization experiments the unresolved radiation from a G.E. mercury arc was focused upon the aluminum surface by a quartz lens. For the threshold measurements the predominant 2653A and 2536A lines of the same arc were used. The high voltage source consisted essentially of a filament transformer a high voltage transformer and an RCA 866 rectifier tube. With 3000 volts applied to the terminals, currents varying from 0.0005 amp. to 0.008 amperes were obtained.

A preliminary set of measurements of the effect of a 10 sec. hydrogen glow discharge, with the target which had not been outgassed as cathode, showed a twenty-fold increase in the photo-current measured one minute after the discharge ceased. The increase was only temporary; a rapid decay ensued, the current decreasing to half its value within a few minutes. Therefore, in addition to the anticipated factors affecting the sensitivity, the decay factor had also to be considered.

In the first group of experiments upon aluminum which had not been outgassed, the following order was observed:

1. The hydrogen pressure kept constant, the time of sensitization (t) varied, and the decay curves run for each (t).
2. The time of sensitization held constant and the decay curves plotted for various pressures of hydrogen.
3. The time (t') since the cessation of discharge held constant, and the sensitization curves plotted for various hydrogen pressures.

In the measurements made upon freshly evaporated aluminum which had been sensitized by the oxygen of the air, only the variation of sensitivity with time of discharge was recorded, since in this case no decay effects were in evidence.

Current-voltage curves, from which the threshold values were calculated, were run both for sensitized aluminum and for a freshly evaporated film approaching bulk thickness.

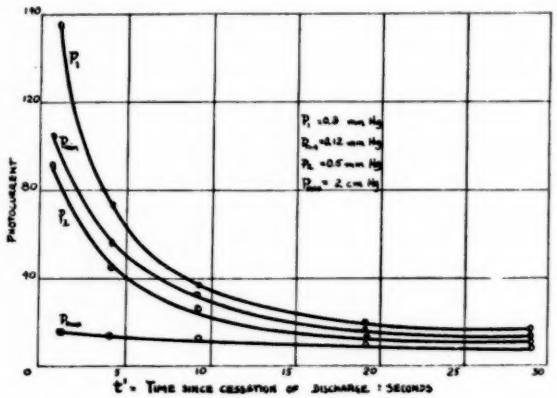

FIG. 4. Decay curves of un-outgassed aluminum. Various pressures.

[2] Poindexter, Phys. Rev. **28**, 208 (1926).
[3] Brown and DuBridge, Rev. Sci. Inst. **4**, 532 (1933).

Results

Sensitization of un-outgassed aluminum

In Fig. 2 the photo-current is plotted against the time of decay (t') the pressure being constant and the time of sensitization varying for each curve thus: A, 1 sec.; B, 3 sec.; C, 10 sec.; D, 30 sec.; E, 2 min. In these experiments the hydrogen was removed at different times during the run, as indicated by the small vertical bars of Fig. 2, but no decided deformation of the curves was noted. All the decay curves seem to be exponential in character.

Figure 3 illustrates the variations in photo-current with time of discharge (t), the pressure again being constant. In addition each particular curve has a constant (t'). The steep slope of all the curves at the beginning indicates that the initial short periods of sensitization are relatively more effective than the longer and later periods.

In Fig. 4, the time of sensitization was a constant (2 min.), and the individual curves show the decay in photo-current for the pressures: $P_{\min}$, 1.2×10^{-1} mm Hg; P_1, 3×10^{-1} mm Hg; P_2, 5×10^{-1} mm Hg; $P_{\max}$, 2 cm Hg. The outstanding feature of these curves is not their form (approximately exponential as in the previous case) but the order of their vertical arrangement: P_1, $P_{\min}$, P_2, $P_{\max}$. This order shows there is an optimum pressure in the neighborhood of P_1 (0.3 mm Hg), and that the higher pressures are ineffective in producing sensitization. By extrapolation of the P_1 curve a sensitization factor of about 80 was obtained for $t'=\frac{1}{2}$ min.

The occurrence of an optimum pressure in the region of 0.3 mm Hg is brought out more clearly in the curves of Fig. 5; the same data being plotted with current and hydrogen pressure as the coordinates.

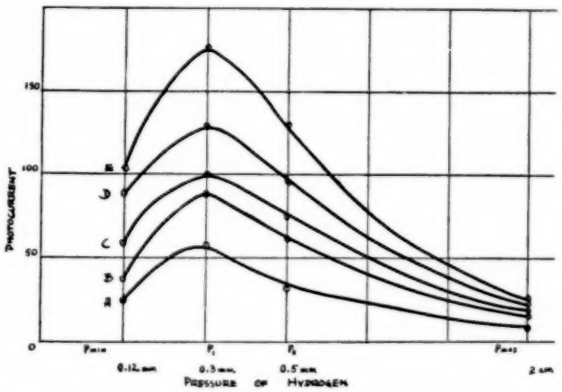

FIG. 5. Optimum pressure curves. Un-outgassed aluminum.

Glow discharges with the aluminum target as anode, produced only an extremely slight increase in the photoelectric sensitivity (Fig. 6).

A preliminary trial of the effect of the hydrogen discharge upon a freshly evaporated film of aluminum yielded a negligibly small decrease in the photoelectric current. An extended set of such tests which had been planned were prevented by the exhaustion of the aluminum in the spirals.

Effect of hydrogen glow discharges on complex surfaces

Pure aluminum was deposited on the target by slow evaporation in a high vacuum (10^{-6} mm Hg) and the new surface was then sensitized by admission of air in minute quantities. The procedure and the results were similar to those obtained by Cashman and Huxford[4] on the sensitization of magnesium by air and oxygen. Successive admissions of air up to the pressure 10^{-3} mm Hg increased the photo-current to a value about 800 times that obtained from the original un-outgassed specimen. Further additions of air produced a decrease in the emission, the lowest value of the yield being characteristic of aluminum oxide. For the high sensitivity surface the threshold was shifted definitely into the visible region. An attempt to determine the exact threshold by the DuBridge graphical method was unsuccessful, since the data for such a surface do not follow the theoretical curve.

Figure 7 shows the effect of the hydrogen glow discharge upon the emission from an aluminum surface which had been highly sensitized by small amounts of dry air. The effect is a rapid desensitization. Although each successive discharge produced further decrease in the photoelectric

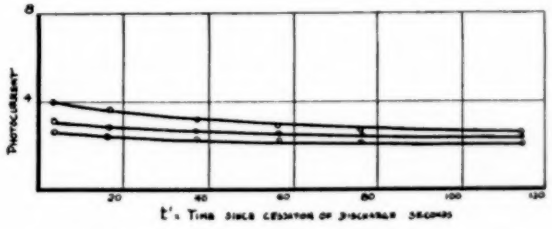

FIG. 6. Decay curves. Aluminum target as anode.

[4] Cashman and Huxford, Phys. Rev. **48**, 734 (1935).

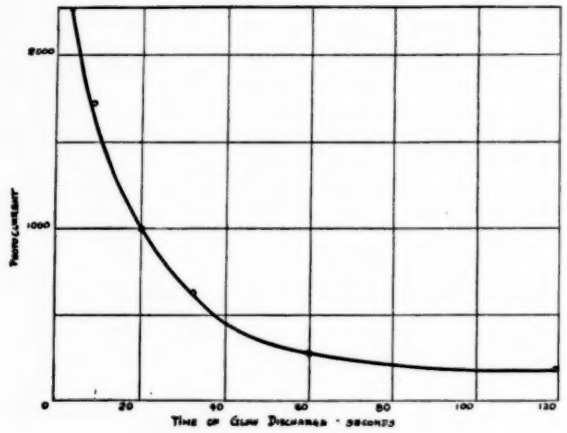

FIG. 7. De-sensitization of an air-sensitized aluminum surface.

current no decay was observed between discharge times. A complete pump-out of the hydrogen was made preceding each measurement of current. With the aluminum surface as anode in the discharge, the same desensitization effect was observed, but to a less marked extent, that is, the slope of the descending curve was less steep.

A surface which had been sensitized by air and subsequently de-sensitized by excess of air was also subjected to the glow discharge. The effect shown in Fig. 8 is a sharp increase to a maximum in the photoemission, followed by a steady decrease down to an end value, at which stage even protracted periods of discharge produced no further variation.

In the process of depositing aluminum by evaporation, the current-thickness curve of Fig. 9 was run. This curve shows a definite film effect with one intermediate maximum point. Readings were made after extended pumping. Analogous results had been observed by Stuhlmann[5] Compton and Ross[6] and others. In some cases a double maximum in the current thickness curve was obtained. The final stationary value of the emission from the freshly evaporated aluminum upon attaining bulk thickness was 135 times that obtained from the original un-outgassed specimen.

Threshold measurements

In the analysis of the current-voltage curves obtained from pure aluminum and from aluminum sensitized by air, the graphical method developed by DuBridge[7] in his theory of the energy distribution of photoelectrons, was applied in order to determine the threshold value. The expression he derived for the slope and tail of the curves of Figs. 10 and 11 is,

$$\log (I/x) = B + f(x - x_0),$$

where I is the photo-current, B a constant (including the temperature constant),

$$x_0 = V_m e/kT$$

and $$f(x-x_0) = \log \left[e^{-(x-x_0)} - \tfrac{1}{4} e^{-2(x-x_0)}\right].$$

Plotting $f(x-x_0)$ *vs.* (x_0-x) yields a theoretical curve of the same form as that obtained experimentally by plotting $\log (I/x)$ *vs.* x. To bring the curves into coincidence a vertical and a horizontal shift are needed, the latter being x_0 from which V_m the maximum energy at 0°K, and also ν_0, the photoelectric threshold, are determined.

An attempt to apply the theory to the curve of Fig. 10, obtained from an aluminum surface

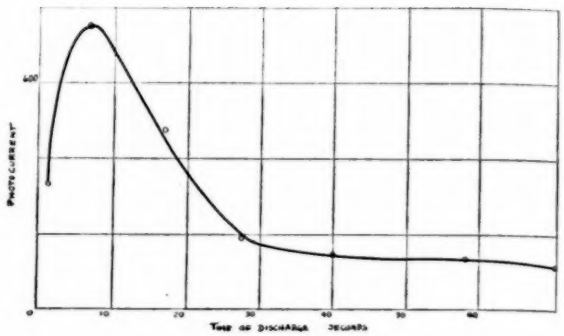

FIG. 8. Effect of the hydrogen glow discharge on a low sensitivity complex aluminum surface.

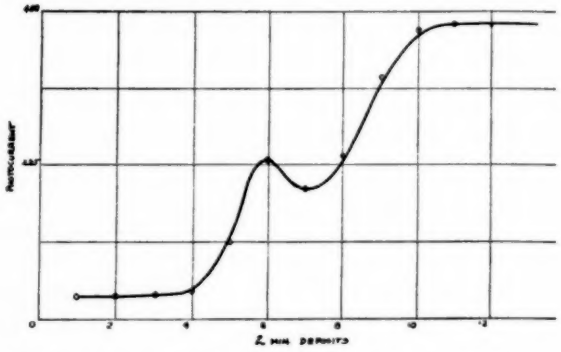

FIG. 9. Variation in photoemission with film thickness. Freshly distilled aluminum.

[5] Stuhlmann, Phys. Rev. **13**, 109 (1919).
[6] Compton and Ross, Phys. Rev. **13**, 374 (1919); Rosenthal, Zeits. f. Physik **99**, 607 (1931).
[7] DuBridge, Phys. Rev. **43**, 726 (1933).

sensitized by air, failed completely. It was not found possible to fit the experimental curve upon the theoretical. This curve exhibits the long "tail" which was found by Roehr[8] and others to be characteristic of high temperatures as well as of contaminated surfaces.

The Fig. 11 measurements were made using freshly evaporated aluminum, approaching bulk thickness, as the photoelectric emitter. The result of the DuBridge analysis is shown in Fig. 12. Although the experimental and theoretical curves do not coincide as closely as those obtained by Roehr in his analysis of molybdenum, nevertheless the agreement is good, considering the small number of readings taken and the fact that the incident light was only approximately monochromatic. The results seem to justify the conclusion that at 300°K the DuBridge theory is valid for a pure aluminum surface but not for the complex surfaces produced by air sensitization. The photoelectric threshold of aluminum as determined by the analysis was 2840A, in good agreement with recent measurements by Gaviola and Strong.[9]

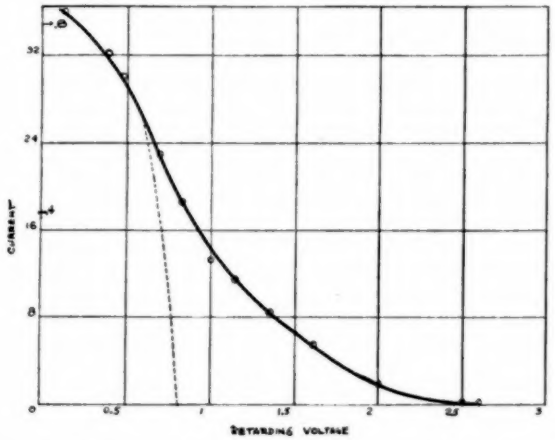

FIG. 10. Current-voltage curve. Complex aluminum surface.

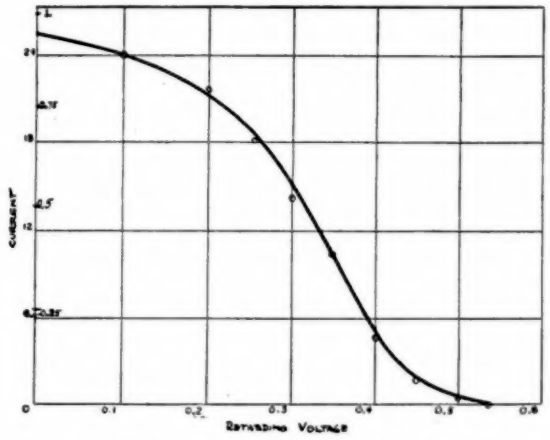

FIG. 11. Current-voltage curve for freshly evaporated aluminum.

INTERPRETATION OF RESULTS

Any attempt to picture the processes involved in the sensitization of aluminum by hydrogen glow discharges must take into account these possibilities:

1. A clean-up of the surface by dissociation of the aluminum oxide coating.
2. The sputtering effect, producing detachment of neutral aluminum atoms.
3. The formation of compounds of aluminum, oxygen and hydrogen.

All of these factors may enter into the process under a given set of conditions; or one may predominate to the practical exclusion of the others. The experiments on sensitizing unoutgassed aluminum, (Fig. 3) suggest that here the predominant action is the dissociation of surface oxide molecules, exposing more pure aluminum. This clean-up action should then proceed as the sensitization time is increased, until the photoemission reached is that of pure aluminum. This upper limit was never actually attained in the experiments described, but could be approached by longer treatment.

The temporary nature of the sensitization of an

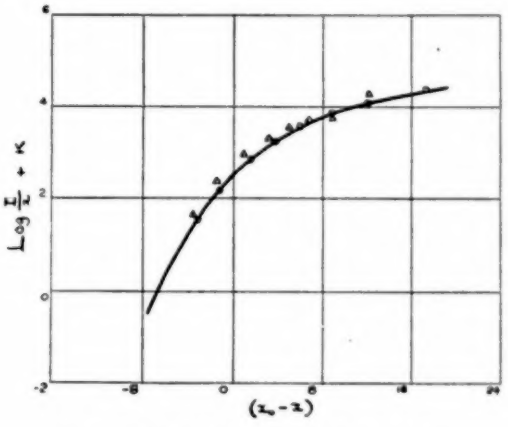

FIG. 12. DuBridge analysis for freshly evaporated aluminum.

[8] Roehr, Phys. Rev. **44**, 866 (1933).

[9] Gaviola and Strong, Phys. Rev. **49**, 441 (1936).

un-outgassed target may be attributed to the diffusion to the surface, of the oxygen contained within the body of the untreated metal. This is borne out by the fact that after the un-outgassed metal had been covered by a layer of fresh aluminum the decay ceased.

The current-pressure curves (Fig. 5), reveal the inefficiency of the higher pressures as well as the existence of an optimum pressure in producing sensitization. If the process is predominantly one of dissociation a fixed minimum amount of energy for dissociation is required. At the higher pressures, the bombarding hydrogen ions are relatively numerous but the velocity over the small mean free path is not sufficient. The optimum pressure would be that at which there would exist the largest number of hydrogen ions, each possessing energy sufficient to break up the surface molecules. In the light of this minimum energy requisite, the ineffectiveness of the discharge with the target as anode is also understandable. Dember[10] observed an increase in the photo-current from aluminum bombarded by electrons from a heated filament. This effect, however, took place only with light shining and electron stream bombarding simultaneously.

The phenomena observed in the experiments on the sensitization of pure aluminum by oxygen are in good accord with the similar observations on uranium, caesium, thorium[11] and magnesium[12] by other investigators. The results may be explained by assuming that the surface produced is one characterized by a sparse distribution of isolated aluminum atoms bound on all sides by aluminum oxide molecules; that is, the type of surface described by de Boer[13] and Kluge and Rupp[14] for alkali-metals and subsequently referred to as the "sensitive spot" type. For a pure surface with a Fermi distribution of electrons, the photo-current should be relatively low, since only the electrons in the highest states are available for ejection. In the complex surface produced by air-sensitization no Fermi distribution exists in the surface layer—individual atoms are exposed. Every quantum absorbed by these isolated atoms would free an electron either downward into the metal or outwards. This one-in-two chance is however greatly diminished by the fact that the great majority of incident quanta are absorbed not by the aluminum atoms but by the aluminum oxide whose work function is relatively high.

Either a detachment of these "sensitive spots" in the complex surface or their widening by dissociation of the surrounding aluminum oxide molecules should produce a decrease in the emission probability. The descending curve of Fig. 7 thus fits well into this tentative picture of the process. The sputtering effect, producing detachment of aluminum atoms may be the major factor in this case—the dissociation effect playing only a supporting role.

The rise and fall of sensitivity in the experiment on the effect of the glow discharge upon a surface desensitized by excess of air (Fig. 8) may be explained by assuming that the discharge first removes excess oxygen exposing individual atoms, and then detaches these by sputtering. Further discharges produce a decrease in the current down to a low limiting value, where the sensitivity remains constant, unaffected even by prolonged discharges. From the present results, the chemical nature of the photoelectrically insensitive end-product cannot be determined. A clue to its identity would probably be found in the exact measurement of the variations in threshold value.

The assumption that the complex surface formed by oxygen sensitization is of the "sensitive spot" type is in harmony with the current-voltage analyses. For the pure aluminum curve of Fig. 11 analysis yielded the agreement predicted by the DuBridge theory based on the Fermi distribution. No such agreement between the experimental and theoretical curves for air-sensitized aluminum could be found; indeed none is predicted by the DuBridge theory, since the Fermi distribution upon which the theory is based does not here exist.

In conclusion the author wishes to express his grateful appreciation to Dr. J. J. Brady who proposed this problem and whose helpful suggestions were of great value throughout the investigation.

[10] Dember, Zeits. f. Physik **33**, 529 (1925).
[11] Rentschler and Henry, J. Opt. Soc. Am. **26**, 30 (1936).
[12] Cashman and Huxford, Phys. Rev. **48**, 734 (1935).
[13] De Boer, *Electron Emission and Absorption Phenomena*, p. 210.
[14] Kluge and Rupp, Physik. Zeits. **32**, 163 (1931).

The Effect of Cathode Material on the Second Townsend Coefficient for Ionization by Collision in Pure and Contaminated N_2 Gas

W. E. Bowls
University of California, Berkeley, California
(Received November 1, 1937)

Experiments for the measurement of the Townsend coefficients for ionization by collision were performed on pure N_2 and N_2 contaminated with Na vapor and Hg vapor. Cathodes of Pt, Na, and Hg were used. Values of α/p in N_2 contaminated with Hg vapor agree with the values found by previous investigators using N_2 of similar purity. With pure N_2 at the lower pressures and higher X/p, the values were seventeen percent lower than the corresponding values in the Hg contaminated N_2. At high pressure and low X/p, the curves differed by relatively little. With Na contamination which may have been accompanied by H_2 contamination, a larger increase in α/p was observed, which amounted at low pressure and high X/p to as much as twenty-four percent higher than the value for the pure N_2. The high value of α/p for Hg contaminated N_2 is explained as being partly due to the direct ionization of Hg vapor atoms by electrons and partly being due to the action of metastable N_2 molecules on Hg. Imprisoned radiation is probably not an important factor. Because of the low vapor pressure of the Na, the direct electron ionization and the ionization by metastable molecules can hardly be invoked to explain the increase in α/p. One must conclude either that the vapor pressure of the Na at room temperature is far above the extrapolated values taken from tables, which is unlikely, or that H_2 introduced in the distillation of Na or N_2 make a volatile compound with Na under excitation or action of ultraviolet light. The shapes of the β/p curves plotted as $f(X/p)$ show abrupt rises at certain values of X/p, definite plateaus, and subsequent gradual increases. These effects have not been observed in previous investigations where Hg contamination predominates, those curves rising asymptotically. Greater significance attaches to the $\beta/\alpha=\gamma=\eta\theta g/\alpha$ curves, which in the case of Pt and Na rise abruptly from zero at a given X/p to a high peak, then fall abruptly and rise again gradually at higher X/p. The rise for the Pt electrode at $X/p=60$ is sharp and occurs at a much lower X/p than any previously observed when low electron current densities are used. The curve with the Na cathode rises at a *higher* X/p than that for Pt to a lower maximum and then, after a fall, rises again. This is surprising, in view of the fact that the Na surface has a far lower work function and far greater photoelectric efficiency than Pt. The sharp peak in pure N_2 is ascribed to the action of radiation either via metastable molecules or by some other mechanism in liberating electrons from the cathode. In the presence of either Hg or Na vapor (possibly contaminated with H_2), the metastable or radiative action is completely destroyed, the energy going to the ionization of the Hg or of the Na and H_2 atoms, if present. In the case of Na, it is possible that only the lower energy states are destroyed so that some of the higher energy states are able to reach the Na cathode. Hence, the small peak at higher X/p with Na. Deducting the peaks leads to curves for Na and Pt and to a lesser extent Hg which intercept the axis at an X/p between 200 and 300. In this region, positive ions have an energy of the order of between two and five volts. Such ions can liberate secondary electrons from the cathode, and we have the effect of a true γ.

Introduction

DESPITE the many studies made on the Townsend coefficients α and β for ionization by collision in gases, practically none of the work except that done by Penning[1-3] and his associates has been carried out in such a fashion as certainly to avoid contamination of the gases by Hg vapor. Owing to the use of mercury gauges in measurements of pressure and the evacuation techniques in filling the chambers with otherwise pure gases, this contamination was unavoidably present to about 10^{-3} mm pressure in all previous work. The effect of mercury vapor on the coefficient α in inert gases has been amply shown by Penning.[4] Furthermore, all electrode surfaces in such gases are coated with monomolecular or thicker layers of Hg as a result of evacuation of the chamber. Hence any value obtained in earlier work for the second coefficient β, which recent work has indicated to be a cathode mechanism, has been that due to a Hg contaminated surface.[5] It is the purpose of this investigation by careful elimination of Hg vapor to determine the second Townsend coefficient β, or better its more significant correlate[5] $\gamma=\beta/\alpha$ for surfaces of Pt and Pt coated with Na in a molecular gas, N_2. The choice of N_2 was in a

[1] Kruithof and Penning, Physica **3**, 515 (1936).
[2] Kruithof and Penning, Physica **4**, 430 (1937).
[3] Kruithof and Druyvesteyn, Physica **4**, 450 (1937).
[4] F. M. Penning, Phil. Mag. **11**, 979 (1931).
[5] L. B. Loeb, Rev. Mod. Phys. **8**, 267 (1936).

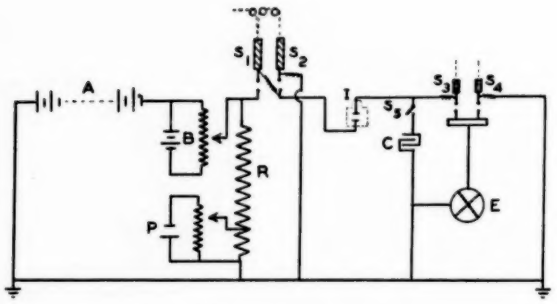

FIG. 1. Diagram of apparatus.

sense unfortunate since N_2 has metastable and active states which complicate the results. Had the importance of these states been recognized at the start the gas used would have been H_2 which is now under investigation in this laboratory instead of N_2.

APPARATUS AND EXPERIMENTAL PROCEDURE

The experimental arrangement is shown in Fig. 1. The potential was supplied by a bank of batteries, *A*. The positive side was connected to ground and the negative side to one fixed terminal of a slide wire rheostat, *B*. A few cells were connected across the rheostat and the sliding contact was connected to the illuminated plate of the ionization chamber through the switch, S_1. The potential was measured by means of a standard cell, the resistance *R* and the potentiometer *P*. The resistances of the plug box, ratio box, and potentiometer and the e.m.f. of the standard cell were accurate to within a few one-hundredths of one percent. Switches S_1 and S_2 were used to connect the cathode of the ionization chamber *I* either to the potential source or to ground. Both were fitted with platinum contacts and mechanically connected so that when one opened the other closed. Switch S_3 connected the anode of the ionization chamber to the electrometer. Under the system of measurement used by the writer S_3 was kept closed but was used in testing for electrical leaks. Switch S_4 was connected to ground and was used during the application of potential to the chamber and was also used to remove charge from the electrometer. Switch S_5 was used to connect the sulphur-insulated cylindrical condenser *C* in parallel with the electrometer when the ionization currents became large. The ionization currents were measured by the rate of deflection method using the quadrant electrometer *E*. As a result of varying the capacity and the interval of making measurements, currents ranging from 3×10^{-14} to 2×10^{-11} amperes were capable of being measured.

The ionization chamber is shown in detail in Fig. 2. The internal parts of the chamber were electrically shielded from the glass walls by the monel metal screen *A*, which was connected to ground. The cathode *B* was 3.8 centimeters in diameter. The cathode consisted of a 0.007″ platinum surface mounted on a quartz plate. The anode *D* was made of nickel and was of the same diameter as the cathode. It was supported by the threaded rod *E*. This rod was connected at its upper end to the iron armature *F* by means of the threaded arms *a*. The armature was held at a constant height by the hollow cylinder *H*, concentric with the hollow cylinder *I* inside of which the rod moved. The armature was turned by an electromagnet. The rod *E* was kept from turning by a set screw *K* which fitted in a vertical slot in the rod. By these arrangements the anode could be set at any desired distance from the cathode. The plates were parallel to within a few tenths of one percent. The plate separation was read through a plane glass window with the aid of a cathetometer. Tube *M* contained the capsule *N*, into which sodium had been distilled, and the ballbearing *R* used for breaking the capsule. The ultraviolet radiation entered through a quartz window and fell on the lower plate.

Before the chamber was assembled, its glass and metal parts were cleaned with acid, grain alcohol, and distilled water, and great care was taken to prevent mercury vapor from coming into contact with any of the parts. After the tube was assembled a lubricated Apiezone stopcock was placed between the tube and a liquid-air trap. The stopcock was kept closed at all times unless liquid air completely surrounded the trap. The chamber was outgassed at 375°C for several hours.

During the course of the experiment, mercury was purposely admitted to the chamber. Complete removal of the mercury necessitated dismantling the entire chamber and cleaning each part with concentrated nitric acid.

The sodium used for coating the cathode was

purified by repeated vacuum distillation before it was distilled into the capsule. Although the sodium may not have been absolutely pure, a surface was obtained that was so sensitive to ordinary light that it was necessary to enclose the chamber in a heavy black cloth and to darken the room to prevent photoelectrons from coming from the surface. In addition, the ultraviolet source was replaced by a Mazda lamp to keep the photoelectric current density from becoming large enough to cause space charge distortion.[6]

The usual source of radiation was a quartz mercury arc operated on 220 volts. A variable aperture was placed near the arc and an image of this aperture was formed at the center of the cathode by a quartz lens. The field between the plates was investigated by means of a full size cross-section model of the plates and found to be sensibly uniform over an area larger than that covered by the ultraviolet light.

Tank nitrogen was passed through a purifying train consisting of heated copper filings, $CaCl_2$, and P_2O_5. It was then passed very slowly through two liquid-air traps and admitted to the chamber. The pressure was measured by a McLeod gauge, which was accurate to one-half of one percent or better. Gas pressures were always reduced to a standard temperature of 22°C and hence all data given in this paper refer to this temperature.

Measurements were made by applying the field and measuring the current by a rate of deflection method. Each current was measured by five deflections which were corrected for leakage currents with no illumination. The usual mean deviation of the five readings was less than one and one-half percent.

The plate separation was varied and similar current measurements were made for the same field strength. The observations usually covered a range of plate separations varying from one to 2.2 cm at intervals of one mm except at the higher plate distances where the intervals were 0.5 mm. In most cases a current was measured for a plate separation within 0.5 mm of sparking. These plate separations were always changed from smaller to larger values.

The sequence of measurements under different conditions were as follows: A few runs using a platinum cathode were first made. Since these indicated a low value of α/p, mercury was admitted and three mercury runs for α/p were taken. The mercury was removed by dismantling and cleaning. The tube was reassembled and runs covering a range of X/p from 65 to 1000 were made. Sodium was then distilled onto the plates and a range of X/p extending from 155 to 1050 was covered. In removing the sodium by use of water, the armature stuck to the threaded rod. The tube was partially dismantled and the armature loosened. After the tube was reassembled, several runs were taken, scattered over the range of 59 to 660. Mercury was then admitted to the chamber and several runs were taken for both α/p and β/p. As a final check the mercury was again removed and two values of α/p and β/p in the lower range of X/p were found for the platinum cathode.

Experimental Results

Curves giving $1/p \log i/i_0$ as a function of plate distance are shown in Figs. 3 and 4. The slopes of the lower portions of these curves give α/p directly.[7] These curves are typical ones

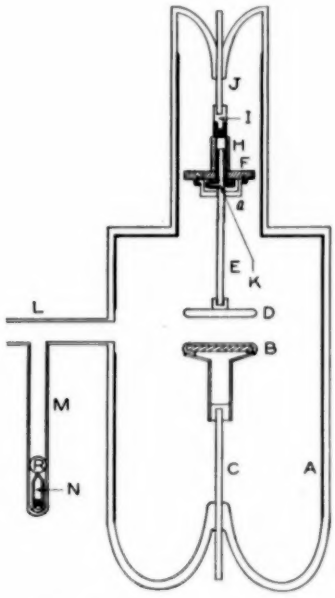

FIG. 2. Ionization chamber.

[6] Varney, White, Loeb and Posin, Phys. Rev. **48**, 818 (1935).

[7] For terminology and the treatment and interpretation of the data the reader is referred to Loeb's summary of this field in Rev. Mod. Phys. **8**, 267 (1936).

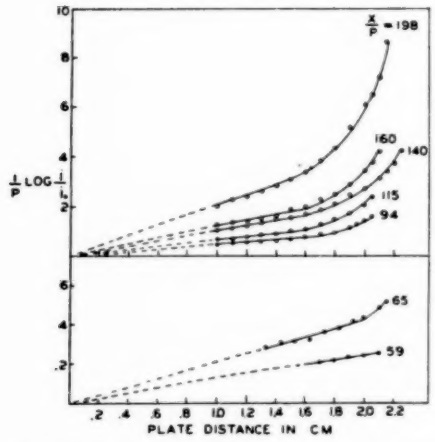

FIG. 3. Curves of various values of X/p from which the value of α/p may be obtained.

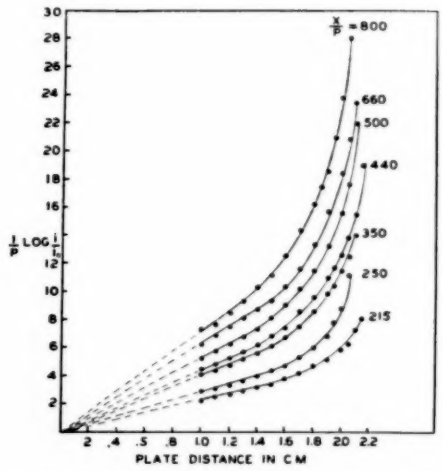

FIG. 4. Curves of various values of X/p from which the value of α/p may be obtained.

obtained with a platinum cathode. Curves of similar forms were obtained for the sodium and mercury covered cathodes. The values of α and of i_0 were determined by the method of least squares from the actual observations, by using data corresponding to the lower parts of the curves, where they are sensibly linear in form. A value of β was obtained for each value of α and i_0 by use of the Townsend equation

$$i = i_0 \frac{(\alpha-\beta)e^{(\alpha-\beta)x}}{\alpha-\beta e^{(\alpha-\beta)x}}.$$ [8]

In general, five to eight values of β were computed from the upcurved portion of the figures. The values of β chosen were *not* least square averages but were determined by the average β that gave the best fit to the observed curves. Similar methods have been used by others.[1, 2]

The first values of α/p that were obtained were several percent lower than corresponding values found by previous investigators. A thorough check of the writer's experimental arrangement and technique of obtaining results was made and no cause for the apparently low values was found. Next, a survey of the literature revealed that mercury was probably present in the ionization chambers of the previous investigators. In the chambers of Townsend and Hurst[9] and of Posin,[10] liquid mercury was present as a necessary part of the chambers. In the papers of Masch,[11] Gill[12] and of Ayres[13] no mention was made of keeping the mercury of the McLeod gauges out of the chambers. While these chambers were evacuated, mercury vapor from the McLeod gauges would have passed into the ionization chambers and contaminated the nitrogen. In order to ascertain if mercury vapor was a contributing factor to the high results of these workers, mercury was admitted to the writer's ionization chamber. The values of α/p then obtained were in close agreement with those of Townsend.

The values of α/p as $f(X/p)$ for the three cathodes investigated are shown in Fig. 5. The

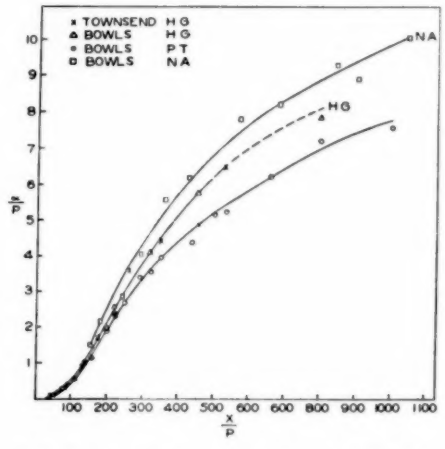

FIG. 5. Values of α/p as a function of X/p.

[8] J. S. Townsend, *Electricity in Gases*.
[9] H. E. Hurst, Phil. Mag. **11**, 535 (1906).
[10] D. Q. Posin, Phys. Rev. **50**, 650 (1936).
[11] K. Masch, Archiv. f. Elek. **26**, 589 (1932).
[12] E. W. Gill, Phil. Mag. **42**, 852 (1921).
[13] T. L. R. Ayres, Phil. Mag. **45**, 353 (1923).

values of Townsend are represented by crosses and the values obtained by the writer for mercury-contaminated nitrogen are represented by triangles. A curve drawn through Townsend's observed points is seen to fit my observations as closely as it fits his. At the lower values of X/p this curve is scarcely distinguishable from my curve for pure nitrogen drawn through the circled observed points. At higher values of X/p the curve for pure nitrogen is as much as seventeen percent lower than the Townsend curve. The results for the case of a sodium cathode are shown as squares. At the higher values of X/p the nitrogen curve is approximately twenty-four percent lower than the sodium curve. The values of α/p in the latter case are more erratic than in the other cases studied. The probable errors are correspondingly larger.

In the case of a platinum cathode a value of β was obtained for an X/p of 65, but no value of β existed at an X/p of 59. These results are shown graphically in Fig. 3. A complete variation of β/p with X/p for the three cathodes is shown in Fig. 6. The same designations are employed as were previously used for α/p.

The variation of $\beta/\alpha=\gamma$ or $\eta\theta g/\alpha$ with X/p is shown in Fig. 7. The values of Posin[6] for a mercury-covered cathode are shown as black circles, and a curve is drawn through his points. The other designations are the same as those previously used.

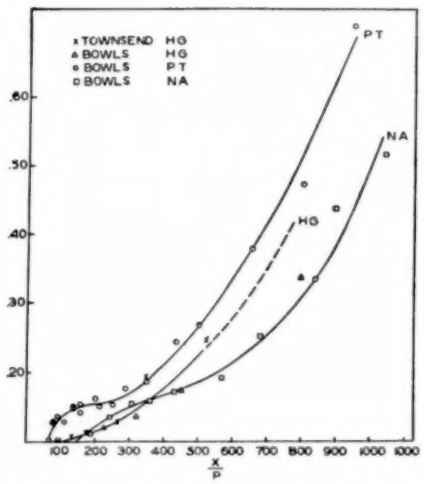

FIG. 6. Values of β/p as a function of X/p. (The circle appearing at an X/p of about 840 on the Na curve should be a square.)

DISCUSSION AND INTERPRETATION

The three methods by which α/p could be increased by the presence of impurities of mercury or sodium vapor in the nitrogen are ionization of the impurity by (1) electron impact, (2) metastable nitrogen, and (3) imprisoned radiation.

MERCURY

1. Quantitative calculations show that the high values of α/p that were obtained when mercury vapor was present may be partly explained as direct ionization of the mercury atoms by electrons. The vapor pressure of mercury at 22°C is 1.43×10^{-3} mm and consequently the number of mercury atoms present in the nitrogen is quite large. Since the first ionization potential of nitrogen is 16.7 volts and that of mercury is 10.4 volts, the latter should show a preferential ionization relative to that for nitrogen despite the paucity of mercury atoms.

The calculations utilized (1) the above data, (2) the efficiencies of ionization of electrons of known energies in nitrogen and mercury vapor as given by P. T. Smith,[14] (3) the Maxwell law of distribution of energies of electrons in an electric field, and (4) the experimental value of Townsend[15] for the average energy of an electron in nitrogen in an electric field.

These calculations showed that direct electron ionization of mercury vapor could account for an increase of α/p of the order of one percent at a

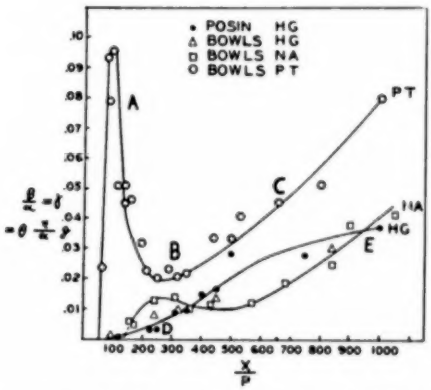

FIG. 7. Values of the ratio β/α as a function of X/p.

[14] P. T. Smith, Phys. Rev. **37**, 808 (1931).
[15] J. S. Townsend, Phil. Mag. **42**, 873 (1921).

value of X/p of 100. At this value of X/p the α/p value for the mixture is higher than that for pure nitrogen by about six percent. We must, however, remember that this result was obtained by assuming a Maxwell distribution of energies. It has been shown in the recent work of Nielsen and Bradbury[16] and H. W. Allen that, depending on the change of electron free paths with energy, the distribution law may be far different from the Maxwell law. Since in nitrogen the Ramsauer free paths vary rapidly with energy, the calculated contribution of mercury to α/p may be too small.

For large values of X/p the gas pressure is smaller than for low values of X/p and therefore the fraction of mercury atoms present in the nitrogen is larger for the high values of X/p. Although the efficiency of ionization in mercury relative to that in nitrogen is less at high values of X/p than it is at low values, calculations showed that because of the fractional increase of mercury atoms the percent contribution of mercury to α/p should be greater for the high values of X/p.

2. Although the energy of the metastable state of the nitrogen molecule that is generally quoted is about 8.2 volts, a value of 9.77 volts is given as the probable energy by Saha and Mathur.[17] The latter value is still too small by 0.62 volt to ionize mercury, but Mulliken[18] has found that energies of 10.4 volts can be transferred by active nitrogen. This latter amount of energy is sufficient to ionize mercury, and it is possible that metastable molecules of nitrogen contribute to the high values of α/p in the case of a mercury contamination. Kruithof[1, 2] and Penning found that the values of α/p in neon containing a small amount of argon were very much higher than the values found in pure neon. As an example of the increase of α/p, the values at $X/p=10$ are chosen. In pure neon the value is 0.050 and in the mixture containing one-tenth percent argon the value is 0.322. This increase was proven to be due to ionization of argon by metastable neon atoms.

If more data regarding the energies and lifetimes of the metastable states of nitrogen were available, calculations could be made to determine the percent contribution of this mechanism to α/p. Since, however, we know nothing about the metastable states we can state only that this mechanism *may* have been active and *could* have been the predominating one. There is evidence that mercury vapor removes some exceedingly active agent instead of permitting it to reach the cathode. This agent cannot be a positive ion and must be either a radiation or a metastable state.

3. There is a possibility of ionization of the mercury vapor by radiation imprisoned in the gas. This process might account for some of the rise of α/p in the mixed gas, but it is the least likely mechanism and may not even exist in nitrogen.

Sodium

The three mechanisms that cause the high values of α/p in the case of a mercury contamination must also be active in the case of a sodium contamination. The problem, however, is complicated in the case of sodium by its exceedingly low vapor pressure at ordinary temperatures. On the other hand, it is simplified by the low ionization potential of sodium (5.12 volts). This potential is so low that there is no doubt as to the ability of metastable and active nitrogen to ionize sodium.

The vapor pressure of sodium is not known at room temperature but estimates place it at about 10^{-10} mm of mercury. This means that there are present only 10^6 atoms of sodium per cm^3. For this reason ionization of the sodium vapor by electron impact can contribute very little to the value of α/p in spite of the low ionization potential. Ionization by imprisoned radiation and metastable ionization may be important but they could not contribute sufficient ionization to cause the observed increases of α/p in the case of the sodium contamination. One might question the validity of the extrapolated value for the vapor pressure of sodium. It is doubtful however if these could be so badly in error as to account for the effects observed with sodium which requires a pressure of at least 10^{-6} mm to be effective.

There is a possibility suggested by N. E. Bradbury that, despite repeated fractional distil-

[16] Nielsen and Bradbury, Phys. Rev. **51**, 69 (1937): Phys. Rev. **50**, 950 (1936).
[17] Saha and Mathur, Proc. Nat. Acad. Sc. India **6**, 120 (1936).
[18] R. S. Mulliken, Phys. Rev. **32**, 186 (1928).

lation of the Na in vacuum, it still carried with it some H_2 gas. The danger of contamination by H_2 from the Na is sufficiently well known so that one cannot ignore the possibility. With the technique of filling the chamber, it would not have been impossible to have had 10^{-5} to 10^{-6} mm pressure of H_2 gas present in the N_2 as a result of distillation of Na into the chamber. According to Joseph Kaplan, H_2 is a most active agent in destroying the metastable states of N_2. In the present chamber with baking out and in the absence of Na the chance of H_2 contamination is small. The distillation of the Na, however, could introduce the pressure of H_2 suggested. H_2 ionizes at 15.3 volts and dissociates at 4.36 volts. H is ionized at 10.3 volts. It is clear that the H_2 cannot be directly much more effectively ionized by electron impact than N_2 of ionization potential 16.7 volts. Nor can H_2 be ionized directly by metastable states in N_2. Hence, one cannot ascribe the increase in α to the direct ionization of H_2 by electron impact or metastables, as was possibly the case with Hg. On the other hand with many metastables the H_2 could be completely dissociated by the N_2 metastables of low energy. The metastables of higher energy could ionize the H atoms, or, if these were present in appreciable numbers, they might be ionized by electron impact more effectively than is N_2. In this fashion, it is conceivable that α in N_2 in the presence of Na with its H_2 contamination could be increased above that in the absence of Na.

While the process suggested may seem somewhat unlikely, it is, if one accepts the low concentration of Na atoms, the only possible way to account for the increase of α with Na in N_2.*

The Significance of β

By referring to Fig. 6, we see that the β/p curve for platinum differs greatly from the curves for mercury and sodium. The platinum curve starts at an X/p of about 65 and rises rather abruptly to a plateau extending from 140 to 240. The spread of values in this region is rather large but a sufficient number of points was obtained to indicate a definite flattening of the curve. The rise at an X/p of 65 was unexpected because of the fact that other observers had not obtained a measurable β below 100. Townsend had observed a slight departure from ionization by electrons alone, as low as 44, but stated that β was very small and the first numerical value quoted by him was for an X/p of 131. Posin[6] had obtained a value of β at 100. No one had observed a flattening of the curve. At the high values of X/p the curve for platinum lies above the other curves and is of the same form as those found by previous investigators.

The curve for sodium starts at an X/p of about 140 or possibly somewhat lower. There appears to be a plateau, after the gradual rise of β/p, extending from 300 to 350. In general, the sodium curve rises more slowly than the platinum one and the β/p values are very much smaller than for platinum.

The mercury curve is typical of the results obtained by former investigators,[6, 8] regardless of the apparent material of the cathode, since a mercury coating was probably always present on the cathode. The data of Townsend were somewhat erratic at the higher values of X/p. At the lower values the writer's results lay on the Townsend curve. The results were higher than those obtained by Posin, who used a brass cathode heavily coated with Hg. The differences in the shapes of the β/p curves for different cathode materials indicate that *the secondary ionizing mechanism is not ionization by positive ions in the gas*. This is in agreement with the cumulative evidence from other fields, which indicates that under the conditions of these experiments a positive ion cannot possibly gain enough energy to ionize a gas molecule.[5, 19, 20] Other mechanisms must, therefore, be considered.

Cathode Mechanisms

For the discussion of these mechanisms, considerations presented by Loeb[5] show that we

* *Note added in proof.*—The results of Florence Ehrenkrantz on sparking potentials in N_2 with Na and Pt electrodes in progress here are in perfect agreement with these findings. Miss Ehrenkrantz has just shown that contamination of pure N_2 with Hg free Pt electrodes by up to 5 percent H_2 does not alter the sparking potential appreciably. Thus H_2 in the absence of Na cannot cause the increase of α observed. The results indicate the presence of some volatile Na compound formed in the process of sparking.

[19] Holst and Oosterhuis, Phil. Mag. **46**, 1117 (1923).

[20] Sutton and Mouzon, Phys. Rev. **35**, 695 (1930); O. Beeck, Physik. Zeits. **35**, 36 (1934); R. N. Varney, Phys. Rev. **47**, 483 (1935).

should plot $\beta/\alpha=\gamma=\eta\theta g/\alpha$ as a function of X/p, representing electron liberation at the cathode by positive ion impact (γ) or photoelectric liberation at the cathode ($\eta\theta g/\alpha$). By referring to Fig. 7, we see quite striking curves for the variation of γ or $\eta\theta g/\alpha$ with X/p. The curve for platinum rises steeply at low values of X/p. A sharp peak is reached at about 100. The curve then falls rapidly until it arrives at the X/p region of 240. It then rises more slowly with increasing values of X/p. The sodium curve rises less steeply and at higher values of X/p. The peak is broader and very much lower. The gradual rise resembles that of platinum. Complete curves of this character have never been observed previously. The curves of Penning and his co-workers, however, indicate that such a peak exists at low values of X/p for both very pure neon and very pure argon. The values of γ or $\eta\theta g/\alpha$ observed by the writer for the mercury surface agree fairly well with those of Posin.

The average *electron* energy at which the platinum curve first rises is about 4.8 volts.[16] At this average energy value the probability of ionizing nitrogen will be distinctly smaller than the probability of exciting it. As the values of X/p increase the average electron energy increases and the probability of excitation increases relative to the probability of ionization. When still higher values of X/p are reached, the probability of ionization increases relative to the probability of excitation. Under these conditions θ/α should at first rise and then decline with increasing X/p. It is likely that the point at which θ/α decreases is at considerably higher energies than the point $X/p=100$ at which the curve begins to decline. It is, therefore, doubtful whether the expected behavior of θ/α will account for the curve observed for a platinum cathode. Again, because of the absence of experimental data on the relative values of θ and α and a distribution of electron energies in nitrogen, we are unable to speculate further regarding this matter.

The curves of Penning[1–3] and his co-workers were obtained by using pure neon and pure argon, and copper cathodes. The current densities of the order of 10^{-8} amp./cm^2 used in the experiments were so high that really accurate values of γ could not have been obtained because of space charge distortion. It was, furthermore, impossible in these experiments to evaluate γ in the X/p region equivalent to low values of X/p in nitrogen.

Penning's curves in argon and in neon indicated a behavior similar to that in the region *ABC* of the curve for platinum. With the introduction of a small amount of argon to the neon, the curve partook characteristically of the shape of my mercury curve between *D* and *E*. It is thus seen that with the removal of the neon metastable atoms as a result of impact with the argon atoms, the shape of the curve changed and the values of γ were less than they had been in pure neon.

It is, therefore, not unreasonable to assume that in the present experiments the peak at low values of X/p in the absence of mercury is due to some action at the cathode depending on excited molecules. The effect of adding mercury was to destroy the ionizing agent (imprisoned radiation or metastable molecules) before it reached the cathode. That this action took place was also indicated by the increase in α/p with the addition of mercury vapor.

In the case of sodium the resulting γ curve is quite surprising. A sodium coated surface in vacuum has a work function of the order of two volts whereas that of platinum is about 4.8 volts. One would, therefore, have expected an enormous photoelectric liberation from the sodium surface relative to that from platinum. That the surface of the cathode was effectively coated and that it had a low work function was shown by the copious electron emission when light from a Mazda lamp was incident on the surface.

The curve for sodium does show an effect similar to that found in the case of platinum, but it rises at a higher energy and has a much lower and broader peak. It is possible to ascribe the shift of the peak toward higher energies to the great efficiency of sodium vapor in destroying the low energy states and so the soft radiation, and to ascribe the appearance of the small peak to the ability of high energy states and hard radiation to reach the cathode.

In view of the small concentration of Na vapor, the action suggested above might be questioned. It is, however, possible that with

the Na there was present perhaps as much as 10^{-5} mm pressure of H_2. The possibility of some contamination by H_2 is indicated by the extreme photosensitivity of the Na coated cathode. Such activity in photo-cells is indicative of hydride formation on the Na surface. In any case, it would not be difficult to ascribe a very material destruction of the N_2 excited and metastable states which could have been active at the cathode in the absence of Na to the presence of H_2 contamination.

When the effects of the peaks are deducted, all of the curves indicate a rise from zero that is fairly sharp and in the X/p region between 200 and 300. In this region the positive ions strike the cathode with energies in the range of two to five volts. It is natural to ascribe these rises to positive ion bombardment of the cathodes. These rises, then, represent the true γ proposed by Townsend and Thomson and strongly favored by Holst, Oosterhuis, Penning and Druyvesteyn.

In conclusion the writer desires to express his thanks to Professor L. B. Loeb under whose direction this work was done, for his guidance in its prosecution and for his aid in the interpretation of the results. His thanks are also due to Mr. W. R. Stamper for his aid in the construction of the apparatus.

FEBRUARY 15, 1938 PHYSICAL REVIEW VOLUME 53

Magnetic Interaction in Homogeneously Strained Ferromagnetic Crystals

L. W. McKeehan
Sloane Physics Laboratory, Yale University, New Haven, Connecticut

(Received January 3, 1938)

A well-known method of computing magnetostrains, as the strains necessary to minimize the sum of magnetic and elastic potential energies, is improved in detail, extended to include terms dependent upon the structure of atomic magnets, and is applied in the cases of body-centered cubic iron, face-centered cubic nickel and hexagonal close-packed cobalt. It is shown that magnetostriction is not important in fixing directions of easiest magnetization in these crystals.

IN a crystal composed of atoms having permanent magnetic moments the potential energy density includes terms depending upon these moments and upon their mean relative positions. Such magnetic terms are therefore strain-sensitive. The potential energy density also contains terms depending only upon the strain components of any existing strain and upon the several elastic moduli characteristic of the crystal. It is apparent, therefore, that a crystal under no applied forces will assume whatever state of strain and magnetization that may be required to make the sum of its magnetic and elastic potential energies minimum. If both strain and magnetization are uniform throughout the crystal the total potential energy is proportional to the potential energy density, also homogeneous, which will be denoted by E.

In nonferromagnetic crystals the magnetization under no forces will be zero and the self-imposed strain associated with the presence of atomic magnets cannot be separated from strains associated with other interatomic forces. In a ferromagnetic crystal the magnetization persists under no applied magnetic forces, so that the equilibrium between magnetic and elastic forces can be investigated. The magnetic part of the energy E, say E_m, will in general depend upon the direction along which the axes of the atomic magnets are lined up, that is upon the unit vector $\mathbf{p}$ in the direction of magnetization. In one case of great interest E_m seems at first glance to be independent of $\mathbf{p}$.

If the atomic magnets are magnetic dipoles (point magnets) and if their loci have strictly cubic symmetry, E_m in an unbounded crystal is independent of $\mathbf{p}$. As Akulov[1] first pointed out, this equilibrium at zero strain is unstable. If the elastic potential energy is denoted by E_e the

[1] N. S. Akulov, Zeits. f. Physik **52**, 389–405 (1928).

state of affairs gives $E_m=0$ and $E_e=0$ so that $E_m+E_e=0$. But E_m is a linear function of strain components, E_e is a quadratic function, so that a type of strain can always be found for which E_m begins to grow negatively faster than E_e grows positively, so that $E_m+E_e<0$ for small strains of this type. The same difference in the functions E_m and E_e ensures that a limiting strain will be reached, so that E_m+E_e will always have a minimum. At this minimum it is easy to see that $E_m=-2E_e$. It is also clear that the necessary strain (magnetostrain) will not be a mere dilatation.

In the absence of an applied magnetic field, $\mathbf{p}$ will automatically find one of the so-called directions of easiest magnetization, for which the minimum in (E_m+E_e) is lowest. In a magnetic field $\mathbf{H}_a$ not along one of the directions of easiest magnetization the potential energy density contains the additional term $-(\mathbf{H}_a\cdot\mathbf{I})=-(\mathbf{H}_a\cdot\mathbf{p})I$ and a different state of strain will be necessary to minimize

$$E=E_m+E_e-(\mathbf{H}_a\cdot\mathbf{p})I. \tag{1}$$

For random directions of $\mathbf{H}_a$ the problem is complicated by the difficulty of finding the equilibrium direction for $\mathbf{p}$, which is explicitly involved in the last term on the right-hand side of Eq. (1), implicitly in E_m. If $\mathbf{H}_a$ is along any axis of symmetry in the crystal it is possible to find a magnitude for H_a high enough to keep $\mathbf{p}$ parallel to $\mathbf{H}_a$. Under these conditions it is only necessary to minimize (E_m+E_e) with $\mathbf{p}$ constant.

In noncubic dipole arrays and in all cases where atomic magnets are more extensive than dipoles E_m is no longer zero at zero strain for all directions of $\mathbf{p}$. Denote its more general value at zero strain by ${}_0E_m$.

In an earlier paper,[2] hereafter designated as l.c., formulae for ${}_0E_m$, there called E, are given for cubic and hexagonal crystals with atomic magnets more complicated than dipoles, and distributions of magnetic moment making differences in ${}_0E_m$ fairly consistent with observed differences in (E_m+E_e) for various important directions of $\mathbf{p}$ in iron, nickel, cobalt and some of their alloys, are suggested. In this analysis the quantities compared actually differed by $(E_m-{}_0E_m+E_e)=-E_e$, and it was pointed out in l.c.[2] that including this difference might somewhat alter the results there presented. The present analysis allows a direct computation of the magnetostrain as above defined and shows that the error committed in ignoring $-E_e$ was actually negligible.

The method here used for computing E_m is based upon that of Akulov,[1] and is straightforward. We start with Eq. (6) of l.c.,[2] omit sextupole terms to shorten subsequent work, and have

$${}_0E_m=-(NP^2/Va^3)[F_2S_2+F_4S_4]. \tag{2}$$

Then in general

$$E_m=(1+\mathbf{A})_0E_m, \tag{3}$$

where $\mathbf{A}$ is an operator equivalent to the application of a homogeneous strain of tensor components, A_{ii}, A_{ij}. The convention regarding subscripts is that i, j, k always refer to different rectangular coordinate axes, as many of which as possible are chosen parallel to crystallographic axes. This necessitates writing both A_{ii} and A_{ij} for the unrestricted tensor component. Furthermore, each permutation of subscripts is counted separately, so that, for example, $\sum A_{ij}$ contains six terms rather than three.

In the notation of Eqs. (2) and (3) what Akulov really did was to compute an energy density

$${}_VE_m=-(NP^2/V)(1+\mathbf{A})(a^{-3}F_2S_2). \tag{4}$$

This amounts to supposing that the volume, V, of a unit cell of the space-lattice remains unaltered no matter how its dimensions are changed by straining. In first recomputation of the coefficients appearing in E_m this procedure was followed,[3] but now the more logical procedure of Eq. (3), in which V may vary, is preferred.

Both S_2 and S_4 are put into rapidly convergent forms before operator $\mathbf{A}$ is applied. The magnetic moment per atom, P, and its distribution about the atom center, which fixes F_4, are regarded as invariant under $\mathbf{A}$. The integers N and $F_2(=1)$ are naturally also invariant. The assumption that P is unaffected by strain re-

[2] L. W. McKeehan, Phys. Rev. **52**, 18–30, 527 (1937). It may be noted, though unimportant here, that Eq. (29a) really gives $(21/20)S_{60}$, Eq. (29b) gives $(99/10)S_{60}$, not S_{60} in each case as printed.

[3] L. W. McKeehan, Phys. Rev. **43**, 1022–1024 (1933).

TABLE I. (Part 1) *Formula for the coefficients of* S_{2+}.

$\gamma_1 = \epsilon^3 \Sigma n_r g_1(x)$
$\gamma_2 = \epsilon^3 \Sigma n_r x^2 g_2(x)$
$\gamma_3 = \epsilon^3 \Sigma n_r x^4 g_3(x)$
$\gamma_4 = \epsilon^3 \Sigma n_r [r_i^2 r_j^2]^* r^{-4} x^4 g_3(x)$
$\gamma_5 = \epsilon^3/3(\pi)^{\frac{1}{2}}$
$\gamma_6 = \pi \Sigma f n_q \exp(-\pi^2 q^2/\epsilon^2)$
$\gamma_7 = \pi \Sigma f n_q (1+\pi^2 q^2/\epsilon^2) \exp(-\pi^2 q^2/\epsilon^2)$
$\gamma_8 = \pi \Sigma f n_q [q_i^2 q_j^2] q^{-4} (1+\pi^2 q^2/\epsilon^2) \exp(-\pi^2 q^2/\epsilon^2)$

Coefficients in Eq. (6)

	γ_1	γ_2	γ_3	γ_4	γ_5	γ_6	γ_7	γ_8
S_{200}	$-1/2$	$+1/6$			$+2$	$-2/3$		
S_{2ii}	$+1/2$			$-1/2$	-2	$+4/3$		-4
S_{21111}		$+1/3$	$-1/6$	$+3/2$		$+4/3$	$-4/3$	$+12$
S_{22323}		$+1/3$		-1		$+4/3$		-8

* Square brackets are used to indicate mean values of the quantities enclosed.

quires further justification. If this be admitted, however, the constancy of F_4 is highly probable.

Equation (3) can be expanded like Eq. (2) so as to separate terms arising in S_2 from those arising in S_4. Thus

$$E_m = -(NP^2/Va^3)[F_2 S_{2A} + F_4 S_{4A}] \qquad (5)$$

where the terms in square brackets are pure numbers, F_2 and F_4 being the same as in Eq. (2). Also as before S_{2A} and S_{4A} can be separated into terms depending upon individual strain components and functions of p_1, p_2, p_3 the components of **p**, that is the direction cosines of the magnetization. The results are, for cubic crystals,

$$S_{2A} = S_{200} + S_{2ii}\sum A_{ii} + S_{21111}\sum A_{ii}p_i^2 + S_{22323}\sum A_{ij}p_i p_j, \qquad (6)$$

TABLE II. *Numerical values of* S_{2+} *and* S_{4+} *for cubic crystals.*

	PRIMITIVE	BODY-CENTERED	FACE-CENTERED
S_{200}	2.0944	4.1888	8.3776
S_{2ii}	-1.0162	-8.1417	-15.9639
S_{21111}	9.5177	-0.7077	-2.3736
S_{22323}	2.1564	-7.9058	-15.1727
S_{400}	3.1082	-3.1065	-7.5257
S_{4ii}	-6.7567	12.9293	0.3118
S_{41111}	27.5736	83.6175	-355.6216
S_{42323}	0.9471	23 7591	-66.4842
$S_{4111111}$	-32.1692	-97.5538	414.8918
$S_{4ii2233}$	9.9984	-53.2277	88.1260
$S_{4232311}$	-6.6296	-166.3138	465.3894

$$S_{4A} = S_{400}\{1-(5/2)\sum p_i^2 p_j^2\} + S_{4ii}\sum A_{ii} + S_{41111}\sum A_{ii}p_i^2 + S_{42323}\sum A_{ij}p_i p_j + S_{4111111}\sum A_{ii}p_i^4 + S_{4ii2233}(\sum A_{ii})\sum p_i^2 p_j^2 + S_{4232311}\sum A_{ij}p_i p_j p_k^2. \qquad (7)$$

Subscripts to S are assigned by adding to 2 or 4 all the subscripts appearing in the unabbreviated first term in the affected sum when arranged in natural cyclic order. Letters ii appear if $(\sum A_{ii})$ is a factor, and terms of this sort have been picked out wherever possible so that the effect of dilatationless strains will be easier to calculate.

All the coefficients S_{2+} and S_{4+} are numbers to be found by suitable summations over the points at which atomic magnets are centered, which usually include points of the space-lattice defining the crystal, and over the points of a lattice reciprocal to that of the crystal. Some of these have been given in l.c.[2] and in previous papers

TABLE I. (Part 2) *Formulas for the coefficients of* S_{4+}.

$\delta_1 = \epsilon^5 \Sigma n_r g_2(x)$
$\delta_2 = \epsilon^5 \Sigma n_r x^2 g_3(x)$
$\delta_3 = \epsilon^5 \Sigma n_r x^4 g_4(x)$
$\delta_4 = \epsilon^5 \Sigma n_r [r_i^2 r_j^2] r^{-4} x^4 g_4(x)$
$\delta_5 = \epsilon^5 \Sigma n_r x^6 g_5(x)$
$\delta_6 = \Sigma^5 \Sigma n_r [r_i^2 r_j^2] r^{-4} x^6 g_5(x)$
$\delta_7 = \epsilon^5 \Sigma n_r r_1^2 r_2^2 r_3^2 r^{-6} x^6 g_6(x)$
$\delta_8 = \epsilon^5/5(\pi)^{\frac{1}{2}}$
$\delta_9 = \pi^3 \Sigma f n_q q^2 \exp(-\pi^2 q^2/\epsilon^2)$
$\delta_{10} = \pi^3 \Sigma f n_q [q_i^2 q_j^2] q^{-2} \exp(-\pi^2 q^2/\epsilon^2)$
$\delta_{11} = \pi^3 \Sigma f n_q q^2 (1+\pi^2 q^2/\epsilon^2) \exp(-\pi^2 q^2/\epsilon^2)$
$\delta_{12} = \pi^3 \Sigma f n_q [q_i^2 q_j^2] q^{-2} (1+\pi^2 q^2/\epsilon^2) \exp(-\pi^2 q^2/\epsilon^2)$
$\delta_{13} = \pi^3 \Sigma f n_q q_1^2 q_2^2 q_3^2 q^{-4} (1+\pi^2 q^2/\epsilon^2) \exp(-\pi^2 q^2/\epsilon^2)$

Coefficients in Eq. (7)

	δ_1	δ_2	δ_3	δ_4	δ_5	δ_6	δ_7	δ_8	δ_9	δ_{10}	δ_{11}	δ_{12}	δ_{13}
S_{400}	$+1/8$	$-1/12$	$+1/72$	$-1/12$				-1	$+2/9$	$-4/3$			
S_{400}			$-1/180$	$+1/12$					$-4/45$	$+4/3$			
S_{4ii}	$-1/8$	$+1/24$	$-1/72$	$+1/3$		$-1/48$	$+1/48$	$+1$	$-4/9$	$+8/3$		$+2/3$	$-2/3$
S_{41111}		$-1/6$	$+1/12$	$-1/4$		$-1/8$	$+3/8$			-8		$+4$	-12
S_{42323}		$-1/6$	$+1/36$	$+7/12$		$-1/12$	$+1/12$		$-4/9$	$-4/3$		$+8/3$	$-8/3$
$S_{4111111}$			$+1/18$	$-5/6$	$-1/72$	$+13/48$	$-7/16$		$-8/9$	$+40/3$	$+4/9$	$-26/3$	$+14$
$S_{4ii2233}$			$+1/72$	$-5/24$		$+1/48$	$-7/48$		$+4/9$	$-20/3$		$-2/3$	$+14/3$
$S_{4232311}$			$-1/36$	$+5/12$		$+1/12$	$-7/12$		$+4/9$	$-20/3$		$-8/3$	$+56/3$

of this series, but formulae for all of them are presented in Table I, Parts 1 and 2 which assigns an abbreviating symbol to each different summation needed and expresses each S in terms of these symbols.

Numerical values of each S are given in Table II for the three cubic arrangements. All values given have been checked to or beyond the last digit here recorded by computations with two different values of ϵ. (Values of S_{200} have also been checked by simpler formulae.)

For hexagonal crystals Eq. (5) splits up differently and yields the following equations:

$$\begin{aligned}S_{2A}&=S_{200}+S_{20033}p_3^2+S_{2ii}\textstyle\sum A_{ii}+S_{233}A_{33}\\&+S_{21111}(A_{11}p_1^2+A_{22}p_2^2)+S_{2ii33}(\textstyle\sum A_{ii})p_3^2\\&+S_{23333}A_{33}p_3^2+S_{21212}(A_{12}+A_{21})p_1p_2\\&+S_{21313}(A_{13}p_1+A_{23}p_2)p_3\\&+S_{23113}(A_{31}p_1+A_{32}p_2)p_3,\end{aligned}\tag{8}$$

$$\begin{aligned}S_{4A}&=\{S_{400}+S_{4ii}\textstyle\sum A_{ii}+S_{433}A_{33}\}\\&\times\{1-10p_3^2+(35/3)p_3^4\}+S_{41111}A_{11}p_1^2\\&+S_{41122}A_{11}p_2^2+S_{41133}A_{11}p_3^2+S_{42211}A_{22}p_1^2\\&+S_{42222}A_{22}p_2^2+S_{42233}A_{22}p_3^2\\&+S_{41212}(A_{12}+A_{21})p_1p_2+S_{41313}(A_{13}p_1+A_{23}p_2)p_3\\&+S_{43113}(A_{31}p_1+A_{32}p_2)p_3+S_{4111111}A_{11}p_1^4\\&+S_{4112222}A_{11}p_2^4+S_{4113333}A_{11}p_3^4\\&+S_{4221111}A_{22}p_1^4+S_{4222222}A_{22}p_2^4\\&+S_{4223333}A_{22}p_3^4+S_{4121112}(A_{12}+A_{21})p_1^3p_2\\&+S_{4121222}(A_{12}+A_{21})p_1p_2^3\\&+S_{4131333}(A_{13}p_1+A_{23}p_2)p_3^3\\&+S_{4311333}(A_{31}p_1+A_{32}p_2)p_3^3.\end{aligned}\tag{9}$$

Not all the coefficients in Eqs. (8) and (9) are unequal, for $S_{21212}=S_{21111}$; $S_{43113}=S_{41212}$; $S_{4221111}=-S_{4111111}$; $S_{4222222}=-S_{4112222}$.

In an earlier paper[4] Akulov's method was carried out, with respect to S_2 only, in hexagonal crystals. The new assumption concerning the variability of V changes several coefficients, so formulae for all the S are here given in Table III, similar in arrangement to Table II. For details of notation consult l.c.[2]

Numerical values for each S have been computed for the particular axial ratio $c=2(6)^{\frac{1}{2}}/3$ appropriate to close-packing of spheres, both for a primitive array and for hexagonal close-packing.

The elastic energy density in cubic crystals is

$$E_e=\tfrac{1}{2}c_{11}\textstyle\sum A_{ii}^2+\tfrac{1}{2}c_{12}\sum A_{ii}A_{jj}+c_{44}\sum A_{ij}^2\tag{10}$$

and in hexagonal crystals is

$$\begin{aligned}E_e&=\tfrac{1}{2}c_{11}(A_{11}^2+A_{22}^2)+\tfrac{1}{2}c_{33}A_{33}^2\\&+\tfrac{1}{2}c_{12}(A_{11}A_{22}+A_{22}A_{11})\\&+\tfrac{1}{2}c_{13}(A_{11}A_{33}+A_{33}A_{11}+A_{22}A_{33}+A_{33}A_{22})\\&+c_{44}(A_{13}^2+A_{31}^2+A_{23}^2+A_{32}^2)\\&+\tfrac{1}{2}(c_{11}-c_{12})(A_{12}^2+A_{21}^2).\end{aligned}\tag{11}$$

The summations in Eq. (10) are to be interpreted like those in preceding equations but c_{11}, c_{12} and c_{44} are the elastic moduli as usually defined with a different rule of summation. This explains the unsymmetrical occurrence of the factor $\frac{1}{2}$ in Eqs. (10), (11).

In the next step we seek tensor components A_{ii}, A_{ij} to minimize E_m+E_0 for various assignments of p_i, p_j, p_k. The work is much simplified by the fact that for directions of $\mathbf{p}$ naturally of interest the crystal and with it the strain tensor $\mathbf{A}$ possess high symmetry. The results are particularly interesting for dilatationless strains. Not only does the number of terms to be considered decrease, but this assumption about $\mathbf{A}$ supports the assumption already made regarding the invariance of P, and is in itself plausible as a first approximation. Experiments usually show small relative changes in volume in applied fields that result in considerable shearing strains. On the theoretical side the enormous molecular field is supposed to be largely affected by small changes in mean interatomic distance. It follows directly that changes in energy resulting from changes in direction of the relatively tiny magnetic fields used in magnetostriction experiments can have little effect on mean interatomic distance, that is, they cannot produce important dilatations. Finally, the assumption that $\sum A_{ii}=0$ makes minimum total energy occur for minimum energy density, a decided simplification.

[4] L. W. McKeehan, Phys. Rev. **43**, 1025–1029 (1933). Eq. (35) should be changed by adding $+H_{1\varphi}$ to the right-hand side.

TABLE III. (Part 1) *Formula for the coefficients of S_{2+} for hexagonal crystals.*

$\eta_1=\epsilon^3\Sigma n_r g_1(x)$
$\eta_2=\epsilon^3\Sigma n_r r_{12}{}^2 r^{-2}x^2 g_2(x)$
$\eta_3=\epsilon^3\Sigma n_r c^2 r_3{}^2 r^{-2}x^2 g_2(x)$
$\eta_4=\epsilon^3\Sigma n_r r_{12}{}^4 r^{-4}x^4 g_3(x)$
$\eta_5=\epsilon^3\Sigma n_r r_{12}{}^2 c^2 r_3{}^2 r^{-4}x^4 g_3(x)$
$\eta_6=\epsilon^3\Sigma n_r c^4 r_3{}^4 r^{-4}x^4 g_3(x)$
$\eta_7=\epsilon^3/3(\pi)^{\frac{1}{2}}$
$\eta_8=(\pi/c\sqrt{3})\Sigma f n_q q_{12}{}^2 q^{-2}\exp(-\pi^2q^2/\epsilon^2)$
$\eta_9=(\pi/c\sqrt{3})\Sigma f n_q c^{-2}q_3{}^2 q^{-2}\exp(-\pi^2q^2/\epsilon^2)$
$\eta_{10}=(\pi/c\sqrt{3})\Sigma f n_q q_{12}{}^4 q^{-4}(1+\pi^2q^2/\epsilon^2)\exp(-\pi^2q^2/\epsilon^2)$
$\eta_{11}=(\pi/c\sqrt{3})\Sigma f n_q q_{12}{}^2 c^{-2}q_3{}^2 q^{-4}(1+\pi^2q^2/\epsilon^2)\exp(-\pi^2q^2/\epsilon^2)$
$\eta_{12}=(\pi/c\sqrt{3})\Sigma f n_q c^{-4}q_3{}^4 q^{-4}(1+\pi^2q^2/\epsilon^2)\exp(-\pi^2q^2/\epsilon^2)$

Coefficients in Eq. (9)

	η_1	η_2	η_3	η_4	η_5	η_6	η_7	η_8	η_9	η_{10}	η_{11}	η_{12}
S_{200}	−1/2	+1/4					+2	−2				
S_{20033}		−1/4	+1/2					+2	−4			
S_{244}	+1/2			−1/16			−2	+4		−1		
S_{233}		−1/4	+1/2	+1/16	−1/4					+1	−4	
S_{21111}		+1/2		−1/8				+4		−2		
S_{24433}		+1/4	−1/2	+1/16	−1/4			−4	+8	+1	−4	
S_{23332}			+1	−1/16	+1/2	−1/2			+8	−1	+8	−8
S_{21313}			+1		−1/2			+4			−8	
S_{23113}		+1/2			−1/2				+8		−8	

TABLE III. (Part 2) *Formula for the coefficients of S_{4+} for hexagonal crystals.*

$\tau_1=\epsilon^5\Sigma n_r g_2(x)$
$\tau_2=\epsilon^5\Sigma n_r r_{12}{}^2 r^{-2}x^2 g_3(x)$
$\tau_3=\epsilon^5\Sigma n_r c^2 r_3{}^2 r^{-2}x^2 g_3(x)$
$\tau_4=\epsilon^5\Sigma n_r r_{12}{}^4 r^{-4}x^4 g_4(x)$
$\tau_5=\epsilon^5\Sigma n_r r_{12}{}^2 c^2 r_3{}^2 r^{-4}x^4 g_4(x)$
$\tau_6=\epsilon^5\Sigma n_r c^4 r_3{}^4 r^{-4}x^4 g_4(x)$
$\tau_7=\epsilon^5\Sigma n_r r_{12}{}^6 r^{-6}x^6 g_5(x)$
$\tau_8=\epsilon^5\Sigma n_r r_1{}^2 r_2{}^2(r_1-r_2)^2 r^{-6}x^6 g_5(x)$
$\tau_9=\epsilon^5\Sigma n_r r_{12}{}^4 c^2 r_3{}^2 r^{-6}x^6 g_5(x)$
$\tau_{10}=\epsilon^5\Sigma n_r r_{12}{}^2 c^4 r_3{}^4 r^{-6}x^6 g_5(x)$
$\tau_{11}=\epsilon^5\Sigma n_r c^6 r_3{}^6 r^{-6}x^6 g_5(x)$
$\tau_{12}=\epsilon^5/5(\pi)^{\frac{1}{2}}$
$\tau_{13}=(\pi^3/c\sqrt{3})\Sigma f n_q q_{12}{}^4 q^{-2}\exp(-\pi^2q^2/\epsilon^2)$
$\tau_{14}=(\pi^3/c\sqrt{3})\Sigma f n_q q_{12}{}^2 c^{-2}q_3{}^2 q^{-2}\exp(-\pi^2q^2/\epsilon^2)$
$\tau_{15}=(\pi^3/c\sqrt{3})\Sigma f n_q c^{-4}q_3{}^4 q^{-2}\exp(-\pi^2q^2/\epsilon^2)$
$\tau_{16}=(\pi^3/c\sqrt{3})\Sigma f n_q q_{12}{}^6 q^{-4}(1+\pi^2q^2/\epsilon^2)\exp(-\pi^2q^2/\epsilon^2)$
$\tau_{17}=(\pi^3/c\sqrt{3})\Sigma f n_q q_1{}^2 q_2{}^2(q_1+q_2)^2 q^{-4}(1+\pi^2q^2/\epsilon^2)\exp(-\pi^2q^2/\epsilon^2)$
$\tau_{18}=(\pi^3/c\sqrt{3})\Sigma f n_q q_{12}{}^4 c^{-2}q_3{}^2 q^{-4}(1+\pi^2q^2/\epsilon^2)\exp(-\pi^2q^2/\epsilon^2)$
$\tau_{19}=(\pi^3/c\sqrt{3})\Sigma f n_q q_{12}{}^2 c^{-4}q_3{}^4 q^{-4}(1+\pi^2q^2/\epsilon^2)\exp(-\pi^2q^2/\epsilon^2)$
$\tau_{20}=(\pi^3/c\sqrt{3})\Sigma f n_q c^{-6}q_3{}^6 q^{-4}(1+\pi^2q^2/\epsilon^2)\exp(-\pi^2q^2/\epsilon^2)$

Coefficients in Eq. (10)

Subscript of S	τ_1	τ_2	τ_3	τ_4	τ_5	τ_6	τ_7	τ_8	τ_9	τ_{10}	τ_{11}	τ_{12}	τ_{13}	τ_{14}	τ_{15}	τ_{16}	τ_{17}	τ_{18}	τ_{19}	τ_{20}
400	+1/8	−1/8		+1/64								−1	+1/2							
400		−1/80	+1/40	+1/320	−1/80								+1/10	−2/5						
400				+3/2240	−3/280	+1/280							+3/70	−12/35	+4/35					
4ii	−3/8		−1/8	+9/64	+1/8		−1/64		−1/64			+3	−5			+1		+1		
4ii		+1/80	−1/40	+1/64	−1/40	−1/40	−1/320		+3/320	+1/80			−1	+4		+1/5		−3/5	−4/5	
4ii				+3/2240	−3/280	+1/280	−3/2240		+3/320	+1/140	−1/280		−3/7	+24/7	−8/7	+3/35		−3/5	−16/35	+8/35
433	+1/4	+1/8		−5/32			+1/64					−2	+4			−1				
433			+1/20	−3/160	+1/40		+1/320		−1/80				+4/5	−12/5		−1/5		+4/5		
433				−3/1120		+1/140	+3/2240		−3/280	+1/280			+12/35	−72/35	+16/35	−3/35		+24/35	−8/35	
41111	+1/4	−3/16	+1/8	−1/32			+3/256	−27/512	−1/64			−2	+3	−4		−1/4	−8	+1		
41122	+1/4	+1/16	+1/8	−3/32	−1/4		+3/256	−27/512	+3/64			−2	+3	+4		−1/4	−8	−3		
41133	+1/4	+1/16	+1/8		−1/4	−1/4	−3/256	+27/512	+3/64	+1/8		−2	−3	+28		+1/4	+8	−3	−8	
42211	+1/4	+1/16	+1/8	−3/32	−1/4		+1/256	+27/512	+3/64			−2	+3	+4		−3/4	+8	−3		
42222	+1/4	−3/16	+1/8	−1/32			+1/256	+27/512	−1/64			−2	+3	−4		−3/4	+8	+1		
42233	+1/4	+1/16	+1/8		−1/4	−1/4	−1/256	−27/512	+3/64	+1/8		−2	−3	+28		+3/4	−8	−3	−8	
41212		−1/4		+1/16	+1/4				−1/16					−8				+4		
41313			−1/2		+1/2				−1/16				−2					+4		
4111111				+1/32	−1/8		−1/96	+9/128	+1/32				−1	+4			+32/3	−2		
4112222				−1/32	+1/8			+9/128	−1/32				+1	−4		−2/3	+32/3	+2		
4113333					+1/8	−1/12	+3/256	−27/512	−3/64	−5/48	+1/24		+3	−28	+32/3	−1/4	−8	+3	+20/3	−8/3
4223333					+1/8	−1/12	+1/256	+27/512	−3/64	−5/48	+1/24		+3	−28	+32/3	−3/4	+8	+3	+20/3	−8/3
4121112				+1/16	−1/4		−1/192	−9/128	+1/16				−2	+8		+1	−32/3	−4		
4121222				+1/16	−1/4		−1/64	+9/128	+1/16				−2	+8		+1/3	+32/3	−4		
4131333					−1/4	+1/6			+1/16	−1/12			+2	−8				−4	+16/3	
4311333				−1/16	+1/4				+1/16	−1/12				+8	−16/3			−4	+16/3	

Table V shows what strain components still need to be computed for several interesting directions of **p** in cubic and hexagonal crystals. The last column in Table V, headed "Cases," refers for comparison to items in a table given by Bitter[5] in an analysis of the experimental material.

The strain components in lines 2 and 3 of

[5] F. Bitter, *Introduction to Ferromagnetism* (1937), pp. 253–254.

TABLE IV. *Hexagonal arrangements.*

Axial ratio $c=2/3(6)^{\frac{1}{2}}=1.6330$.

SUBSCRIPT OF S	NUMERICAL PRIMITIVE	VALUE OF S CLOSE-PACKED	SUBSCRIPT OF S	NUMERICAL PRIMITIVE	VALUE OF S CLOSE-PACKED
200	2.75741	2.96023	400	0.95461	0.33815
20033	−3.82936	0.00507	4ii	−7.6369	−2.7052
2ii	−4.8288	−4.8920	433	6.6382	5.6646
233	2.0848	0.7779	41111	35.1298	29.6909
21111	−4.1428	−3.8634	41122	16.2140	9.7378
2ii33	9.7435	0.7678	41133	−60.2145	−18.6979
23333	−10.3972	−6.1972	42211	−26.4942	−29.9450
21313	0.0268	−2.3076	42222	−7.5784	−9.9920
23113	7.7123	−2.3177	42233	−17.5062	20.9850
			41212	18.9158	19.9530
			41313	−0.1765	13.1900
			4111111	−39.5064	−38.0945
			4112222	−17.4380	−14.8160
			4113333	71.7286	18.3590
			4223333	29.0204	−21.3238
			4121112	6.4038	3.1767
			4121222	−50.5406	−49.7338
			4131333	0.4117	−30.7766
			4311333	−44.1369	−46.5571

Table V may be simplified by referring them to the principal axes of the strains. In line 2 this gives $A[110]=A_{11}+A_{12}$; $A[1\bar{1}0]=A_{11}-A_{12}$; $A[001]=-2A_{11}$. In line 3 it gives $A[111]=2A_{23}$; $A[1\bar{1}0]=-A_{23}$; $A[11\bar{2}]=-A_{23}$.

In applying the formulae here derived for E_m to iron and nickel the values of N, P, a, F_4 given in Table III of l.c.[2] are used. In case of cobalt a slight improvement over l.c.[2] is introduced by making $a=2.5024\times10^{-8}$ cm, instead of using the experimental value, $a=2.507\times10^{-8}$. This changes ρ enough to raise F_4 at $\lambda=\pi/2$ from 0.9090 to 0.9124. The calculated value of ${}_0E_m$ now corresponds to a fictitious crystal having precisely the axial ratio $c=2(6)^{\frac{1}{2}}/3$ used in computing Table IV. The strain **A′** necessary to change this fictitious crystal to the actual strain-free cobalt crystal, with $c=1.624$, $a=2.507\times10^{-8}$ cm, is dilatationless, as is also the further strain **A″** necessary to minimize (E_m+E_e). The strains **A′** and **A″** both affect E_m but only the strain **A″** (the magnetostrain) affects E_e. The value of E_m under **A′** alone will be denoted by E_m'.

TABLE VI. *Elastic moduli* ($erg\cdot cm^{-3}$).

METAL	$10^{-12}\times$ c_{11}	c_{12}	c_{44}
Iron[6]	2 369	1.406	1.160
Nickel	3.42	1.98	0.789
Cobalt	3.47	1.95	0.76

The computation of E_e requires values for elastic moduli appropriate to single crystals, not all of which are as yet known. In case of iron the experiments of Goens and Schmid[6] yield all needed data. In the case of nickel new (unpublished) values were furnished by Quimby, who has supplemented the work of Zacharias[7] on a single crystal with measurements of Young's modulus and shear modulus on a polycrystalline rod like that used by Siegel and Quimby[8] in studies on Young's modulus only. In the case of cobalt there seem to be no accepted values of moduli for use in Eq. (12). Making the very daring assumptions that cobalt is elastically isotropic, and that it is otherwise indistinguishable from hickel allows using Quimby's newly measured moduli for polycrystalline nickel together with the added conditions for elastic isotropy. About the only justification for these assumptions is the fact that Young's moduli[9] for nickel and cobalt and the compressibilities as well[10] are nearly indistinguishable in polycrys-

[6] E. Goens and E. Schmid, Naturwiss. **19**, 520–524 (1931).
[7] J. Zacharias, Phys. Rev. **44**, 116–122 (1933).
[8] S. Siegel and S. L. Quimby, Phys. Rev. **49**, 663–670 (1936).
[9] J. Zacharias, reference 7; K. Nakamura, Sci. Rep. Tohoku Imp. Univ. Honda Volume, 146–157 (1936).
[10] P. W. Bridgman, Proc. Am. Acad. **58**, 163–242 (1923).

TABLE V. *Characteristics of magnetostrictive strains.*

CRYSTAL SYMMETRY	INDICES OF **p**	COMPONENTS OF **p**			STRAIN COMPONENTS						CASES[5]
		p_1	p_2	p_3	A_{11}	A_{22}	A_{33}	A_{23} AND A_{32}	A_{31} AND A_{13}	A_{12} AND A_{21}	
Cubic	[100]	1	0	0	A_{11}	$-A_{11}/2$	$-A_{11}/2$	0	0	0	*a, b, c*
	[110]	$1/\sqrt{2}$	$1/\sqrt{2}$	0	A_{11}	A_{11}	$-2A_{11}$	0	0	A_{12}	*d, e, f*
	[111]	$1/\sqrt{3}$	$1/\sqrt{3}$	$1/\sqrt{3}$	0	0	0	A_{23}	A_{23}	A_{23}	*g, h*
Hexagonal	[001]	0	0	1	A_{11}	A_{11}	$-2A_{11}$	0	0	0	
	[100]	1	0	0	A_{11}	A_{22}	A_{33}	0	0	0	
	[120]	0	1	0	A_{11}	A_{22}	A_{33}	0	0	0	

TABLE VII. *Calculated strains, and energy densities in erg·cm^{-3}.*

METAL	$10^6\times$					$10^{-6}\times$	
	p	A_{11}	A_{22}	A_{33}	A_{23}	${}_0E_m$	E_e
Iron	[100]	5.62	−2.81	−2.81	—	−8.5037	−0.000023
	[110]	−4.17	−4.17	8.34	−6.01	−5.9381	−0.000134
	[111]	—	—	—	1.26	−5.0829	−0.000011
Nickel	[100]	0.70	−0.35	−0.35	—	−0.3974	−0.0000005
	[110]	−0.51	−0.51	1.02	−0.95	−0.6667	−0.0000026
	[111]	—	—	—	0.30	−0.7564	−0.0000004
Cobalt*	[001]	−2.73	−2.73	+5.46	—	−5.3933	−0.0000340
	[100]	−11.48	+6.44	+5.04	—	−4.6513	−0.0001509
	[120]	−4.97	−0.07	+5.04	—	−4.6513	−0.0000381

* Corrected for preliminary strain: $A_{11}'=0.001839$, $A_{22}'=0.001839$, $A_{33}'=-0.003678$, to make $c=1.624$, and $a=2.507\times10^{-8}$ cm.

talline specimens. The assumption of isotropy leaves only two independent moduli, c_{11} and c_{12}, instead of the five appearing in Eq. (12), since $c_{33}=c_{11}$ and $c_{44}=(c_{11}-c_{12})/2$.

The moduli used in the final calculations are collected in Table VI. The strain components for minimum (E_m+E_e) are presented in Table VII, together with values of ${}_0E_m$ (or ${}_0E_m'$), the energy density in unstrained crystals for the same directions of **p**, and the energy density increase, $(E_m-{}_0E_m+E_e)=-E_e$, arising from magnetostrain. It is obvious that the energy densities associated with magnetostriction are trivial, and this remains true whether the theoretical magnetostrains of Table VII or experimental values[5] are used. This justifies the principal results of l.c.[2] which ignored strain effects altogether.

The calculated magnetostrains in iron are much nearer to experimental values than are those in nickel. The signs of all components agree with the single exception of $A[001]$ for **p** along [110]. In nickel the calculated values are much too low in absolute magnitude and do not exhibit the approximate isotropy, both of longitudinal contraction and of transverse expansions, so striking in the experiments. In cobalt the calculated values are again too small and do not give all the details of the experiments[11] with which they must be compared. The fit, such as it is, is almost certainly fortuitous, in view of the roughness with which the elastic moduli have been estimated. Better data are badly needed.

The inadequacy of purely magnetic interactions to account for magnetostriction in nickel suggests that the nonmagnetic interactions, collectively accounting for the molecular field, do not produce mere dilatation (here contraction in volume) as hitherto supposed.

[11] Z. Nishiyama, Sci. Rep. Tohoku Imp. Univ. **20**, 323–341 (1931).

FEBRUARY 15, 1938 PHYSICAL REVIEW VOLUME 53

Magnetic Interaction in Pyrrhotite and in Magnetite

L. W. MCKEEHAN
Sloane Physics Laboratory, Yale University, New Haven, Connecticut

(Received January 3, 1938)

Magnetic potential energy densities, including quadrupole terms, have been computed for important directions of magnetization in pyrrhotite and in magnetite. In pyrrhotite the results are in contradiction with experiment, suggesting that other causes of ferromagnetic anisotropy greatly predominate. In magnetite the results suggest that all the iron atoms contribute to the ferromagnetism, neither ferric nor ferrous iron being adequate separately to explain the observed behavior. With this assumption the results are in qualitative agreement with experiment, calculated anisotropy being greater than that reported in the literature of the subject.

Pyrrhotite

PYRRHOTITE is an anomalous ferromagnetic in at least two respects. The preference for magnetization normal to the hexagonal axis is so strong that crystals can hardly be said to be ferromagnetic parallel to this axis.[1] The gyromagnetic ratio is very different from that for all other ferromagnetics yet investigated.[2] It therefore seemed worth while to compute the ferromagnetic anisotropy of pyrrhotite on the same basis as that which gave reasonably good results for iron and nickel and their cubic alloys, less satisfactory results for hexagonal cobalt.[3]

The computation involves no special difficulty. The coordinates of the two iron atoms in the hexagonal unit cell are (0, 0, 0) and (0, 0, $\frac{1}{2}$) so that the formulae for a simple hexagonal lattice can be used by halving the c axis of the true unit cell. This makes[4] the axial ratio $c=0.844$, with $a=3.43\times10^{-8}$ cm. The number of atomic magnets per cell is now $N=1$, the volume of the cell $V=58.99\times10^{-24}$ cm³. The reported saturation magnetization varies widely. The highest reported value in the *International Critical Tables* ($I=72.8$) gives for the average magnetic moment per iron atom $P=2.147\times10^{-21}$. This makes $(NP^2/Va^3)=1.937\times10^3$. The value of P is far below that for one electron per atom, so axial concentration of magnetic moment ($\lambda=\pi/2$) may be expected. The magnetic moment may be supposed to be spread at the same distance from the nucleus that was assumed in metallic iron,

Table I. *Coordinates of iron atom centers.*

Fe″				Fe‴											
0	0	0		$\frac{1}{4}$	$\frac{1}{4}$	$\frac{1}{4}$		$\frac{3}{8}$	$\frac{3}{8}$	$\frac{3}{8}$		$\frac{3}{8}$	$\frac{1}{8}$	$\frac{7}{8}$	
0	$\frac{1}{2}$	$\frac{1}{2}$		$\frac{1}{4}$	$\frac{3}{4}$	$\frac{3}{4}$		$\frac{3}{8}$	$\frac{7}{8}$	$\frac{7}{8}$		$\frac{3}{8}$	$\frac{5}{8}$	$\frac{3}{8}$	
$\frac{1}{2}$	0	$\frac{1}{2}$		$\frac{3}{4}$	$\frac{1}{4}$	$\frac{3}{4}$		$\frac{7}{8}$	$\frac{3}{8}$	$\frac{7}{8}$		$\frac{7}{8}$	$\frac{5}{8}$	$\frac{3}{8}$	
$\frac{1}{2}$	$\frac{1}{2}$	0		$\frac{3}{4}$	$\frac{3}{4}$	$\frac{1}{4}$		$\frac{7}{8}$	$\frac{7}{8}$	$\frac{3}{8}$		$\frac{7}{8}$	$\frac{1}{8}$	$\frac{7}{8}$	

[1] P. Weiss, J. de phys. **8**, 542–544 (1899).
[2] F. Coeterier, Helv. Phys. Acta **8**, 522–564 (1935).
[3] L. W. McKeehan, Phys. Rev. **52**, 18–30 (1937). Note that S_{200} and S_{20033} of the present paper are S_{20} and S_{22} of this reference.
[4] Assuming c for the true unit is 1.688. Since the calculations here reported were finished a different value, $c=1.644$ has been announced by S. S. Sidhu and V. Hicks, Phys. Rev. **52**, 667 (1937). The discrepancy emphasized herein would be about as serious for either assumption regarding c so that recomputation with the new value seemed unprofitable.

Table II. *Lattice sums.*

Atoms Considered	S_2	S_{400}
8 Fe″	16.75516	−106.9607
16 Fe‴	33.51032	−177.6685
(8 Fe″+16 Fe‴); Fe″ at origin	50.26548	33.4852
(8 Fe″+16 Fe‴); Fe‴ at origin	50.26548	−107.4455
(8 Fe″+16 Fe‴); mean value	50.26548	−60.4686

giving a different value to the ratio ρ, *viz.* $\rho=0.223$.

The computation of lattice sums yields $S_{200}=2.4034$, $S_{20033}=1.3860$, and $S_{400}=2.1804$. These, with the assumptions regarding λ and ρ, give the following energy densities for important directions:

$$E[001]=-14.06\times10^3 \text{ erg}\cdot\text{cm}^{-3},$$
$$E[100]=E[120]=-7.18\times10^3 \text{ erg cm}^{-3}.$$

The wrong direction is indicated as preferred and the energy difference is much too small. It does not help to take $\lambda=0$, for this yields

$$E[001]=-3.79\times10^3 \text{ erg}\cdot\text{cm}^{-3},$$
$$E[100]=E[120]=-3.40\times10^3 \text{ erg cm}^{-3}$$

showing still a slight preference for the direction, [001], which is energetically avoided.

It must be concluded that gross magnetic interaction between atoms is relatively unimportant in establishing ferromagnetic anisotropy in pyrrhotite.[5]

Magnetite

Magnetite was the first cubic crystal shown to be magnetically anisotropic.[6] The chemical formula may be written $FeO\cdot Fe_2O_3$, and it is customary to distinguish ferrous (Fe″) and ferric (Fe‴) atoms in its unit cell, which contains 8 of the former, 16 of the latter. With the usual choice of origin the coordinates of the iron atom centers are given in Table I.

The lattice parameter is $a=8.41\times10^{-8}$ cm ($V=594.8\times10^{-24}$ cm³) which, with the same distance of magnetic moment from the center of each atom as was assumed in metallic iron, makes

[5] F. Bitter has pointed out in private conversation since this paper was written that the room temperature preference for magnetization in the basal plane, (001), may be replaced at low temperature by a preference for magnetization along the normal to this plane, [001].
[6] P. Weiss, J. de phys. **5**, 435–453 (1896).

$\rho=0.091$. We assume the saturation magnetization as the highest reported in the *International Critical Tables*, $\sigma=98.6$ per gram. If all iron atoms contribute equally to the observed magnetization this gives $P=1.263\times10^{-20}$ (gaussian units), if only ferric iron counts, $P=1.894\times10^{-20}$, if only ferrous iron counts, $P=3.789\times10^{-20}$. It is noticed at once that the last assumption gives higher average moment to each iron atom than occurs in metallic iron, which seems very unlikely. It is difficult to attribute all the magnetization to ferric iron, either, for if this is done it is hard to see why magnetite is so far superior magnetically to isomorphous crystals (ferrites) of formulae $MO\cdot Fe_2O_3$, which in general have very low magnetizations.[7] Additional reasons for dividing the magnetization among all the available iron atoms are discussed later.

It is apparent from the coordinates of the atoms that Fe″ and Fe‴ are differently surrounded by neighbors. Even the symmetries differ, centers of inversion occurring at Fe″ but not at Fe‴. It is therefore necessary to compute lattice sums separately for Fe″ as origin and for Fe‴ as origin and to compute a mean value by suitably weighting the two. Table II gives the separate and combined results computed in the usual way.[3]

In these computations care must be taken with factors which differ with choice of origin atom when the origin is not at a center of inversion. Such factors $([r_i^2r_j^2]^*=(r_2^2r_3^2+r_3^2r_1^2+r_1^2r_2^2)/3$ and f) occur in numerous lattice sums.[8] The values of ϵ chosen for numerical work were $\epsilon=4$ and $\epsilon=2(3)^{\frac{1}{2}}$.

All the values of S_{400} in Table II are new, except for the first, which was directly computed by Forrest[9] (his value corresponds to $S_{400}=-107.04$).

Table III gives values of K_0 and K_1 computed with the values of S_2 and S_{400} in lines 1, 2 and 5 of Table II both for axial ($\lambda=\pi/2$) and equatorial ($\lambda=0$) concentrations of magnetic moment.

An experimental value of K_1 can be derived from data given by Weiss, who first studied this crystal.[6] From graphical quadrature of curves which he has published[10] one finds approximately $E[100]=1.0374$; $E[110]=0.0176$; $E[111]=0.0145$ (all in 10^6 erg·cm^{-3}); from which

$$K_1=-0.0792\times10^5;\quad K_2=+0.094\times10^5.$$

(This is a very small value of K_2, not significantly different from zero.)

The sign of K_1 evidently requires an axial concentration of magnetic moment. This is easy to admit if the average moment per atom is as low as 1.263×10^{-20} (corresponding to less than two electrons per atom) a third reason for favoring distribution over 24 atoms per cell rather than some smaller number. The calculated value of K_1, which drops in absolute magnitude as the number of atoms possessing magnetic moment is made greater, is, even for 24 atoms per cell, more negative than the experimental value. The least distance between iron atom centers in magnetite is 2.973×10^{-8} cm, which may be compared with a least distance of 2.478×10^{-8} cm in metallic iron at room temperature. The lower value of P in magnetite may be due entirely to this larger separation.

On the whole the case of magnetite may be considered as adequately covered by the simple sort of magnetic interaction previously proposed for metal crystals.

No account has been taken in this analysis of the nonmagnetic element present in each case, sulphur in pyrrhotite, oxygen in magnetite. As far as purely magnetic interaction goes this is entirely reasonable. If other types of interaction are important this simplification is probably not justified.

TABLE III. *Energy densities.*

	Energy Densities (erg·cm^{-3}) $10^{-6}\times$			
	$\lambda=\pi/2$		$\lambda=0$	
	K_0	K_1	K_0	K_1
8 Fe″	−0.197	−1.74	−0.718	+0.869
16 Fe‴	−0.255	−1.44	−0.688	+0.720
(8 Fe″+16 Fe‴)	−0.478	−0.326	−0.576	+0.163

[7] D. P. Raychaudhuri, Ind. J. Phys. **9**, 425–432 (1935).

[*] Square brackets are used to indicate mean values of the quantities enclosed.

[8] L. W. McKeehan, Phys. Rev. **53**, 301 (1938) designates these sums as follows: γ_4, γ_6, γ_7, γ_8, δ_4, δ_6, δ_8, δ_{10}, δ_{11}, δ_{12}, δ_{13}.

[9] J. Forrest, detailed references and recomputation of the quantity in question have been given by L. W. McKeehan, Phys. Rev. **44**, 38–42 (1933).

[10] P. Weiss, G. Foëx, *Le Magnétisme* (Armand Colin, 1926), p. 122.

Van der Waals Forces Between Symmetrical Rotators

KENNETH G. CARROLL
Sloane Physics Laboratory, Yale University, New Haven, Connecticut
(Received December 23, 1937)

Work of F. London on the van der Waals forces between linear dipole molecules has been extended to polyatomic molecules which are representable as symmetrical tops. The results obtained by a second-order perturbation calculation are compared with those of a variational calculation for the specific case of the interaction between two tops in one-quantum states.

IN a recent paper by Margenau and Warren[1] the first-order perturbation energy between symmetrical top molecules carrying permanent dipole moments along their figure axes was calculated. The results were applied to the pressure broadening of the near infra-red spectral lines of ammonia, and qualitative agreement with experiment obtained. This indicates that these long range forces play a significant role in line broadening even at atmospheric pressure. It was there assumed that the second-order forces would be negligibly small over the range for which their calculation was valid, a conclusion based on the results of London[2] for linear dipole molecules. In the present work, the second-order perturbation to the van der Waals forces is calculated for symmetrical top molecules. The results show that the second-order effect is indeed negligible in line broadening. Actually the addition of another degree of freedom (spin about the figure axis) to the calculation for linear molecules reduces the second-order interaction. An independent calculation of the effect is made by the variation method.

The Schrödinger second-order perturbation formula may be used to find the energy change, averaged over degenerate states, resulting from the approach of two molecules carrying dipole moments μ along their figure axes:

$$\langle \Delta E_i \rangle_{Av}^{(2)} = \frac{1}{g_i} \sum_j{}' \frac{\sum_{\lambda,\mu} |V_{\lambda\mu}{}^{ij}|^2}{E_i{}^0 - E_j{}^0}. \qquad (1)$$

$V_{\lambda\mu}{}^{ij}$ is the matrix element of the perturbing potential V between the degenerate states λ and μ belonging to the energy states i and j respectively, g_i is the degree of degeneracy of the ith state. The perturbing potential (interaction of the dipole moments) is

$$V = -(\mu^2/R^3)[2\cos\theta_1\cos\theta_2 - \sin\theta_1\sin\theta_2\cos(\phi_1-\phi_2)]$$

where the orientations of the molecules are expressed in the Eulerian angles θ, ϕ, χ relative to the line joining them, and R is the separation of the two molecules. A state j is characterized by the product of two unperturbed symmetrical top eigenfunctions, each of which is dependent on the three quantum numbers J, K, M. Since the energy of the symmetrical top is

$$E = \frac{h^2}{8\pi^2}\left\{\frac{J(J+1)}{A} + \left(\frac{1}{C}-\frac{1}{A}\right)K^2\right\}, \qquad (2)$$

where A and C are the moments of inertia about the principal axes, summing over degenerate states involves summing the numerator of (1) over permissible values of the M's (from $-J$ to $+J$) and the two possible values of the K's. If the quantum numbers of the two molecules belonging to the ith state are denoted by J_i, K_i, M_i and J_i', K_i', M_i' the numerator of Eq. (1) becomes

$$\sum \left| V^{J_iK_iM_i;\, J_i'K_i'M_i'}_{J_jK_jM_j;\, J_j'K_j'M_j'} \right|^2 = \frac{6\mu^4}{R^6}\sum \left(\cos\theta_1 {}^{J_i, K_i, M_i;\, J_i', K_i', M_i'}_{J_j, K_j, M_j;\, J_j', K_j', M_j'}\right)^2 \cdot \left(\cos\theta_2 {}^{J_i, K_i, M_i;\, J_i', K_i', M_i'}_{J_j, K_j, M_j;\, J_j', K_j', M_j'}\right)^2. \qquad (3)$$

The summation in (3) is over degenerate quantum numbers of both initial and final states. It

[1] H. Margenau and D. T. Warren, Phys. Rev. **51**, 748 (1937).
[2] F. London, Zeits. f. Physik **63**, 245 (1930).

has been carried out over degenerate quantum numbers of the final state (j) in calculations on transition probabilities, for example, in the work of Dennison.[3] Because the result at this stage is independent of the degenerate quantum numbers of the initial state (i), the remainder of the summation yields only the degeneracy factor, g_i. In terms of Dennison's transition probabilities

$$\Sigma\begin{pmatrix}\cos\theta & J_iK_iM_i\\ & J_jK_jM_j\end{pmatrix}^2=\frac{g_i}{3}\begin{pmatrix}A & J_iK_i\\ & J_jK_j\end{pmatrix}^2.$$

The factor $\frac{1}{3}$ arises from the three possibilities of polarization which contribute equally to the total transition probability A^2. Expressed in these terms, the numerator of (1) becomes

$$\frac{2\mu^4}{3R^6}g_ig_i'\begin{pmatrix}A & J_iK_i\\ & J_jK_j\end{pmatrix}^2\begin{pmatrix}A & J_i'K_i'\\ & J_j'K_j'\end{pmatrix}^2$$

and

$$\langle\Delta E_i\rangle_{\text{Av}}^{(2)}=\frac{2\mu^4}{3R^6}\sum_j{}'\frac{\begin{pmatrix}A & J_iK_i\\ & J_jK_j\end{pmatrix}^2\begin{pmatrix}A & J_i'K_i'\\ & J_j'K_j'\end{pmatrix}^2}{E_i^0-E_j^0}.$$

The elements A^2 are different from zero only when $\Delta J=0,\ \pm1$ and $\Delta K=0$ (selection rules for $\|$-type bands). With Dennison's[3,4] expressions for the A's, the final result is

$$\langle\Delta E\rangle_{\text{Av}}^{(2)}=-\frac{\mu^4}{3R^6B}\left\{\frac{(J+1)^2-K^2}{(J+1)(2J+1)}\left[\frac{(J'+1)^2-K'^2}{(J'+1)(2J'+1)(J+J'+2)}+\frac{K'^2}{J'(J'+1)(J+1)}\right.\right.$$
$$\left.+\frac{J'^2-K'^2}{J'(2J'+1)(J-J'+1)}\right]+\frac{K^2K'^2}{J(J+1)J'^2(J'+1)^2}+\frac{J^2-K^2}{J(2J+1)}\left[\frac{(J'+1)^2-K'^2}{(J'+1)(2J'+1)(1+J'-J)}\right.$$
$$\left.\left.-\frac{K'^2}{JJ'(J'+1)}-\frac{J'^2-K'^2}{J'(2J'+1)(J+J')}\right]\right\},\quad(3)$$

where the subscripts i have been dropped throughout. Table I gives a few values of this expression. It is seen that an increase in K, the "spin" quantum number, weakens the interaction between molecules of fixed J and J'. Since this energy perturbation would be described classically as the tendency of one dipole molecule to line up its neighbors, it may be said that an increase in the "spin" energy of a top strengthens its resistance to orientation.

If K is set equal to zero, the wave functions of the symmetrical top go over into those of the linear molecule. If the K's in (3) are allowed to vanish, the resulting expression is identical with that obtained for linear dipole molecules by F. London.[2] It is to be noted that (3) has the familiar form of the $1/R^6$ law which is characteristic of this effect. It does not apply, of course, to cases of close approach where the numerators of terms in (1) become comparable to the denominators. For a typical molecule, calculations indicate that Eq. (3) is quite accurate for distances of separation greater than 9 or 10A.

Since the first-order splitting of levels is symmetrical, the "center of gravity" of a degenerate group of levels is unchanged by this interaction. Hence Eq. (3) contains the total average effect of these long range forces.

An upper bound to the energy of interaction can be found by the variation method, by using a linear combination of unperturbed wave functions. The mathematical complexity, how-

TABLE I. *Values of* $\langle\Delta E\rangle_{\text{Av}}^{(2)}$ *for various energy states.*

Energy State	$\langle\Delta E\rangle_{\text{Av}}^{(2)}$ in Units of μ^4/R^6B	Energy State	$\langle\Delta E\rangle_{\text{Av}}^{(2)}$ in Units of μ^4/R^6B
$J=J'$, $K=K'=0$	$-\frac{1}{6}$	$J=1$ $J'=2$, $K=1$ $K'=2$	$-\frac{23}{270}$
$J=1=J'$, $K=1=K'$	$-\frac{5}{48}$	$J=2$ $J'=2$, $K=2$ $K'=2$	$-\frac{1}{18}$
$J=0$ $J'=1$, $K=0$ $K'=0$	$-\frac{2}{27}$	$J=2$ $J'=2$, $K=1$ $K'=1$	-0.158
$J=0$ $J'=1$, $K=0$ $K'=1$	$-\frac{2}{9}$		

[3] D. M. Dennison, Rev. Mod. Phys. **3**, 280 (1931).

[4] The expressions given by Dennison are here to be multiplied by 4.

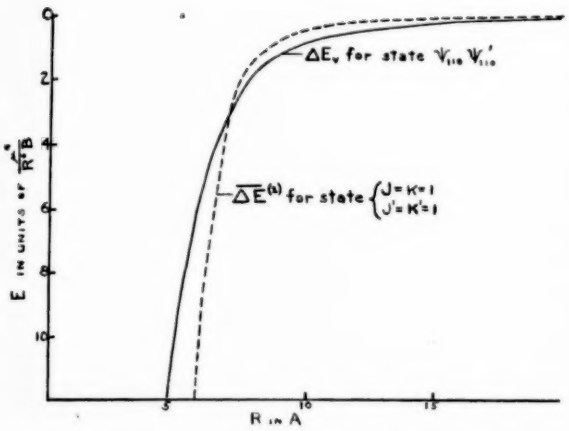

FIG. 1. Energies of state as functions of R.

ever, prevents an explicit calculation for the general case. It has been carried out for the special case where both interacting molecules are in the state $J=1$, $K=1$, $M=0$. Here the variation function suggested by the problem is a linear combination of the ten unperturbed wave functions with which the given state ($\psi_{110}\psi'_{110}$) combines, i.e.,

$$\psi_{111}\,\psi'_{11-1},\quad \psi_{11-1}\psi'_{111},\quad \psi_{211}\,\psi'_{21-1},$$
$$\psi_{111}\,\psi'_{21-1},\quad \psi_{210}\,\psi'_{210},\quad \psi_{21-1}\psi'_{211},$$
$$\psi_{11-1}\psi'_{211},\quad \psi_{211}\,\psi'_{11-1},\quad \psi_{21-1}\psi'_{111}.$$

Minimizing the energy of the system with respect to the constants in the variation function leads to a secular determinant of ten rows and columns, but which possesses only four distinct roots, reducing to an equation of the fourth degree in E_v, the variation energy. The various matrix elements in the secular equation were constructed from a table of integrals involving symmetrical top wave functions published by Reiche and Rademacher.[5] The resulting fourth degree equation was solved numerically for various values of the molecular separation, R, using reasonable values of the molecular constants ($\mu=1.5\times10^{-18}$ e.s.u., $A=3\times10^{-40}$ g cm^2, from which B, the separation of the rotational levels$=1.8\times10^{-15}$ ergs, or about 0.001 ev.). The lowest root of the secular equation is an upper bound to the energy of the given state. This energy is shown in Fig. 1 as a function of R. Included for comparison is a plot of $\langle\Delta E\rangle_{Av}^{(2)}$ for the energy state $J=|K|=J'=|K'|=1$. Neglecting the effect on E_v of averaging over degenerate states, it is seen that it is larger than the second-order perturbation for $R>8$A, since E_v contains also the first-order effect, which obeys a $1/R^3$ law. At distances less than about 8A, the second-order perturbation diverges markedly. This shows that Eq. (3) is valid only for R greater than this value.

I wish to express my gratitude to Professor H. Margenau for his kind supervision of this work.

[5] F. Reiche and H. Rademacher, Zeits. f. Physik **41**, 453 (1927).

The Binding Energy of the Deuteron

H. A. BETHE
Cornell University, Ithaca, New York
(Received January 21, 1938)

IN a recent paper,[1] Chadwick, Feather and Bretscher have published their results on the photodisintegration of the deuteron. For the determination of the energy of the photo-protons from their range they use the range-energy relation of Blackett and Lees;[2] this gives 185 kv for the energy of the photo-protons produced by the 2.62 Mev γ-rays from Th C″, and therefore 2.25 Mev for the binding energy of the deuteron. However, recent experimental[3–5] and theoretical[3] investigations show that the energy of a slow proton is, for a given range, considerably higher than is indicated by the relation of Blackett and Lees. Because of the fundamental importance of the binding energy of the deuteron for nuclear theory, it seems worth while to analyze the data of Chadwick, Feather and Bretscher in terms of the most recent range-energy data.

A very careful study of the range-energy relation of slow (up to 2 Mev) protons in air was recently carried out by Parkinson, Herb, Bellamy and Hudson.[4] We have applied some obvious corrections to the data published by P. H. B. H. such as using the mean[6] instead of the extrapolated voltage, using the distance to the center of the ionization chamber as the "mean range" and reducing the data to standard conditions (15° and 760 mm). The range-energy relation thus obtained[7] was used in the following. Its accuracy is difficult to estimate; probably the greatest error arises from the definition of the end of the range which may be different in cloud chamber and ionization chamber work; we shall assume that this error amounts to 0.1 mm standard air (depth of ionization chamber in experiments was 0.4 mm, range of photo-protons about 2 mm).

Chadwick, Feather and Bretscher used in their cloud chamber a mixture of about 60 percent He and 40 percent CH_4. In this mixture, the mean range of the photo-protons was 0.613 cm, with a mean error (due to statistics) of 0.010 cm or 1.6 percent. The stopping power (S.P.) of the mixture was calibrated with α-particles of about 2 cm range, and it was found that 2.91 cm of the gas were equivalent to a mica foil of 0.902 cm air equivalent.[8] If the S.P. of the gas relative to air were the same for slow protons as for 2 cm alphas, the range of the photo-protons in air would be $0.613 \times 0.902/2.91 = 0.190$ cm.

Actually, the S.P. of the gas is considerably higher for slow particles. The S.P. of hydrogen and helium relative to air were measured by Gurney[9] for α-particles of various energies and by Gerthsen[10] for very slow protons. Blackett and Lees[2] have given an interpolation table for the S.P. of hydrogen for protons and α-particles. From this table, the average S.P. for protons in the last 0.23 cm of their range[11] is 0.33, that for alphas of 2 cm range[12] 0.217.

For helium as a stopping gas, Gurney found a very small variation of the S.P. from about 0.175 at medium to 0.179 at small velocities. This result may seem somewhat surprising since helium is so much lighter than air. However, it is

[1] Chadwick, Feather and Bretscher, Proc. Roy. Soc. **163**, 366 (1937).
[2] Blackett and Lees, Proc. Roy. Soc. **134**, 658 (1932).
[3] Livingston and Bethe, Rev. Mod. Phys. **9**, 246 (1937), especially §95, p. 261–68. (Theory, and discussion and references to experimental papers up till 1936.)
[4] Parkinson, Herb, Bellamy and Hudson, Phys. Rev. **52**, 75 (1937).
[5] Blewett and Blewett, private communication (Experiments on the range-nergy relation of slow α-particles, carried out in the Cavendish laboratory).
[6] I.e. the voltage at which, for a given position of the ionization chamber, the number of protons reaching the chamber has dropped to one-half the number at high voltage.
[7] A limited number of blue-prints of this relation has been sent to some of the chief laboratories in nuclear physics.
[8] It is not stated how the mica foil itself was calibrated. We assume in the following that it was also calibrated with 2 cm alphas. If, instead, Ra C′ alphas were used, its actual air equivalent would be about 1.1 percent less, owing to the variation of the stopping power of mica. This would increase the binding energy of the deuteron by 5 kv. This correction is negligible compared with the uncertainty in the range-energy relation.
[9] Gurney, Proc. Roy. Soc. **107**, 341 (1925).
[10] Gerthsen, Ann. d. Physik **5**, 657 (1930).
[11] Actual range in air found for the photo-protons.
[12] For this case, Fig. 33a of reference 3 gives 0.231. This difference may indicate the probable error. Since only the *relative* stopping powers for slow protons and 2 cm alphas matter, we prefer to use one set of data (those of Blackett and Lees) consistently.

immediately understood theoretically because the important quantity for the S.P. is the average excitation potential of the electrons of the stopping atoms. Now, the K electrons of air contribute only a very small amount to the S.P. for slow particles (about 5 percent for 2 cm alphas). The average excitation potential of the *L electrons* of air is 40.3 volts (from experimental data, reference 3, p. 267); that of helium (K electrons) is 42.7 volts,[13] i.e., almost the same.[14] Therefore the relative S.P. of He should remain almost constant up to about 2 or 3 cm range, and should decrease slowly for greater ranges when the K electrons of air become effective.

The S.P. of carbon changes very slightly, from about 0.935 at 2 cm range to 0.945 at zero range (cf. Fig. 33a, reference 3).

The stopping power of the mixture of 60 percent He and 40 percent CH_4 becomes then for 2 cm alphas:

$$0.6\cdot 0.175+0.2\cdot 0.935+0.8\cdot 0.217=0.466,$$

for slow protons (last 2.2 mm of range):

$$0.6\cdot 0.179+0.2\cdot 0.945+0.8\cdot 0.33=0.560.$$

Therefore the range of the photo-protons in standard air

$$0.190\times 0.560/0.466=0.228 \text{ cm}.$$

According to the range-energy relation of P.H.B.H. this corresponds to an energy of 228 kv. Since the energy of the Th C'' γ-rays is 2.62_3 Mev, the binding energy of the deuteron becomes

$$\epsilon=2.62_3-0.45_6=2.17 \text{ Mev}.$$

The probable errors may be estimated as follows:

Statistical error in determination of range of protons	1.6 percent
Error in range-energy relation of P.H.B.H.	5 percent
Error in relative stopping power of gas for slow protons and 2 cm alphas	5 percent
Error in calibration of stopping power for 2 cm alphas, including error due to variation of S.P. of mica	2 percent

Mean square total error about 8 percent (of 0.46 Mev), i.e., 0.04 Mev.

Therefore the binding energy of the deuteron is

$$\epsilon=2.17\pm 0.04 \text{ Mev}.$$

This value agrees very closely with the original result of Chadwick and Goldhaber[15] who used the ionization produced by the photo-protons (2.14 Mev$\pm$0.16). It also makes it understandable why Ra C γ-rays, of maximum energy 2.198, cause an observable photo-disintegration of the deuteron.[16] From the mass-spectroscopic difference between the masses of H_2 and the deuteron, *viz.* 1.53$\pm$0.04 milli-mass-units = 1.43 $\pm$0.04 Mev, we obtain for the difference between the masses of neutron and hydrogen atom

$$n-H=0.74\pm 0.06 \text{ Mev}$$
$$=0.80\pm 0.06\times 10^{-3} \text{ mass units}$$

and for the mass of the neutron

$$n=1.008\ 93\pm 0.000\ 05$$

as against 1.008 97 in Table 73 of reference 3.

The masses of all nuclei which are obtained from disintegrations involving neutrons must be changed accordingly. The most important changes in Table 73 of reference 3 are

$$\text{He}^3=\ 3.017\ 11 \text{ (against } 3.017\ 07),$$
$$\text{C}^{14}=14.007\ 63 \text{ (“ } 14.007\ 67),$$
$$\text{N}^{13}=13.010\ 08 \text{ (“ } 13.010\ 04).$$

From the new mass of N^{13} and $C^{13}=13.00761$ the expected energy of the nitrogen positron comes out to be 1.28 Mev (previously 1.24 Mev), still in good agreement with the "inspection limit" of 1.25 Mev and in disagreement with the Konopinski-Uhlenbeck limit of 1.45 Mev.

The changes in the calculations of nuclear force constants are very small.

[13] For K electrons, $I_k=1.103\ Z_{\text{eff}}{}^2 Ry$ (reference 3, p. 264), where $Z_{\text{eff}}=Z-0.31$, the screening constant 0.31 being obtained from the well-known variation calculation. For $Z=2$, this gives $I_k=1.103\cdot 1.69^2\cdot 13.54=42.7$ volts.

[14] The slight excess of I_{He} over I_{air} compensates partly the influence of the K electrons of air.

[15] Chadwick and Goldhaber, Proc. Roy. Soc. **151**, 479 (1935).

[16] Banks, Chalmers and Hopwood, Nature **135**, 99 (1935); Mitchell, Rasetti, Fink and Pegram, Phys. Rev. **50**, 189 (1936).

LETTERS TO THE EDITOR

Prompt publication of brief reports of important discoveries in physics may be secured by addressing them to this department. Closing dates for this department are, for the first issue of the month, the eighteenth of the preceding month, for the second issue, the third of the month. Because of the late closing dates for the section no proof can be shown to authors. The Board of Editors does not hold itself responsible for the opinions expressed by the correspondents.

Intrinsic Variability of the So-Called Fundamental Physical Constants

Several years ago I pointed out[1-3] that formulations of natural laws which imply the possibility of *absolute* verification through a finite number of observations are intrinsically inadequate and must in course of time give way to statistically flexible formulations of natural laws. The considerations which led to the conclusion just stated were illustrated by predictions regarding the necessarily to be expected variability of physically significant pure numbers, such as the fine structure constant $\alpha=2\pi e^2/hc$, the ratio of the rest masses of proton and electron $r=m_p/m_e$ and the ratio of the electric radius to the gravitational radius of the electron $R=e^2/\Gamma m_e^2$, (Γ=universal gravitational constant), numbers which previously had been considered as absolute constants. The programmatic value of these considerations is accentuated by recent developments in the physics of elementary particles as well as in cosmology.

It was for instance stated,[1-4] that, if $p=e$, m, μ, etc., is the charge, the rest mass, the magnetic moment and so on of an elementary particle, p would occasionally be found to assume values different from those generally accepted for the known elementary particles. The actual occurrence in cloud chamber photographs was pointed out of particles whose e/m is *different* from that of any conventional elementary particle.[1] It was suggested that easily observable deviations from the conventional values of p might be expected, especially under the following circumstances:

(a) If time intervals are considered which are long enough to change the general physical conditions in the universe, such as for instance the wholesale distribution of matter and radiation, a distribution which by present theories is made responsible for the values of the inertial mass of matter.

(b) If accidental happenings, such as impacts among particles and among particles and photons, possess characteristics which may especially facilitate the realization of intrinsic transformations of the considered elementary units.

Considerations of the type (a) have since been elaborated and in part tested experimentally by the writer,[3, 5] as well as by other authors[6] in an attempt to arrive at a deeper understanding of the redshift of light from distant nebulae and other astronomical phenomena. The possible variability of R, r and α has been shown to open up entirely new outlooks if time intervals of the order of a billion years are considered.

Processes of the type (b) have recently been suggested by many authors[7] in discussions of the penetrating cosmic-ray particles whose existence confirms the prediction that the assumption of the variability of the physical properties p of elementary particles would prove indispensible for a rational understanding of cosmic-ray phenomena, as I stated long before the recent developments.[1-4]

In this connection a trebly reflected cloud chamber track of a charged particle described by G. Herzog and P. Scherrer[8] is of considerable interest. The succession of curvatures on this track would seem to point to a violation of the principle of conservation of energy, and the mentioned authors therefore dismiss it as accidental. The track, however, also admits of an interpretation in terms of changing values of e/m caused by violent collisions.

Gains in energy, as in the track just mentioned, as well as the excessive losses of energy, described for instance by W. Bothe,[9] might often be only apparent, because of a decrease or an increase in the value of e/m of an elementary particle during a collision. This possibility suggests a systematic reexamination of single and multiple reflections of very fast electrons on for instance solid surfaces and in gases. Positive results of such experiments would put on a new basis the interpretation of changes in curvature of the path of particles passing through matter.

Finally it can be shown that the preceding considerations suggest important modifications in the formulation of the uncertainty principle of quantum mechanics, and I therefore intend to present the implications involved in more detail in another place.

F. ZWICKY

California Institute of Technology,
Pasadena, California,
January 26, 1938.

[1] F. Zwicky, Phys. Rev. **43**, 1031 (1933).
[2] F. Zwicky, Phil. Sci. **1**, 353 (1934).
[3] F. Zwicky, Proc. Nat. Acad. Sci. **23**, 169 (1937).
[4] F. Zwicky, Phys. Rev. **48**, 169 (1935).
[5] F. Zwicky, Phys. Rev. **48**, 802 (1935).
[6] J. A. Chalmers, V. B. Chalmers, Phil. Mag. **19**, 436 (1935); P. A. M. Dirac, Nature **139**, 323 (1937); P. Jordan, Naturwiss. **25**, 513 (1937).
[7] See for instance H. Euler, Physik. Zeits. **38**, 943 (1937); G. E. M. Jauncey, Phys. Rev. **52**, 1256 (1937); S. H. Neddermeyer, Phys. Rev. **53**, 102 (1938).
[8] G. Herzog and P. Scherrer, J. de phys. **6**, 489 (1935).
[9] W. Bothe, *Kernphysik* (Ed. E. Bretscher), (Verlag J. Springer, Berlin, 1936) p. 76.

Modified High Speed Geiger Counter Circuit

Although the speed of the circuit designed by Neher[1] is quite satisfactory, it suffers from the disadvantages of requiring insulation for the cylinder and shielding if two or more Geiger counters are used to count coincidences. Also, the capacity of the cylinder for large counters introduces a longer reaction time. With the circuit to be described the cylinder of the counter is grounded.

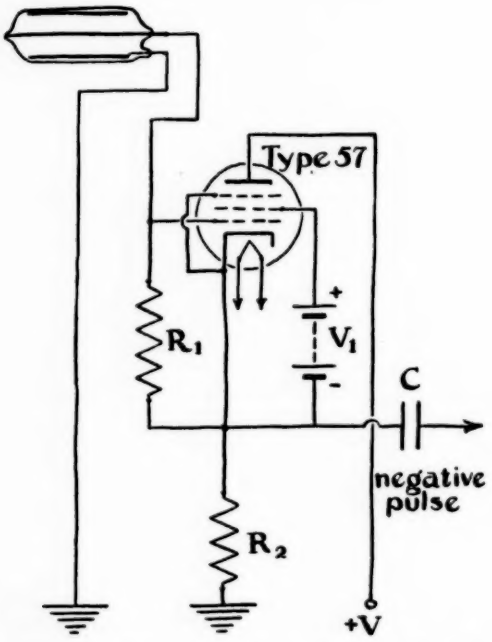

FIG. 1. High speed Geiger counter circuit. $R_1 = 5 \times 10^6$ ohms; $R_2 = 10^6$ ohms; $V_1 = 45$ volts; V = counter threshold + 100 v; $C = 50$ to 100 $\mu\mu f$.

The circuit is shown in Fig. 1. Since there is no bias on the control grid the radio tube is normally in a conducting state. Since the drop in potential across the tube is small, practically the full potential, V, is across the Geiger counter. When an ionizing particle passes through the counter a negative charge flows to the wire and thence to the control grid. The 57 tube then becomes nonconducting and the resistance R_2 pulls the cathode, grid, etc. toward ground potential. Cathode-ray oscillograph figures indicate that in all cases the potential of the cathode drops only to threshold potential or at most only a few volts below. The potential then recovers itself either partially or completely depending upon the time before the beginning of the next pulse. If the threshold of the counter becomes greater than 1500 volts, it is advisable to place a resistance of say 5×10^6 ohms between the high voltage supply and the cathode to by-pass some of the current. This keeps the drop in voltage in the 57 tube from becoming too large, because of the grid current.

The advantages offered by this circuit over the previous one are: (1) The cylinder of the Geiger tube is grounded. (2) High potentials are not applied across the radio tube. (3) No grid bias is necessary. (4) Either a positive or negative pulse may be taken off. (A positive pulse may be obtained from the plate by inserting a resistance of, say, 2×10^5 ohms in the plate lead.) The disadvantages are: (1) An insulated heater supply must be provided. (2) There is a constant drain of about one milliampere on the high voltage supply. If it is desired a self-bias may be used for the screen potential.

Further details will be published in this journal at a later date.

H. V. NEHER
W. H. PICKERING

Norman Bridge Laboratory of Physics,
California Institute of Technology,
Pasadena, California,
January 25, 1938.

[1] H. V. Neher and W. W. Harper, Phys. Rev. **49**, 940 (1936).

Multivibrator Geiger Counter Circuit

Recently Getting[1] has described a Geiger counter circuit which may be called a choked multivibrator. Brammer, Miss Hodge and the writer have employed this circuit for more than a year, obtaining the fundamental idea from a paper by Gingrich, Evans and Edgerton.[2] There are several features of its operation which deserve further discussion.

(1) When one is not attempting to secure very high speeds of operation, the constants of the circuit can be varied widely. We have used '32 tubes as well as '57 tubes. We have had no success with the '53 double triode, no doubt because of its large grid current. With either '57 or '32 tubes, plate voltages as low as 135 (with correspondingly low screen grid voltages) are satisfactory.

(2) The circuit shown by Getting is asymmetrical. Referring to his figure, the time constant of the second grid circuit is much lower than that of the first. The constants of our circuits are similar. The advantage is this: when the second tube initiates the return of the circuit to its normal condition after a count, and the output pulse is taken from the plate circuit of the *first* tube, the output capacity can be varied considerably without affecting the total recovery time. This facilitates the use of different recording circuits and mechanisms.

(3) There are two slight modifications which greatly increase the convenience of operation. (a) In practice, when the circuit recovers, the voltage at the plate of the first tube may "overshoot," going below the normal value and finally returning to normal. Unless controlled, this can result in doubling the number of pulses which actuate the recording circuits. The trouble can be cured by merely cutting down the regeneration; a potentiometer replaces the plate resistance of the second tube and the coupling condenser is connected between the first grid and the variable tap of the potentiometer. (b) Similarly, when the output pulse is secured from the plate of the first tube, it can be varied in magnitude by substituting a potentiometer for the plate resistance of that tube.

(4) Getting states that the Neher-Harper circuit requires the first vacuum tube to stand the entire counter voltage, and remarks that all the tubes are used within their ratings in the multivibrator circuit. However, the writer tried a modification of the Neher-Harper circuit in which the tube operated at rated potential; the source of high voltage for the counter was inserted between one counter terminal and the plate of the first tube; this source was an *unshielded* bank of B batteries, about 1000 volts in all, but no trouble was experienced in getting the arrangement to count. It was used both with the counter wire on the grid of the first tube and with the cylinder of the counter on the grid. (Of course the circuit constants were appropriately changed in going from one of these arrangements to the other. The counter wire was always positive to the cylinder in these tests.) A real advantage of the multivibrator over the Neher-Harper arrangement is that it works with the first grid normally at ground potential. When the grid potential is adjusted in the Neher-Harper circuit the voltage applied to the counter is altered, and this change must be compensated in many types of work.

(5) Dr. Getting remarks that the statistics of the multivibrator circuit are different from those of previous ones. Brammer and the writer[3] have treated the corrections for recovery time in any circuit which controls the counter voltage during the discharge and the subsequent period in which the ions are swept out of the counter. It is believed that in general the analysis given applies to both the multivibrator circuit and the Neher-Harper circuit.

ARTHUR RUARK

Department of Physics,
University of North Carolina,
Chapel Hill, N. C.,
January 15, 1938.

[1] Getting, Phys. Rev. **53**, 103 (1938).
[2] Gingrich, Evans and Edgerton, Rev. Sci. Inst. **7**, 450 (1936).
[3] Ruark and Brammer, Phys. Rev. **52**, 322 (1937).

Note on the Existence of Heavy Beta-Rays

During the winter of 1936–37 the author, together with J. J. Turin, E. R. Gaerttner and D. S. Bayley, carried out some rather extensive experiments in an effort to determine whether or not beta-rays of nuclear origin behaved differently from those of extranuclear origin. The results of a comparison of nuclear beta-rays with recoil electrons produced by gamma-rays seemed at the time to indicate that a difference in penetrating power existed.[1] The idea that the total energy (mass plus kinetic) might be the same for all the beta-rays from a given kind of emitter, and equivalent to the energy lost by the nucleus was at that time discussed as an alternative to the neutrino hypothesis. In the course of discussion of this idea at the Washington Conference on Theoretical Physics[1] many grave objections to such a mechanism were brought forward, the principal of which were the results of calorimetric experiments on Ra E, measurements on the primary ionization of beta-rays, and the stopping power of matter for beta-rays of various momenta from a given source. However, in spite of these arguments, experiments specifically designed to test such a hypothesis were carried out by the group of which the author was a member, and also by C. T. Zahn and A. H. Spees. The latter have already published a preliminary note[2] on their results. Inasmuch as the same question has again been raised[3] (this time in regard to Ra E it seems appropriate to describe briefly an experiment performed in this laboratory which bears directly upon the question raised, even though a different beta-ray emitter (Li^8) was used.

Li^8 emits a continuous spectrum of beta-rays having an upper limit of 12 Mev.[4] Using the cloud chamber method already described[5] we measured the absorption in ½ cm of carbon of a group of beta-rays coming from about the center of the spectrum. We next carried out the same absorption measurements on a group of beta-rays which originated near the upper limit of the spectrum, but which had been slowed down to the same momentum as those measured in the first case, by passage through about 1½ cm of carbon surrounding the source. The results indicated that the beta-rays from these two widely separated parts of the spectrum were absorbed very nearly alike when brought to the same momentum. On the hypothesis considered by us, and later by Jauncey,[3] the beta-rays originating near the middle of the spectrum (say 10 mC momentum) should have lost roughly six times as much energy as those taken from the upper end of the spectrum. In fact a consideration of the kinetic energy shows that they should not have passed through the ½ cm carbon absorber in the cloud chamber at all. Results for the fractions stopped by the carbon are given below, based upon a total of about 1000 tracks.

Momenta of incident particles, in units mC	6 to 8	8 to 10	10 to 12	12 to 14
Unfiltered	64%	45%	34%	15%
Filtered	63%	41%	27%	17%

In addition to this, the loss of momentum suffered by those particles which passed through the carbon absorber was found to be the same for the filtered and unfiltered groups, and agreed with the theoretical predictions for ordinary electrons. It therefore appears that if in the case of Ra E the rest mass is continuously variable and is a function of the initial momentum,[3] the phenomenon does not extend to all beta-ray emitters, and cannot be thought of as clearing up the question of the conservation of energy in beta-ray emission.

In the course of the experiments described a few individual beta-rays (amounting to only a small fraction of a percent of the total number) appeared to behave in an anomalous way, but a satisfactory interpretation of these cases has not been found.

H. R. CRANE

University of Michigan,
Ann Arbor, Michigan,
January 25, 1938.

[1] Breit, Rev. Sci. Inst. **8**, 141 (1937).
[2] Zahn and Spees, Phys. Rev. **52**, 524 (1937).
[3] Jauncey, Phys. Rev. **52**, 1256 (1937); Phys. Rev. **53**, 106 (1938); Phys. Rev. **53**, 197 (1938).
[4] Bayley and Crane, Phys. Rev. **52**, 604 (1937).
[5] Turin and Crane, Phys. Rev. **52**, 63 (1937); Phys. Rev. **52**, 610 (1937).

A New Method of Measuring Nuclear Magnetic Moment*

It is the purpose of this note to describe an experiment in which nuclear magnetic moment is measured very directly. The method is capable of very high precision and extension to a large number and variety of nuclei.

Consider a beam of molecules, such as LiCl, traversing a magnetic field which is sufficiently strong to decouple completely the nuclear spins from one another and from the molecular rotation. If a small oscillating magnetic field is applied at right angles to a much larger constant field, a re-orientation of the nuclear spin and magnetic moment with respect to the constant field will occur when the frequency of the oscillating field is close to the Larmor frequency of precession of the particular angular momentum vector in question. This precession frequency is given by

$$\nu = \mu H/hi = g(i)\mu_0 H/h. \qquad (1)$$

To apply these ideas a beam of molecules in a $^1\Sigma$ state (no electronic moment) is spread by an inhomogeneous magnetic field and refocused onto a detector by a subsequent field, somewhat as in the experiment of Kellogg, Rabi and Zacharias.[1] As in that experiment the re-orienting field is placed in the region between the two magnets. The homogeneous field is produced by an electromagnet capable of supplying uniform fields up to 6000 gauss in a gap 6 mm wide and 5 cm long. In the gap is placed a loop of wire in the form of a hairpin (with its axis parallel to the direction of the beam) which is connected to a source of current at radiofrequency to produce the oscillating field at right angles to the steady field. If a re-orientation of a spin occurs in this field, the subsequent conditions in the second deflecting field are no longer correct for refocusing, and the intensity at the detector goes down. The experimental procedure is to vary the homogeneous field for some given value of the frequency of the oscillating field until the resonance is observed by a drop in intensity at the detector and a subsequent recovery when the resonance value is passed.

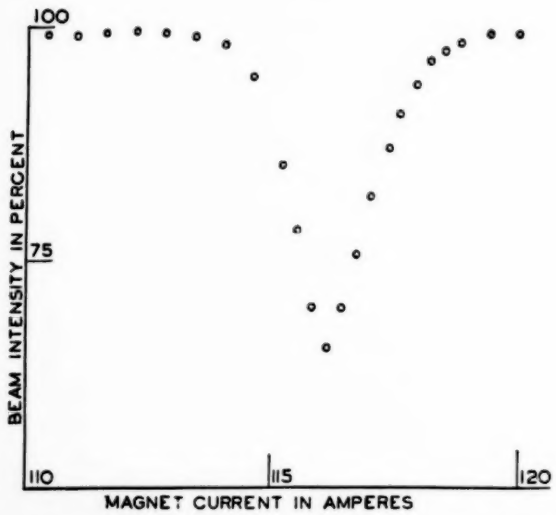

FIG. 1. Curve showing refocused beam intensity at various values of the homogeneous field. One ampere corresponds to about 18.4 gauss. The frequency of the oscillating field was held constant at 3.518×10^6 cycles per second.

The re-orientation process is more accurately described as one in which transitions occur between the various magnetic levels given by the quantum number m_i of the particular angular momentum vector in question. An exact solution for the transition probability was given by Rabi[2, 3] for the case where the variable field rotates rather than oscillates. However, it is more convenient experimentally to use an oscillating field, in which case the transition probability is approximately the same for *weak* oscillating fields *near* the resonance frequency, except that ϑ is replaced by $\vartheta/2$ in Eq. (13). With this replacement and with passage to the limit of weak oscillating fields, the formula becomes for the case of $i = \frac{1}{2}$

$$P(\tfrac{1}{2}, -\tfrac{1}{2}) = \frac{\vartheta^2}{(1-q)^2+q\vartheta^2} \sin^2 \{\pi t r[(1-q)^2+q\vartheta^2]^{\frac{1}{2}}\}, \qquad (2)$$

where ϑ is $\frac{1}{2}$ the ratio of the oscillating field to the steady field, q is the ratio of the Larmor frequency of Eq. (1) to the frequency r of the oscillating field. The denominator of the expression is the familiar resonance denominator. The formula is generalized to any spin i by formula (17).[2]

In the theory of this experiment, t, in Eq. (2), is replaced by L/v, where L is the length of the oscillating region of the field, and v is the molecular velocity. $P(\frac{1}{2}, -\frac{1}{2})$ must then be averaged over the Maxwellian distribution of velocities. However, the first term is not affected by the velocity distribution if t is long enough for many oscillations to take place. The average value of the $\sin^2$ term over the velocity distribution is approximately $\frac{1}{2}$.

To produce deflections of the weakly magnetic molecules sufficient to make the apparatus sensitive to this effect, the beam is made 245 cm long; the first deflecting field is 52 cm in length and the second 100 cm.

We have tried this experiment with LiCl and observed the resonance peaks of Li and Cl. The effects are very striking and the resonances sharp (Fig. 1). A full account of this experiment, together with the values of the nuclear moments, will be published when the homogeneous field is recalibrated.

I. I. RABI
J. R. ZACHARIAS
S. MILLMAN
P. KUSCH

Hunter College (J. R. Z.),
Columbia University,
New York, N. Y.
January 31, 1938.

* Publication assisted by the Ernest Kempton Adams Fund for Physical Research of Columbia University.

[1] Kellogg, Rabi and Zacharias, Phys. Rev. **50**, 472 (1936).
[2] Rabi, Phys. Rev. **51**, 652 (1937).
[3] C. J. Gorter, Physica **9**, 995 (1936). We are very much indebted to Dr. Gorter who, when visiting our laboratory in September 1937, drew our attention to his stimulating experiments in which he attempted to measure nuclear moments by observing the rise in temperature of solids placed in a constant magnetic field on which an oscillating field was superimposed. Dr. F. Bloch has independently worked out similar ideas but for another purpose (unpublished).

Heavy Electrons from Radium E—Discussion of the Evidence

The evidence for the existence of heavy beta-rays as given in the previous two letters[1, 2] has been subject to the following objections: (a) the voltage across the velocity selector is not that determined by the voltage measuring device, (b) the resolving power of the velocity selector is zero, and/or (c) the "heavy electron" band on the film is due to ordinary electrons being multiply reflected or scattered within the selector.

Objection (a) is ruled out by the presence of the line due to the ordinary electrons in the photograph shown in my last letter.[2] This line occurs at the position on the film required by the selector velocity, $\beta_s c = E/H$.

To answer (b), we consider the velocity selector.[3] Making the approximations that the force Ee on the electron is opposite to the force $He\beta c$ on it and that the curvature $1/\rho'$ inside the selector is constant, we obtain

$$\beta_s = \beta + pm_0\beta^2 c/He\rho'(1-\beta^2)^{\frac{1}{2}}, \qquad (1)$$

where pm_0 is the mass of the electron. To obtain the resolving power, we put $\rho' = \pm l^2/8w = \pm 29.8$ cm (see previous letter). At the moment it is only necessary to show that the "heavy electron" band is not produced by ordinary electrons. The ranges of $\beta = v/c$ for the ordinary electrons allowed through the selector for the films described in my last letter are from β_1 to β_2 and from β_3 to unity, as follows:

Film	β_s	β_1	β_2	β_3	s_1	s_2	s_3	s_h
5	0.34	0.33	0.37	0.96	—	—	0.32	1.02
8	0.33	0.29	0.43	0.77	1.95	1.05	0.40	0.47

The corresponding displacements on the films are shown under s_1, s_2, and s_3. The blanks indicate that the magnetic field was great enough to prevent the ordinaries from reaching the film. The displacement of the center of the "heavy electron" band is shown under s_h. *Obviously this band could not have been produced by ordinary electrons.* Although for film 8 the selector will pass ordinaries of β from 0.29 to 0.43 and so should give a width of 0.90 cm for the ordinary line, yet the observed width is about 0.2 cm. In agreement with the theory of the selector, this indicates that the probability of the selector passing ordinary electrons is highest when $\beta = \beta_s$. For the heavies the range of β depends on the mass pm_0. Consider film 5. For $p=2$, the range of β is from 0.30 to 0.41 and from 0.85 to 1.0, while for $p=3.33$ the range is from 0.29 to 1.0. In the latter case the resolving power may be said to approach zero. In this case the magnetic field outside the selector spreads the heavies out into a combination of mass and velocity spectrum. The distribution in this spectrum depends upon the probability that an electron of a certain velocity will get through the selector and upon the relative prevalence of the beta-rays with the mass corresponding to this velocity. Although the values of p in the previous letters are not exact, they cannot be very far wrong since they are calculated from the displacement of the center of the "heavy" band. I am now using higher resolving power and shall report my results shortly.

To answer (c), I need only report the following: Using a new selector with $E = 100{,}000$ volts/cm, I have found that with $H = 740$ gauss ($\beta_s = 0.45$) both ordinary and heavy electrons are recorded, but that with $H = 830$ gauss ($\beta_s = 0.40$) no heavy electrons (or very few) are recorded although the ordinary line was quite distinct. This means that the selector was passing very few or no heavies. It also means that the multiple reflection of ordinaries is not responsible for the "heavy" band.

G. E. M. Jauncey

Wayman Crow Hall of Physics,
Washington University,
St. Louis, Missouri,
January 31, 1938.

[1] Jauncey, Phys. Rev. **53**, 197 (1938).
[2] Jauncey, Phys. Rev. **53**, 265 (1938).
[3] Dr. C. Zahn gave an excellent description of the theory of the selector at an informal meeting on January 30, 1937.

On Magnetic Anisotropy in Ferromagnetic Crystals in Weak Fields

The *Physical Review* recently published important results of Williams[1] who first studied the magnetic properties of crystals in specimens of closed form. Williams showed that the magnetization curves of crystals are different along different directions even in weak fields. The initial magnetic susceptibilities along the [100], [110] and [111] directions were found to be approximately in the ratio 6 : 3 : 2.

The fact that magnetic anisotropy may exist, even in weak fields, was indicated by Akulov.[2] Akulov came to this conclusion on the basis of the assumption that the work expended on magnetization in any direction is one and the same function of the sum of the components of the magnetization vector along the axes of easy magnetization. From this Akulov finds that in weak fields the values of the susceptibilities along the [100], [110] and [111] axes should be in the ratio of 6 : 3 : 2.

In order to explain magnetic anisotropy in weak fields Bozorth[3] assumed that when H is applied, for example, along the [110] direction the component of H along [100] will produce a magnetization in that direction given by the [100] magnetization curves. On the basis of this assumption Bozorth also comes to the conclusion that the initial susceptibility along the [100], [110] and [111] axes should be as 6 : 3 : 2.

It should be noticed that these conclusions inevitably contain certain implicit assumptions concerning the initial state of the crystal before magnetization. It is interesting to examine this question from the viewpoint of a model of the process of magnetization in weak fields, as a process of displacement of boundaries between regions of spontaneous magnetization. The model was originated in the works of Sixtus and Tonks[4] and was further developed theoretically by Becker[5] and Bloch,[6] and also in part in a recent work of the writer.[7] Starting with this model we find that in weak fields, when the spins remain directed along the

axes of easy magnetization, the susceptibility of iron may be divided into two parts, $\kappa_{||}=I_{||}/H$ and $\kappa_{\perp}=I_{\perp}/H$, where $I_{||}$ is the magnetization arising from the displacement of boundaries between regions with antiparallel resultant spins; and $I_{\perp}$ is the magnetization arising from the displacement of boundaries between regions with resultant spins forming an angle of 90°.[8] To obtain formulae for magnetic anisotropy in weak fields it is necessary to calculate $\kappa_{||}$ and $\kappa_{\perp}$ for an arbitrary direction in the crystal. After carrying out the corresponding calculations the following formula for initial susceptibility κ_0 is obtained:

$$\begin{aligned}&\kappa_0=\kappa_{||}+\kappa_{\perp},\\&\kappa_{||}=\kappa_1(n_1h_1^2+n_2h_2^2+n_3h_3^2),\\&\kappa_{\perp}=\kappa_2[n_2n_3(h_2^2+h_3^2)+n_3n_1(h_3^2+h_1^2)+n_1n_2(h_1^2+h_2^2)].\end{aligned}\tag{1}$$

where: n_1, n_2, n_3 are the parts of unit volume of the crystals in which the spins are parallel or antiparallel to the axes of easy magnetization [100], [010], [001], respectively: h_1, h_2, h_3, are the cosines of the angles between the directions of the magnetic field and these axes; κ_1 and κ_2 are coefficients independent of the direction of magnetization, provided that in any one direction of easy magnetization the magnitudes of the stress gradients, and their spatial distribution, are on an average the same as in any other.

It follows from (1) that if there is uniform distribution of the spins, i.e., if $n_1=n_2=n_3$, the susceptibility should not depend on the direction of the field. Thus the presence of magnetic anisotropy in Williams' crystals should, from the viewpoint of the model under consideration, be explained as a result of the presence of preferential spin orientations. From the calculations of Kaya and Takaki,[9] made on the basis of measurements of magnetization in crystals of iron, it follows that in the initial condition, the spins are preferentially orientated along the directions of easy magnetization for which the demagnetizing factor has the least value (in a specimen of the given form). From this it follows that in Williams' specimens, the values of n_1, n_2, n_3 could hardly be equal to one another. It is extremely possible that in specimens cut along the direction [100] the greater part of the spins were orientated parallel or antiparallel to this direction, particularly after the specimen has been magnetized once. If it happens that for $H\|[100]$ we have $n_1=1$, $n_2=n_3=0$; for $H\|[110]$ $n_1=n_2$, $n_3=0$ and for $H\|[111]$, $n_1=n_2=n_3$, i.e., if there is a most preferential orientation it follows from (1) that the initial susceptibilities in these cases should be as

$$6:\left(3+\frac{3}{2}\frac{\kappa_2}{\kappa_1}\right):\left(2+\frac{4}{3}\frac{\kappa_2}{\kappa_1}\right).$$

When $\kappa_1\gg\kappa_2$ this gives the ratio 6 : 3 : 2.

There is reason to suppose that $I_{||}$ is either entirely, or to a considerable degree irreversible and $\kappa_{||}$ represents the initial irreversible susceptibility (up to the present time, the initial susceptibility has been supposed equal to the initial reversible susceptibility). Therefore, measurements of the reversible susceptibility of these crystals would be of interest.

E. KONDORSKY

Physical Institute of the State University,
Moscow, U. S. S. R.,
December 21, 1937.

[1] H. J. Williams, Phys. Rev. **52**, 747, 1004 (1937).
[2] N. Akulov, Zeits. f. Physik **69**, 78 (1931).
[3] R. M. Bozorth, J. App. Phys. **8**, 575 (1937).
[4] K. J. Sixtus and L. Tonks, Phys. Rev. **37**, 930 (1931); **42**, 419 (1932); L. Tonks and K. J. Sixtus, **43**, 70, 931 (1933).
[5] R. Becker, Physik. Zeits. **33**, 905 (1932).
[6] F. Bloch, Zeits. f. Physik **74**, 295 (1932).
[7] E. Kondorsky, Physik. Zeits. Sowjetunion **11**, 597 (1937).
[8] It should be noticed, that in his work Akulov also divided the magnetization into two parts, the first being the magnetization arising from longitudinal inversions of spins, and the second from transverse ones, but this author considered the process of inversions of spins from a different point of view.
[9] S. Kaya and H. Takaki, J. Hokkaido. Univ. **1**, 227 (1935).

Proceedings of the American Physical Society

MINUTES OF THE INDIANAPOLIS, INDIANA MEETING, DECEMBER 28–30, 1937

THE 39th Annual Meeting (the 218th regular meeting) of the American Physical Society was held at Indianapolis, Indiana on Tuesday, Wednesday and Thursday, December 28, 29 and 30, 1937 in affiliation with Section B—Physics—of the American Association for the Advancement of Science. The presiding officers were Professor H. M. Randall, president of the Society, Dr. Lyman J. Briggs, vice president, Professor G. Breit, Professor H. A. Erikson and Professor H. H. Marvin. There were about three hundred physicists in attendance at the meeting. All sessions were held at the Indianapolis Athletic Club.

The joint session with Section B of the A.A.A.S. and the American Association of Physics Teachers was held on Tuesday afternoon at two-thirty o'clock. Dr. Harvey Fletcher of the Bell Telephone Laboratories, Inc., vice president of Section B, presided. The retiring vice president of Section B, Dean George B. Pegram of Columbia University made an address. Professor H. M. Randall of the University of Michigan, president of the American Physical Society, delivered an address on "The Spectroscopy of the Infra-Red" and Professor G. Breit of the University of Wisconsin, spoke on "Some Recent Progress in the Understanding of Nuclei."

On Wednesday evening at seven o'clock in the Lantern Room the members and friends of the American Physical Society and the American Association of Physics Teachers convened for dinner. Two hundred and sixty-five were present. President Randall presided and called upon F. K. Richtmyer, president of the American Association of Physics Teachers to speak. Professor Richtmyer in turn called upon Professor D. L. Webster to make the annual award of the American Association of Physics Teachers to Professor Edwin H. Hall of Harvard University. Professor Hall responded with an outline of the early history of the development of laboratory apparatus in the United States. He also recited one of his own sonnets to the delight of all the guests. The Chairman then called upon Dr. Lyman J. Briggs of the National Bureau of Standards and Professor G. W. Stewart of the State University of Iowa for brief remarks.

Annual Business Meeting. The regular annual business meeting of the American Physical Society was held on Tuesday afternoon, December 29, 1937 at two o'clock, President Randall presiding. The President had appointed Messrs. Walker Bleakney and H. W. Webb to canvas the ballots for the officers of the Society. They reported the following elections:

President, LYMAN J. BRIGGS
Vice President, JOHN T. TATE
Secretary, W. L. SEVERINGHAUS
Treasurer, GEORGE B. PEGRAM
Managing Editor, JOHN T. TATE
Members of the Council, four year term, G. W. STEWART, RICHARD C. TOLMAN
Members of the Board of Editors, three year term, A. L. HUGHES, F. A. JENKINS, THOMAS H. JOHNSON.

The Secretary reported that during the year there were 241 who accepted election to membership and seventeen were reinstated to active membership. The deaths of twenty members were reported, fourteen members resigned and twenty-seven members were dropped. The membership as of December 24, 1937 was as follows: Honorary Member, 5; Fellows, 745; Members, 2363; total, 3113.

The Treasurer presented a summary of the financial condition of the society. It was impossible to present a final report for the year at the Annual Meeting because the fiscal year ends on December 31. The Treasurer's financial report will be audited, printed and distributed to members.

The Managing Editor made a brief report on the general status of the publications of the society and stated that a detailed, audited financial report for 1937 would be printed and distributed.

The Annual Business Meeting adjourned at two-twenty P.M.

Meeting of the Council. At the meeting of the Council held on Tuesday morning, December 28, 1937 one candidate was elected to fellowship, eight members were transferred from membership to fellowship and thirty-five candidates were elected to membership. *Elected to fellowship:* Hilario Magliano. *Transferred from membership to fellowship:* Charles S. Fazel, R. G. Herb, Herrick L. Johnson, Edward B. Jordan, R. C. Mason, Richard D. Present, F. Simon, and Dudley Williams. *Elected to membership:* J. M. Anderson, Clarence L. Babcock, Paul D. Bales, E. Irving Bergeson, Robert J. Bessey, Rolf Buchdahl, Harold E. Clark, Vincent Dillon, Joseph D. Elder, W. A. Fowler, Philip W. Froebes, David C. Grahame, Raymond Gustafson, Donald E. Hull, William P. Hurley, F. Joliot, F. London, Myron S. McCay, R. Naidu, Marcel K. Newman, Anna R. Oliver, Robert D. Park, Herbert Schimmel, W. M. Schwarz, Takeo Shimizu, Merle A. Starr, Louis G. Stier, James A. Van Allen, A. E. Vivell, John W. Walker, Ernest T. S. Walton, Yuzuru Watase, George Welch, Gifford E. White and John S. Wiggins.

The regular scientific program of the Society consisted of sixty-four contributed papers, number 25 having been withdrawn. Numbers 19, 36, 37, 49 and 59 were read by title. The abstracts of the contributed papers are given in the following pages. An Author Index will be found at the end.

W. L. SEVERINGHAUS, *Secretary*

ABSTRACTS

1. On the Hydrodynamical Theory of the Viscosity of Suspensions. EUGENE GUTH, *University of Notre Dame,* AND OTTO GOLD, *University of Vienna.* (*Introduced by George B. Collins.*)—Einstein, in his thesis, 1906, developed a theory of the viscosity of a suspension. He calculated the disturbance which a spherical particle causes in a laminar stream of a viscous fluid. From the energy dissipated, he derived an equation connecting the viscosity of the solvent, η, with the viscosity of the suspension, η_0, the total volume, v, of the suspended particles and the volume, V, of the suspension: $\eta=\eta_0(1-2.5v/V)$. This relationship holds only for small concentrations. For higher concentrations one must take into account the mutual disturbance caused by a pair of particles of a laminar stream. This has been done by a special adaptation of the method of reflections, first introduced by H. A. Lorentz for taking into account the influence of walls on Stokes's law. A lengthy calculation leads to the result: $\eta=\eta_0(1-2.5v/V-14.1v^2/V^2)$. This equation is applicable to all solutions of high molecular substances with spherical shape, such as rubber latex solutions, protein solutions, and the changing of the viscosity of lubricating oils by the addition of small quantities of higher molecular compounds. The equation was verified experimentally in the case of suspended glass spheres.

2. The Viscosity of Monolayers: Theory of the Surface Slit Viscosimeter. WILLIAM D. HARKINS AND JOHN G. KIRKWOOD, *University of Chicago.*—The surface viscosimeter which makes use of the flow of a film through a rectangular capillary slit possesses many advantages in comparison with other types. Perhaps the greatest of these is the fact that, since it has no moving parts, no motion is imparted to the substrate (usually aqueous) by the instrument. Since surface viscosimeters which utilize moving rings or disks impart such a motion, their theory is thus made much more complicated. If

$$\alpha=f_1-f_2/l$$
$$\eta=\alpha a^3/12A-a\eta_0/\pi,$$

where a is the diameter of the slit, f the surface pressure, A is the area flux, η the viscosity of the film, and η_0 of the water, and l the length of the slit. The viscosity of a film of arachidic acid, with 20 C atoms in a straight chain, is found, in work with Dr. R. J. Myers, to be 0.0017 surface poises. Expanded films, such as that of oleic acid, have exceedingly small viscosities. Several ring surface viscosimeters have also been developed in the laboratory, and these are suitable for work with plastic films.

3. Arrangement of Molecules in Unimolecular and Multimolecular Layers. L. H. GERMER AND K. H. STORKS, *Bell Telephone Laboratories, Inc., New York, N. Y.*—Our recent study[1] of the structure of films built from many molecular layers of stearic acid by the Langmuir-Blodgett technique has been extended to *unimolecular* layers of stearic acid, and to *unimolecular* and *multimolecular* layers of barium stearate. Electron diffraction patterns from barium stearate prove that films several molecules thick have hexagonal structures with c axes parallel to axes of the hydrocarbon chains and normal to the supporting surface. Details of the patterns vary with pH of the water, which controls the amount of barium in the film. In *single molecular layers* also barium stearate molecules are arranged with axes normal to the supporting surface, but in one layer there exists almost no regularity in lateral spacings. Single layers of stearic acid molecules have the same arrangement as barium stearate in single layers, although multi-layers of the acid have an entirely different struc-

ture.[1] We suggest that this difference is due to combination of the first layer of acid molecules with a metal surface. From multi-layers of stearic acid diffraction patterns differ widely; these represent different polymorphic forms.

[1] Proc. Nat. Acad. **23**, 390 (1937).

4. Electric Moment of the Methyl and Ethyl Alcohol Molecules. J. D. STRANATHAN, *University of Kansas.*—The dielectric constant of methyl alcohol vapor has been determined at 14 temperatures between 25.0° and 206.0°C. At each temperature measurements have been made at an average of 23 different pressures ranging from zero up to near saturation. The polarization at any one temperature was obtained by a least square solution for the slope of the best straight line through observations at various pressures at that temperature. A least square solution for the best Debye line through the polarization data at different temperatures yields a preliminary value $(1.694 \pm 0.003) \times 10^{-18}$ e.s.u. for the electric moment of the methyl alcohol molecule. The moment here found is in essential agreement with values reported by Miles and by Kubo. It is obtained, however, from more extensive data, and has associated with it a smaller probable error. Data on ethyl alcohol previously published by Knowles have been recalculated, using a least square treatment throughout, and making a minor correction to the value he used for the absolute zero of temperature. The resultant moment is $(1.690 \pm 0.005) \times 10^{-18}$ e.s.u. Knowles, using largely a graphical determination of slopes, obtained 1.686×10^{-18}; no probable error was stated.

5. Permanent Electrets as a Function of the Method of Preparation. WILFRED M. GOOD, *University of Kansas. (Introduced by J. D. Stranathan.)*—Preliminary to a proposed study of the effect of the method of manufacture of electrets upon their subsequent behavior, it was deemed advisable to develop a procedure of manufacture which could be accurately controlled, and which would yield electrets with uniformly smooth surfaces and not subject to cracking. Electrets have been made in an oil bath whose temperature is automatically and continuously lowered from 90° to 30°C over a period of from 1 to 10 days. The conventional tin foil electrodes have been replaced by rigid electrodes of solid tin. The resulting electrets have exceptionally smooth and closely parallel surfaces, and show no tendency to crack provided the electric field is applied at the proper temperature (75°C). Application of the field at a higher temperature (90°C) has caused each of the 4 electrets so made to crack in a peculiar manner apparently associated with the fringing of the electric field. Preliminary measurements indicate that electrets made as described above show the same general behavior as those cooled more rapidly in air, though there is some indication that the time of aging is affected.

6. The Variation of Apparent Ionic Volumes with Concentration in Aqueous Solutions. G. W. STEWART, *State University of Iowa.*—The free ion theory of electrolytes leads to a linear relation between the apparent ionic mol volume of an electrolyte, Φ, and the square root of the concentration, c, at dilute solutions, and also to values of the rate of change of the former with the latter. While the theory is of distinct value, it is seriously inadequate. Of 208 strong electrolytes only 62 percent have the $\Phi - c^{\frac{1}{2}}$ linear variation, and with these the values of the rate of change of Φ with $c^{\frac{1}{2}}$ vary widely from the computed values, the divergence being from one-fifth to fifteen times. In 22 percent the linear relation is more nearly c than $c^{\frac{1}{2}}$. Assuming an approximately linear relation at dilute solutions the value of the exponent of c varies from a -0.5 to 2.0. The explanation of the limitation in the free ion theory is the absence of a consideration of liquid structure or of the forces that produce it.

7. The Existence of a Vitreous State in Gelatin Gels. BASILE J. LUYET, *St. Louis University.*—Gelatin gels of concentrations varying from 10 to 60 percent can take the vitreous state, that is, can be brought to temperatures at which their viscosity is of the order observed in solid bodies, but their structure is not crystalline. For that purpose, the gels are immersed in liquid air in thin layers; they then keep their transparency and isotropic properties, but are hard and breakable as glass; when they are warmed up slowly they devitrify, that is, they crystallize, at a temperature of more than 150 degrees above the temperature of ebullition of liquid air. To insure a sufficient cooling velocity during the immersion, the gel layers, when supported on glass plates 50 micra thick, can be as much as 0.5 mm thick, with a 50 percent gel, while they must not exceed a few microns with a 10 percent gel. The experimental demonstration of the fact that a high water content (90 percent) can stay unfrozen in an aqueous gel at some twenty degrees below zero requires a revision of the entire problem of "bound water."

8. Estimates of Age of the Planet from Isotope Ratios. ARTHUR BRAMLEY, *Washington, D. C.*—Recent opinion on radioactivity of potassium supports Muhloffs' value of 1.8×10^9 years.[1] With this value for the half life, the ratio of the rate of formation of argon from potassium to that of calcium is $1/10^3$ whereas considerations based on the intensity of gamma-radiation require for this ratio the value 1/100.[2] The relative abundances of Ca^{40} and K^{40} on the earth's crust taken in conjunction with this value for mean life indicate that the nuclei of Ca^{40} and K^{40} have been in equilibrium for 2×10^{10} years. This is of the same order of magnitude as the age of the stars. If during part of this time the temperature of the earth's atmosphere was over 7000°, the argon formed in that period would have escaped into interstellar space.[3] The reaction rates as calculated from the relative abundance of argon and calcium and from gamma-ray intensity can be brought into harmony provided we assume that the earth's atmosphere was hotter than 7000°, 1×10^{10} years ago. An uncertainty in these calculations arises from difficulty in determining the argon content of the earth's crust.

[1] Klemperer, Proc. Roy. Soc. **148**, 638 (1935).
[2] Bramley, Science **86**, 424 (1937).
[3] Jeans, *Dynamical Theory of Gases*, chapter 15.

9. The Relation Between Stefan's Radiation Law and Nernst's Heat Theorem. ARTHUR E. HAAS AND EUGENE GUTH, *University of Notre Dame.*—Although Nernst's heat theorem represents an independent thermodynamic principle, the vanishing of the zero entropy may be derived from "classical" principles in the special case of the black-body radiation. We start with the energy equation of classical thermodynamics: $(\partial U/\partial V)_T = T(\partial P/\partial T)_V - P$, where U is the energy, V the volume, T the temperature, and P the pressure. In applying this general relation to the black-body radiation we make use of Stefan's law according to which the density of energy u is equal to aT^4, a being a constant. The integration of the resulting differential equation leads to the expression for the radiation pressure: $p = \frac{1}{3}aT^4 + bT$, b being another constant. The insertion of this result into thermodynamical formulas yields the following equation for the entropy: $S = \frac{4}{3}aT^3V + bV$. From Maxwell's electromagnetic theory we have: $p = u/3$. Comparing this with the above expression for the radiation pressure, and remembering that $u = aT^4$, we see that b must be zero. This, however, requires that S be zero when $T = 0$. The statistical interpretation of the entropy of the black-body radiation leads to the result that the number of photons emitted by a black body is proportional to T^3.

10. The Persistence of Molecular Vibration in Collisions. ROBERT J. DWYER, *R.C.A. Institutes, Inc., Chicago, Ill.*—The dispersion of sound, discovered by G. W. Pierce and theoretically interpreted by K. F. Herzfeld and F. O. Rice, indicates a slow transfer of energy between translational and vibrational molecular degrees of freedom. It seemed desirable to find a direct optical method of observing and measuring this effect. Apparatus has been developed in this laboratory for the purpose of investigating molecules present in very small concentration, like radicals, by their absorption spectra.[1] The lines of the rotational structure of any branch of a band indicate by their intensities the relative concentrations in different rotational levels. The relative concentrations of molecules responsible for two absorption spectra may therefore be determined merely by matching rotation lines. The shift of concentrations from lower to upper vibrational levels caused by the electrical discharge was observed in iodine vapor by comparing intensities of the absorption spectrum with those when the discharge was on. By varying the phase between an electric switch and optical shutter snapshots of the absorption spectrum could be taken at different intervals after the discharge was interrupted. Iodine molecules raised from the zero to the first vibrational level were able to persist in this level through several thousand collisions with other iodine molecules before losing their vibration.

[1] A. A. Frost and O. Oldenberg, J. Chem. Phys. **4**, 782 (1936). A. A. Frost, D. W. Mann and O. Oldenberg, J. Opt. Soc. Am. **27**, 147 (1937).

11. A Study of the Anisotropy of the Atomic Vibrations of a Zn-Cu Alloy. R. A. HOWARD, *Washington University, St. Louis, Mo.*—The atomic structure factors for an alloy of zinc and copper in the ϵ phase, containing approximately fifteen atomic percent of copper, have been measured. This alloy has an hexagonal lattice with an axial ratio of 1.56, which is less than the value of 1.633 for close-packed spheres. It has been shown for pure zinc[1] and pure cadmium,[2] which both have an axial ratio greater than 1.633, that the atomic vibrations are greater along the c axis than perpendicular to it. One might, therefore, be led to expect that in the case of a crystal in which the atoms are separated by less than the normal distance along the c axis, as is the case for the Zn-Cu alloy used here, the atomic vibrations would be less along the c axis than in a direction normal to it. The results show this effect very strikingly. The structure factor curve bears a remarkable similarity to that obtained by Wollan[3] for a Cd-Ag alloy, which also possesses a hexagonal lattice and an axial ratio of 1.56.

[1] G. W. Brindley, Phil. Mag. **21**, 790 (1936). G. E. M. Jauncey and W. A. Bruce, Phys. Rev. **50**, 408 (1936). E. O. Wollan and G. G. Harvey, Phys. Rev. **51**, 1054 (1937).
[2] G. W. Brindley, Proc. Leeds Phil. Soc. **3**, 200 (1936).
[3] E. O. Wollan, reported at Thanksgiving meeting (1937).

12. Calculation of Transition Energies of Polymorphous Molecular Crystals. M. BRUCH-WILLSTÄTTER AND H. SPONER, *University of Wisconsin and Duke University.*—A number of crystals show at low temperatures the phenomenon of a transition from an oscillatory motion of their molecules to a rotational one. In many cases the lattice type is preserved during the transition, which is usually not sharp but covers a range of temperature of several degrees. In other cases, however, the transition is connected with a change in crystal structure which sets in sharply at a definite temperature. Transition energies have been determined experimentally for a number of cases by several authors. Here a calculation of these transition energies has been carried out for N_2, CO, HCl and HI by using London's simple theory of van der Waals forces. The first three substances show transitions with a change in crystal structure while HI represents an example of the other type. The calculated values come out larger than the experimental ones, some by a factor 2, but no more can be expected from the approximative treatment. A more accurate calculation is rendered difficult because of lack of experimental data.

13. Segregation of Polonium in Bismuth Crystals. ALFRED B. FOCKE, *Brown University.*—The study of the distribution of polonium as an impurity in bismuth crystals reported some time ago[1] is continued, using improved methods of high speed counting of α-particles. Measurements on over twenty crystals confirm the results of the earlier paper showing that the polonium is segregated into small regions separated by distances of $(0.55 \pm 0.01)\mu$ and $(0.86 \pm 0.03)\mu$ in directions parallel to the [111] and [11$\bar{1}$] axes, respectively. It is also found that where twinning due to cold working occurs the spacing along the original [111] axis changes to that expected along the [11$\bar{1}$] axis, the distribution of impurity thus following the crystallographic change. This must indicate either a large scale migration of the polonium at relatively low temperatures

or that the twinning process is not atomic in nature but that relatively large regions of the crystal change their positions as entities.

[1] A. B. Focke, Phys. Rev. **46**, 623 (1934).

14. Radioactivity of Air, Water, Cave and Soil Gases. OSCAR G. FRYER, *Drury College.* (*Introduced by R. R. Ramsey.*)—An electroscope is described which has new features particularly suited for field work. Tests were made on caves and springs in Ozark, Wichita, and Arbuckle Mountains of Arkansas and Oklahoma. Also a series of tests covering a period of 8 months was made on caves, springs, air, and soil gases in the limestone belt of Indiana. Rainfall affects the radon content in some springs more than in others. Radioactivity is not proportional to rainfall, yet a continued dry period is marked by an appreciable decrease in activity of most springs. There is no correlation between atmospheric pressure and radon content of spring water in the vicinity of Indiana University. In the limestone belt it is thought that the source of activity is in the soil and not in the limestone below as no limestone caves there showed any activity while the soil above was very active. Radon content of soil gases increases with depth. Radioactivity of the soil decreases with continued rainfall but is not affected by barometric pressure. Radon content of soil gases here is much greater than in other countries, while the activity of the air is less.

15. Photographic Measurements of the Brownian Motion. CHAS. HIRE, *Murray State Teachers College.* (*Introduced by W. L. Severinghaus.*)—Gamboge particles of uniform size were suspended in water. Positions of the particles in a suitable sealed microscope slide were recorded instantaneously at intervals of 1/128 second by a photographic method using an electric spark as the light source. Particle diameters were determined from the rate of settling by applying Stokes' formula. In addition to the Brownian agitation, the photographs revealed field vibrations in which all particles moved in the same directions simultaneously. Simple corrections for the field vibrations gave the true Brownian Displacements. Calculations from the corrected data gave for Avogadro's Constant a value of 7×10^{23} molecules per mole, and calculations from the uncorrected data gave results comparable with those of Henri. The paper contains a brief discussion of corrections needed for the law of Stokes. Apparatus and data table are illustrated with lantern slides.

16. The Variation of Contrast with Wave-Length in Photographic Materials. W. R. KOCH, *Materiel Division, U. S. Army Air Corps, Wright Field.*—Contrast data obtained for different wave-lengths with various photographic materials were reported. Measurements extended through the visible and near ultraviolet regions and included the effect of varied development conditions. The relation of these results to the selection of suitable emulsions for photographic photometry was discussed. Applications of the data in the field of chemical analysis by spectrographic methods as well as in the field of color photography were noted.

17. Anodic Properties of the Aluminum Cell. W. B. PIETENPOL AND T. EDWIN DEVANEY, *University of Colorado.*—Further experiments substantiate the previously proposed theory that in the aluminum cell the active film is composed of colloidal aluminum hydroxide which partially traps anions but allows cations to pass. The generally accepted Gunther Schultze theory, which assumes that the high resistance is due to a thin gas film, predicts that the capacitance should decrease with drop in voltage and increase with drop in temperature. Experiments show that, in accord with the hydroxide layer theory, the capacitance remains nearly constant with drop in voltage and decreases slightly with drop in temperature. With ammonium hydroxide the electrolyte, aluminum hydroxide is formed and there is evidence that the high resistance is due to it. With oxalic acid, the electrolyte, the exposure of the anode to air for a time causes the current upon the anode's return to the solution to remain for some time below its former value. For this and similar effects, no explanation can be given by the Gunther Schultze theory. However all results are in accord with the proposed slow hydrolysis of aluminum oxide to aluminum hydroxide.

18. The Width of the Resonance Peaks in Disintegration of Boron by Protons. JAMES S. ALLEN, ROBERT O. HAXBY, JOHN H. WILLIAMS, *University of Minnesota.*—The width of the resonance peak occurring in the reaction $B^{11}+H^1\rightarrow Be^8+He^4+Q$ has been measured for targets of various thicknesses. For a pure Boron target of thickness sufficient to slow 160 kv protons by about 500 volts, the full width at half-maximum was approximately 10 kv. The peak occurred at 159 kv. The transformer kenetron set, ion source, and accelerating tube described by Williams, Wells, Tate and Hill[1] were used. A new voltmeter consisting of 250 10 meg. resistors was used for the voltage measurements. By tapping off a small fraction of the total voltage across the voltmeter, the amount of ripple in the voltage supply was measured with a cathode-ray oscillograph. At 170 kv the total ripple was 4500 volts, or 2.6 percent. The resonance occurring in the reaction $B^{11}+H^1\rightarrow C^{12}+\gamma$ has been studied for thick Boron targets. Using a G.M. tube, the number of γ-rays was determined as a function of the tube voltage. When differentiated the curve was similar to that for the above reaction and the peak occurred at approximately the same voltage.

[1] Williams, Wells, Tate, Hill, Phys. Rev. **51**, 434 (1937).

19. The Angular Distribution of Resonance Disintegration Products. R. D. MYERS, *Purdue University.*—An attempt is made to account by symmetry considerations for the anisotropy observed in the angular distribution of products of nuclear disintegrations. The Bethe-Placzek[1] method of averaging the cross section of a nuclear disintegration over the several spin orientations is adopted so as to be suitable for finding A_L, the average Lth coefficient of the expansion in spherical harmonics of the angular intensity. The dependence of A_L on L is found to occur only through certain coefficients whose variation with L

can be calculated. For resonance the formula simplifies and may even reduce to one term so that the variation with L is known and the slope of the curve for the angular distribution of the products is completely determined. The theory is applied to the disintegrations (1) $D^2+D^2 \rightarrow H^3+H^1$ and (2) $B^{11}+H^1 \rightarrow Be^8+He^4$. With certain assumptions as to the scheme by which the disintegration occurs the distributions of the protons and α-particles are found to agree with those observed experimentally by Neuert.[2]

[1] Bethe and Placzek, Phys. Rev. **51**, 450 (1937).
[2] Neuert, Physik. Zeits. **38**, 122 (1937).

20. Capture Cross Section for Thermal Neutrons. A. H. SPEES, W. F. COLBY AND S. GOUDSMIT, *University of Michigan.*—The density of thermal neutrons in a hydrogenous substance is proportional to their rate of production and inversely proportional to their rate of absorption, provided the density varies linearly around the position of the measurements. The addition of a small amount of cadmium salt does not change the production but increases the absorption. This provides a simple method to determine the capture cross section of various solutions and mixtures in terms of that of cadmium. The neutron density was measured by the activity of silver foils put horizontally at the center of a cylindrical vessel of 26 cm diameter and the same height which was placed near the Michigan cyclotron. The effect of the silver foil (0.067 g/cm²) on the density was estimated by using a few thicknesses and extrapolating (about 7 percent) to zero thickness. It was verified that the reciprocal of the activity (corrected for nonthermal neutrons) is indeed a linear function of the cadmium concentration up to about 0.08 moles of Cd in 100 moles of H_2O when the cross section is increased by a factor five. For water the results gave $\sigma(H_2O)=.00020\sigma(Cd)$, for NaCl a preliminary measurement gives $\sigma(NaCl)=.014\sigma(Cd)$. With $\sigma(Cd)=2600\cdot10^{-24}$ cm² this yields $\sigma(H)=.26\pm.02\cdot10^{-24}$ cm² (neglecting $\sigma(O)$) and $\sigma(NaCl)=36\pm4\cdot10^{-24}$ cm².

21. Neutron Yields from Deuteron Reactions at High Energy. LUIS W. ALVAREZ, *University of California.*—The relative neutron yields from 15 elements bombarded with 7.6 Mev deuterons have been measured with ionization chambers, and in some cases checked with radioactive detectors. The thick target yield *vs.* Z curve is very nearly of the form $Y=ke^{-Z}$, and all 12 elements tried from Li to Sn gave points which lay very closely on a smooth curve. Background neutrons from the cyclotron prevented the curve from being carried to higher Z. Carbon has been most carefully investigated; excitation functions for the production of N^{13} and of neutrons have been compared, and the number of N^{13} atoms at saturation has been compared with the number of neutrons per second from Carbon (determined by standardization with a Ra+Be source). The relative neutron yields for C and Ni have been compared with their relative radioactive yields. All three of these comparisons indicate that the number of neutrons from C is larger than can be accounted for by the reaction leading to N^{13}. The most satisfactory explanation at present is that the following reaction is responsible for the excess: $C^{12}+d \rightarrow C^{12}+n+p$. This represents a capture followed by two Bohr evaporations.

22. Radioactivity Induced in the Rare Earth Elements by Fast Neutrons. M. L. POOL, *Ohio State University.*—With the exception of illinium, thulium and lutecium all the rare earth elements (fifteen in number) have been bombarded with slow and fast neutrons. The fast neutrons were obtained by the lithium plus deuteron reaction. Deuterons of 6.3 Mev were produced by the cyclotron in Professor Cork's laboratory at the University of Michigan. Most of the slow neutron periods have already been found by other observers. However, changes and additions have been necessary in some cases, probably because of the greater slow neutron equivalent of the cyclotron or the higher purity of the elements used. Several of the rare earths were spectroscopically pure. Since it is difficult to assign definitely to a nucleus a radioactive period based upon evidence from slow neutron activation alone, fast neutron activation is of great advantage. Deuteron activation was also used in a few cases. In all, twenty-six different radioactive periods have been observed. Of these, twenty have been placed with reasonable certainty. There are seven cases in which the radioactive body emits positrons. Evidence exists for three new stable rare earth nuclei on which radioactive nuclei terminate.

23. Radioactivities Induced by High Energy Protons. L. A. DUBRIDGE, S. W. BARNES, E. O. WIIG, J. H. BUCK AND C. V. STRAIN, *University of Rochester.*—Studies previously reported on proton induced radioactivities have been extended. It appears that for nearly all elements so far studied above O^{16}, which show induced radioactivity, the reactions must be of the p-n type. In the light elements this leads to a positron emitting isotope and the reactions have thresholds at 1.8 Mev plus the positron energy. For heavier elements electron emission is preferred and such isotopes can be formed at much lower energies (1.4 Mev). The following e^+ emitting isotopes have been formed: O^{15} (2.1 m); F^{18} (107 min.); Mn^{52} (40 m); Cu^{61} (3.2 hr.); Ga^{68} (68 m); Se^{75} (105 m); Ag^{106} (25 min.); Sn^{113} (14 m). The following e^- emitters have been found: Cu^{64} (12 hr.); Ga^{70} (18.2 m); Br^{80} (18 m, 4 hr.); Br^{82} (36 hr.); Ma^x (0.5 m, 31 m); Ag^{108} (2.4 min.). In most cases these periods check with previous observations. Yield curves for + and − emitting isotopes of the same element ($Ga^{68, 70}$) show pronounced differences, as do the curves for the two periods of Br^{80}. The excitation function for the O^{18} p-n reaction shows a peak at 3.6 Mev, the top of the potential barrier.

24. The Radioactive Isotopes of Zinc. R. L. THORNTON, *University of Michigan.*—The radioactive isotopes of zinc have been investigated through the bombardment of Zn and the neighboring elements Cu and Ga with high energy deuterons and with slow and fast (Li+D) neutrons. Chemical separations of the bombarded element were made and the observed half-periods in Zn are shown in the following table.

Bombarded Element	Projectile	Periods Observed in Zn
Zn	*D*	60 min., 14 hr. (4 d., 30 d.)
Zn	Slow neutrons	60 min., ~10 hr. (weak)
Zn	Fast neutrons	40 min., 14 hr.
Cu	*D*	65 min.
Ga	*D*	14 hr. (in addition to other periods)

These results, in combination with those of other workers, make possible a provisional assignment of the observed periods as follows: Zn^{63} 35 min., Zn^{65} 1 hr., Zn^{69} 14 hr. This is on the reasonable assumption that the 40 min. period observed from fast neutron bombardment of Zn is really due to a combination of the known 35 min. period of Zn^{63} with the 1 hr. period found from the other reactions. It would seem reasonable also to ascribe to Zn^{71} a period either of 4 d. or 30 d. These activities however are not strong and must be investigated further. The observation that radioactivity is produced in Zn through deuteron bombardment of copper would suggest either a (D, γ) reaction from Cu^{63} or a $(D, 2n)$ reaction from Cu^{65}, since the observed intensity makes Zn contamination of the Cu unlikely.

25. On the Thermoelastics and Structure of Rubber. F. E. DART AND EUGENE GUTH, *University of Notre Dame.* (*Introduced by George B. Collins.*)—In an exactly analogous manner as for gases, one can formulate for rubber a state equation for unilateral deformations by studying its thermoelastic behavior. From such a state equation important conclusions may be drawn toward a molecular theory of the rubber structure. Experimentally one can get information on the state equation of rubber (or any other material) by investigation of: (1) The stress-strain diagram at different temperatures; (2) The dependency of the stress on the temperature at constant length; (3) The dependency of the length on temperature at constant stress. (1) was handled by Ornstein and his co-workers, but only in the adiabatic case. (2) was handled by Meyer and E. Ferri. (3) was handled by M. L. Braun and also H. Bouasse. Meyer-Ferri and Braun investigated samples of almost the same composition and vulcanization but their results differ. Our general conclusion is, that there are samples of rubber for which a state equation of the van der Waals type holds. This is also in accordance with the new statistical theory of the elasticity of rubber.[1] Further experiments under well-defined conditions are still in progress at University of Notre Dame.

[1] E. Guth, "Statistical Theory of the Elasticity of Natural and Artificial Rubber and Similar Long Chain Compounds," Paper presented at the International Conference on Rubber, Paris, June 1937; "Revue general du Caoutchouc," in print.

26. Air Driven Tubular Vacuum Type Centrifuge. J. W. BEAMS AND C. SKARSTROM, *University of Virginia.*—The method[1] of spinning long tubes and rods in a vacuum has been improved and extended. By reducing the free air space directly beneath the driving turbine, much heavier rotors may be supported upon the air cushion by simply increasing the pressure of the air. Rotors weighing 75 lbs. have been supported and spun with ease. Rods 25 inches long and 2 inches in diameter have been spun with great stability. The maximum rotational speed in all cases is set only by the strength of the rotor. A multi-stage vacuum type centrifuge for vapors consisting of 19 "theoretical" centrifuges connected in series and mounted in an alloy steel tube 14 inches long and 4 inches in diameter has been constructed. The application of the tubular centrifuge to the separation of isotopes is discussed.

[1] Beams, Linke and Skarstrom, Science **86**, 293 (1937).

27. A Convenient Light Source for a Ten Inch Wilson Cloud Chamber. WILSON M. POWELL, *Kenyon College.*—The new Westinghouse coil-coil filament 60 watt clear lamp is arranged with the filament in a straight line. This type of filament will replace the usual type in all common bulbs in the future and can be purchased for 20 cents. It is possible to choose bulbs such that when the back surface is silvered on the outside the image from the mirror falls directly above and in the plane of the filament itself. Two plano-convex lenses six inches in diameter and nine inches in focal length are placed before the bulb with their convex surfaces together. They are adjusted so that an image of the double filament exactly fills the edge of the cloud chamber. A mirror on the far side of the chamber reflects the light back through again. By using four bulbs with their corresponding condensers and operating them on 220 volts d.c., good photographs of cosmic-ray tracks were obtained on "Super-X Panchromatic" film at f: 3.5. The lights were turned on automatically by counter control for about 1/15th of a second. No shutter was used on the camera. The bulbs were still in good condition after 100 flashes. This work was done at the Bartol Research Laboratory.

28. Effect of Valence Electrons on Intensities in Electron Scattering from Zinc Oxide. VIVIAN A. JOHNSON AND HUBERT M. JAMES, *Purdue University.*—A comparison of the intensities in electron and x-ray diffraction patterns from zinc oxide discloses systematic anomalies, if, as is usual, one employs formulas valid for a system of spherically symmetric atoms.[1] The qualitative character of the discrepancies indicates a polarization of the atoms parallel to the line between each zinc atom and the nearest neighboring oxygen. It has been shown that the anomalies cannot be due to polarization of the inner shells of the atoms by intracrystalline fields.[2] To determine whether they can be due to the asymmetrical distribution of the relatively few valence electrons, we have carried out computations with a simple model. Two of the valence electrons of each zinc-oxygen pair of nearest neighbors we have supposed to be in uniform distribution through the crystal, the other two in a uniform linear distribution between the neighboring nuclei. The form factor for this distribution was added to the Pauling-Sherman[3] expression for the symmetrical distribution of the other electrons, and the total used in computing corrected structure factors for the crystal. Within the limits of experimental error these cor-

rected structure factors agree with those obtained from measured electron diffraction intensities.

[1] H. J. Yearian and K. Lark-Horovitz, Phys. Rev. **42**, 905 (1932). K. Lark-Horovitz, H. J. Yearian and J. D. Howe, Phys. Rev. **47**, 331 (1935). H. J. Yearian, Phys. Rev. **48**, 631 (1935).
[2] V. A. Johnson and L. W. Nordheim, Phys. Rev. **51**, 1002 (1937).
[3] L. Pauling and J. Sherman, Zeits. f. Krist. **81**, 1 (1932).

29. Secondary Emission of Electrons from Sodium Films on Tantalum.* PAUL L. COPELAND. *The Research Foundation, Armour Institute of Technology.*—Sodium films condensed on tantalum plates in vacuum lacked luster, and, although the photoelectric work function was very low, secondary emission (as in work by Bruining and Boer[1]) was very low. Mild heat treatment increased luster and the secondary emission rose to maxima of about five secondaries per primary. When logarithms of secondary to primary ratios are plotted against primary energies, slopes just beyond the maxima are characteristic of sodium. For higher primary energies slopes are characteristic of tantalum. The primary energy corresponding to the inflection increases with film thickness. Measurement of films was made by microtitration of the sodium with dilute hydrochloric acid using phenolphthalein as indicator. Inflections at 2.5, 3.5, 3.8, 3.2 and 3.7 kilovolts correspond respectively to measurements of 2, 6, 7, 8, and 9 micrograms of sodium per square centimeter. Inconsistencies in this sequence indicate errors which may be as great as 25 percent. All the evidence, however, indicates that films of sodium 200 monatomic layers thick on tantalum yield secondary emission characteristic of the sodium up to primary energies of about 3 kilovolts; for higher energies the characteristics of the tantalum begin to influence the results.

* Preliminary report of work supported in part by a grant-in-aid from the National Research Council.
[1] Physica **4**, 473 (1937).

30. Design and Construction of an Electron Velocity Analyzer for Ionization Probability Measurements. M. E. BELL, E. A. COOMES, AND W. B. NOTTINGHAM, *Massachusetts Institute of Technology.*—A tube constructed by M. E. Bell used an indirectly heated "oxide" cathode electron source. The electrons were accelerated into a semi-circular "magnetic" analyzer with 0.4 mm entrance and exit slits. Electrons leaving the analyzer were accelerated into the ion chamber, also semi-circular, with slits defining a circle with 3 cm radius. An electron collector at the exit slit converted the chamber into a second velocity "spectrometer." Results obtained were in general agreement with E. O. Lawrence[1] except for an apparent yield of ions at less than 10.4 ev. To distinguish between electrons leaving the ion collector and ions arriving two grids surrounding the collector are needed. E. A. Coomes rebuilt the original tube with this modification but was unsuccessful because the cathode heating current disturbed the magnetic field. A third tube built by W. B. Nottingham used a thoriated filament heated by 300 cycle pulsating current as the electron source and such carefully constructed parts that the tube serves as a means of determining e/m for the electron. ($1.760 \pm .003 \times 10^7$ abs. e.m.u.) Since this is possible, an absolute scale of electron energies is thus available and the ionization probability curve may be accurately placed on the energy spectrum without making any assumptions as to contact difference in potential.

[1] E. O. Lawrence, Phys. Rev. **28**, 947 (1926).

31. Ionization of Mercury Atoms as a Function of the Bombarding Electron Energy. W. B. NOTTINGHAM, *Massachusetts Institute of Technology.*—The experimental tube described in the above abstract has been used to determine the ionization produced in mercury vapor as a function of the electron energy. The salient results obtained are the following: (1) Ionization commences at 10.38 volts with a sharply rising probability curve of small magnitude compared with that of the second mode of ionization. (2) Electrons with an energy of 10.9 electron-volts have about sixteen times higher probability of ionization than those with 10.4 electron-volts. (3) The probability curve has a maximum at this energy as was shown by the experiments of E. O. Lawrence, although he computed its value as 11.29 volts on the assumption that no contact difference in potential existed between the inside and the outside of the ion chamber. (4) The photoelectric emission produced by the radiation from the excited atoms is remarkably strong and shows many sharp maxima and minima which would, of necessity, be confused with "ultra-ionization" potentials unless special provision were made to eliminate this effect. This may very well account for the many critical potentials observed by P. T. Smith.[1]

[1] P. T. Smith, Phys. Rev. **37**, 808 (1931).

32. The Distribution of Energies Among the Incoming Cosmic-Ray Electrons. I. S. BOWEN, R. A. MILLIKAN AND H. V. NEHER, *California Institute of Technology.*—The distribution of energies has been studied by taking cosmic-ray ionization curves practically up to the top of the atmosphere at four different latitudes between 0° and 60° N magnetic. The maximum number of incoming electrons is found at about 5 billion e-volts. The numbers fall off to very small values above 30 billion e-volts and also below 3 billion e-volts. In other words, the incoming particle rays are largely limited to a definite band of energies either because of the mode of origin of the rays or because of this, plus possible blocking effects of celestial magnetic or electric fields.

33. The East-West Effect in Southern India. H. V. NEHER, *California Institute of Technology.*—In the month of November 1936 two sets of three large (37 cm × 7 cm) Geiger-Müller counters were used to measure the East-West effect at Kodaikanal (geomagnetic latitude 0°, elevation 7800 ft.) in southern India. One set was used to measure the azimuthal effect while the other recorded the zenith angle effect. Comparison of one set of readings with the other shows that the data are self consistent. Somewhat larger relative values of the West excess are found than those reported by Johnson[1] in Peru. By using the data of Bowen, Millikan and Neher[2] and of Johnson[1] on the apparent absorption coefficient of the radiation due to charged particles, an empirical relationship is found

connecting μ and E. Further, an empirical formula is found from the balloon data of Bowen, Millikan and Neher[3] for the energy distribution of the particles incident on the top of the atmosphere. An application of these two relationships to the East-West effect explains satisfactorily the West excess at the equator. This indicates that the charged particles responsible for the West excess are of the same nature as those which give the latitude effect—namely, electrons. The analysis further indicates that of the total radiation at 7800 ft. elevation in southern India at least one-fourth is due to positrons.

[1] T. H. Johnson, Phys. Rev. **48**, 287 (1935).
[2] Phys. Rev. **52**, 80 (1937).
[3] Some data are used which will be published in the near future.

34. The Latitude Effect for Cosmic-Ray Showers. W. H. PICKERING AND H. V. NEHER, *California Institute of Technology.*—Two Geiger counter sets have been taken from San Francisco to India via Japan and return via Australia. Both the vertical intensity and the shower intensity were measured as a function of latitude. By using large counters in the Neher-Harper circuit,[1] quite reliable results were obtained. The latitude effect for the vertical rays was found to be 14.5 percent in the region of the East Indies and 10 percent in the Pacific Ocean. Both these results are in good agreement with those found with electroscopes in the same regions.[2] The showers show a much smaller latitude effect amounting to about 6 percent in the East Indies. There is also some evidence that the "plateau" of the curve giving the variation of the showers with latitude extends to lower latitudes than the corresponding "plateau" of the curve for the vertical rays. These results show that the latitude sensitive part of the radiation is relatively not as efficient at producing showers as the nonlatitude sensitive component.

[1] Neher and Harper, Phys. Rev. **49**, 940 (1936).
[2] Millikan and Neher, Phys. Rev. **47**, 205 (1935).

35. The Energy Flux of the Corpuscular Cosmic Radiation. C. G. MONTGOMERY AND D. D. MONTGOMERY, *Bartol Research Foundation of the Franklin Institute.*—Recent improvements in the measurement of very high energies in cloud expansion chambers make it possible to estimate what fraction of the total cosmic ray energy crossing a horizontal surface occurs in the form of kinetic energy of charged corpuscular rays. The total amount of the energy flux may be obtained by integrating the cosmic-ray ionization from the point considered to infinity, since all of the cosmic-ray energy is eventually dissipated in the ionization and excitation of atoms. The energy flux is conveniently expressed by the mean energy per corpuscular ray recorded in a counter telescope. This mean energy is computed for vertical rays from the data of various observers, and is found to increase continuously from a minimum value near the top of the atmosphere as the atmospheric depth increases. The value at sea level is 3.04×10^9 volts. The mean energy measured by P. M. S. Blackett in his expansion chamber is 3.11×10^9 volts. We therefore conclude that, at sea level, practically all of the cosmic-ray energy is carried by charged particles. This is not in accord with the theoretical behavior of a beam of electrons and their secondaries, since in that case half of the energy would be in the form of photons.

36. Cosmic Radiation and the Earth's Magnetism. THOMAS H. JOHNSON, *The Bartol Research Foundation of the Franklin Institute.*—Records during the April 1937 magnetic storm, reported by Forbush[1] and Hess and Demmelmair[2] have shown that a world wide decrease of cosmic ray intensity, j, occurred during the period of weakened horizontal field strength, H. The effect for three widely separated stations can be expressed by (1) $Hdj/jdH=10$. On the assumption that the effect was due to a change in the earth's magnetic moment, M, consistency with the latitude and asymmetry effects requires that (2) $Mdj/jdM=-0.2$. Combining (1) and (2), $dM/dH=50a^3$ which is fifty times the value of this coefficient if the effect were due to internal disturbances. If the disturbance were caused by a system of external circular currents distributed as $\cos\lambda$ over the surface of a sphere of radius a' then[3] $dM/dH=-(2a'^3-a^3)/3$ which reduces to $-a^3/3$ if the currents are in the outer atmosphere. It would be necessary to have $a'=4a$ if numerical agreement is to be realized, but this result is trivial since a system of currents at such a distance would weaken rather than strengthen the field in the space where the cosmic rays suffer most of their deflection. It is concluded that the storm effect is at least 150 times greater than can be accounted for by increased bending of the orbits in any field reconcilable with the magnetic variations.

[1] S. E. Forbush, Phys. Rev. **51**, 1108 (1937).
[2] V. F. Hess and A. Demmelmair, Nature **140**, 316 (1937).
[3] S. Chapman, Nature **140**, 423 (1937).

37. A New Analysis of Cosmic Radiation Including the Hard Component. L. W. NORDHEIM, *Duke University.*—A careful comparison of the high altitude cosmic-ray data at different latitudes[1] gives very strong support to the assumption of practically quantitative validity of the radiation theory up to energies of some 10^{10} ev. The analysis shows further the necessity of a separate "hard component" and allows an estimate of its intensity at high altitudes. These data together with the geomagnetic effect at sea level, the energy distribution near sea level[2] and the absorption curve at great depths below sea level[2] (all pertaining to the hard component) can be explained simultaneously by assuming that, in addition to normal ionization, the hard rays are absorbed by a discontinuous process (probably connected with shower production) the cross section of which decreases for increasing energy. A reasonably good quantitative representation of all the data mentioned is given by a primary distribution[3] proportional to E^{-n} (E=energy; $n\sim3$) for both electronic and hard rays with electrons being the more numerous and behaving according to theory, and the absorption coefficient for the hard rays being proportional to E^{-1} for $E>8\times10^9$ ev. A large number of other facts (especially about showers) gives a qualitative confirmation of this picture.

[1] Pfotzer, Zeits. f. Physik **102**, 41 (1936) (geomagnetic latitude 50°); Bowen, Millikan, Korff and Neher, Phys. Rev. **50**, 579 (1936) (38.5°); Bowen, Millikan and Neher, Phys. Rev. **52**, 80 (1937) (3°).
[2] Blackett, Proc. Roy. Soc. **A159**, 1 (1937).
[3] As already suggested by Heitler, Proc. Roy. Soc. **A161**, 1 (1937), and Nordheim, Phys. Rev. **51**, 1110 (1937).

38. Energy Losses of Pauli-Weisskopf Particles. J. F. CARLSON, *Purdue University.*—The work of Anderson and Neddermeyer[1] and of Street and Stevenson[2] lends plausibility to the idea of the existence of a corpuscular component in the cosmic rays that can be identified neither with particles of electronic nor of protonic mass. Street and Stevenson[3] offer evidence that this mass is in the neighborhood of 100 times the electronic mass. Since the information about these particles is as yet incomplete, it will be of some interest to compare the behavior to be expected if these particles possess a spin of $\frac{1}{2}$ unit, i.e., satisfy a Dirac wave equation, or if they should have zero spin and be described by a scalar wave function proposed by Pauli and Weisskopf.[4] The various methods of energy loss for particles satisfying the Pauli-Weisskopf scalar equation have been investigated and a comparison of these results with the results obtained for a particle possessing spin will be given.

[1] Neddermeyer and Anderson, Phys. Rev. **51**, 884 (1937).
[2] Street and Stevenson, Phys. Rev. **51**, 1005 (1937).
[3] Street and Stevenson, Phys. Rev. **52**, 1003 (1937).
[4] Pauli and Weisskopf, Helv. Phys. Acta **27**, 709 (1934).

39. Cosmic-Ray Observations in the Stratosphere. L. F. CURTISS, A. V. ASTIN, S. A. KORFF, L. L. STOCKMANN AND B. W. BROWN, *National Bureau of Standards and Department of Terrestrial Magnetism, Carnegie Institution.*—Using radio methods it has been found possible to record the response of a Geiger-Müller tube counter to cosmic rays at altitudes up to 116,000 feet. Records were made automatically by means of a recording receiver at a ground station. The averaged results from the 12 highest flights show a gradual rise in cosmic-ray intensity which is clearly evident at a pressure of about 500 millibars and then decreases slightly at a pressure of about 300 millibars after which the rise to maximum intensity at a pressure of about 100 millibars is very rapid. This maximum is about 150 times the count recorded near the ground level and is followed by a rapid decrease in counting rate at pressures below 100 millibars. At the highest altitude reached, approximately 116,000 feet, where the pressure is only 5 millibars, the counting rate falls to a value which is about the same as that observed at a pressure of 500 millibars. The general trend of these observations indicates that as the limit of the atmosphere is approached the counts continue to decrease, confirming the view which has been put forward by other observers that the greater part of cosmic-ray phenomena are due to secondary effects generated within our atmosphere.

40. The Infrared Absorption by the Selenium Hydrides. WILLIAM C. SEARS, DONALD M. CAMERON AND HARALD H. NIELSEN, *Ohio State University.*—The fundamental bands in the infrared absorption spectra of the molecules H_2Se, HDSe and D_2Se have been located and preliminary measurements on their rotational structures carried out. *H_2Se:* The centers of the fundamental bands for H_2Se, adopting Dennison's notation, are as follows: $\nu_1=2300$ cm^{-1}, $\nu_2=1110$ cm^{-1} and $\nu_3=2380$ cm^{-1}. Their identification rests on the fact that the bands at 2300 cm^{-1} and 1110 cm^{-1} appear to have similar structures while that at 2380 cm^{-1} is different, showing a gathered Q branch at the center. The rotational spacings in all three bands, which are quite regular except at the center, appear to be the same and equal to about 7.8 cm^{-1}. *HDSe:* For this molecule the frequencies are: $\nu_1=1610$ cm^{-1}, $\nu_2=910$ cm^{-1}, and $\nu_3=2385$ cm^{-1}. Here the rotational spacings are known only for ν_2 and ν_3 and these are equal to about 5.5 cm^{-1}. The frequency ν_1 shows a gathered Q branch while ν_2 and ν_3 do not. *D_2Se:* For this molecule only ν_2 and ν_3 have been identified. ν_2 occurs near 760 cm^{-1} while ν_3 is found to be at 1700 cm^{-1}. The spacings are known definitely only for ν_2 and are equal to about 4.0 cm^{-1} or approximately one-half of the spacings for the lines in the H_2Se bands.

41. The Zeeman Effect of Gold. H. N. MAXWELL, *Hood College,* AND J. B. GREEN, *Ohio State University.*—Several of the classifications of Au I by Symons and Daley[1] in the region of λλ5000–6000A have been verified by Zeeman effect measurements, and the g values determined. For the $5d^{10}6s$, $5d^{10}6p$, $5d^{10}7s$, $5d^{10}6d$, and $5d^{9}6s^{2}$ the g values are unperturbed; but those for the $5d^{9}6s6p$ and $5d^{9}6s6d$ are perturbed from the *LS*-coupling values. The spectrum of Au II has been investigated by McLennan and McLay,[2] by Rao[3] and by Mack and Fromer.[4] No classifications of Au II lines in the region λλ4760–5726 have been made. This region seems to be rich in lines, but the wavelengths found in the tables are in disagreement (sometimes as much as 1.5A) with our measurements. Several well-defined multiplets appear, which, if the above classifications are correct, indicate transitions between a previously unidentified configuration, $5d^{8}6s6p$, and $5d^{8}6s7s$ or $5d^{9}6d$.

[1] Proc. Phys. Soc. London **41**, 431 (1928).
[2] Proc. Roy. Soc. Canada **22**, 103 (1928).
[3] Proc. Roy. Soc. **A1** and **2**, 118 (1933).
[4] Phys. Rev. **48**, 357 (1935).

42. The Zeeman Effect of Selenium II. J. B. GREEN, *Ohio State University,* AND R. A. LORING, *University of Louisville.*—The Zeeman effect of selenium II has been studied in fields of about 37,500 gauss. The selenium was introduced in powdered form into a brass rod which served as an electromagnetic interrupter and the metal vaporized readily. To date, several of the strongest lines have been measured, principally those involved in transitions between $4s4p^{4}$ and $4s^{2}4p^{2}5s$ with $4s^{2}4p^{2}5p$. The g values are all perturbed from *LS*-coupling values, but the assignments of J values by Martin[1] are generally in agreement with the observed patterns; with the exception (so far) of 21° which has a J value of $\frac{3}{2}$ instead of 5/2 as assigned by Martin.

[1] Phys. Rev. **48**, 938 (1935).

43. Raman Spectra of Disubstituted Acetylenes. FORREST F. CLEVELAND AND M. J. MURRAY, *Lynchburg College, Lynchburg, Virginia.*—The Raman spectra of (a) $C_6H_5\cdot C\equiv C\cdot CH_2\cdot Cl$, (b) $C_6H_5\cdot C\equiv C\cdot CH_2\cdot CH_2\cdot Cl$, (c) $C_6H_5\cdot C\equiv C\cdot CH_2\cdot CH_2\cdot CH_2\cdot Cl$, (d) $C_6H_5\cdot C\equiv C\cdot CH_2\cdot OH$, (e) $C_6H_5\cdot C\equiv C\cdot CH_2\cdot CH_2\cdot OH$, (f) $C_6H_5\cdot C\equiv C\cdot CH_2\cdot Br$ have been measured by means of apparatus previously described.[1] Compounds b and e have also been measured by Faucounau[2] and compound d by Gredy.[3] No measurements on a, c, and f seem to have been reported. The characteristic

acetylenic frequency at 2200–2300 cm^{-1} is double in many disubstituted acetylenes.[4] Gredy has found that if one of the substituents is a phenyl group, the line of lesser intensity is of lower frequency. The present results verify this conclusion for compound *d*, but for compounds *a* and *f*, prepared from *d*, the weaker line has a *higher frequency*. The acetylenic frequency is double in *a*, *d*, and *f*, but is broad, intense, and apparently single in the remainder of the compounds. The sum of the widths (in hundredths of a mm) of the two lines in *a* is 32, the width of the single line in *b* is 27, and in *c* the width is 22. Since the line of comparable intensity at 1600 cm^{-1} has a width of only 16 and since the above widths decrease as additional CH_2 groups are inserted, it seems probable that the single broad line in *b*, and perhaps also in *c*, may be an unresolved doublet. Preliminary attempts to resolve it by use of a grating have proved unsuccessful. Experiments designed to determine qualitatively the depolarization factors of the acetylenic frequencies are now in progress.

[1] Cleveland and Murray, Am. Phys. Teacher **5**, 270 (1937).
[2] Louis Faucounau, Comptes rendus **199**, 605 (1934).
[3] Blanche Gredy, *Theses* (Paris, 1935).
[4] J. H. Hibben, Chem. Rev. **18**, 50–51 (1936).

44. Raman Spectra of Some Inorganic Compounds. J. Rud Nielsen, N. E. Ward and H. Dodson, *University of Oklahoma*.—The Raman spectra of aqueous solutions of sodium metaborate, borax and sodium aluminate and of crystalline sodium metaborate, borax, boric acid, halides of cadmium, zinc and mercury, and potassium cyanate have been investigated. With sodium metaborate solutions prolonged exposures yielded two faint and diffuse frequencies in addition to that already reported.[1] The latter frequency was found, practically unchanged, in crystalline metaborate. These facts show that the metaborate ion cannot be triatomic and linear, as previously assumed.[1] The crystal powders were observed with the technique developed by Ananthakrishnan.[2] New frequencies were found with most of the crystals already studied. Thus, with mercuric chloride two new low frequencies were observed, while with boric acid twice as many frequencies were found as observed by Ananthakrishnan.[3] Attempts are being made to correlate the Raman spectra with the crystal structures.

[1] J. Rud Nielsen and N. E. Ward, J. Chem. Phys. **5**, 201 (1937).
[2] R. Ananthakrishnan, Proc. Ind. Acad. Sci. **5**, 76 (1937).
[3] R. Ananthakrishnan, Proc. Ind. Acad. Sci. **5**, 200 (1937).

45. The Signs of the Nuclear Magnetic Moments of Li^6 and K^{41}. John E. Gorham, *Columbia University*.—Nonadiabatic transitions between magnetic quantum states of atoms in an atomic beam were used to show that the signs of the nuclear magnetic moments of Li^6 and K^{41} are positive.[1] A beam of atoms 230 cm in length was passed through a weak nonhomogeneous field 153 cm long, a selecting slit, a weak transition field whose direction changed rapidly with respect to the atoms, a strong field, and was detected on a hot tungsten wire.

[1] I. I. Rabi, Phys. Rev. **49**, 324 (1936).

46. Absolute Nuclear Moment of Indium 115. S. Millman, I. I. Rabi, *Columbia University*, and J. R. Zacharias, *Hunter College*.—The atomic beam method of zero moments has been applied to indium to measure the nuclear spin and the hfs $\Delta\nu$ of the normal $^2P_{1/2}$ state. The spin was found to be 9/2 and the $\Delta\nu = 0.381$ cm^{-1} in agreement with spectroscopic results. The resolving power attained was sufficiently high to allow a measurement of the fine structure of the zero moment peaks. From the separation of the two $m=-3$ peaks of $\Delta H/H = 0.0193$ we calculate the moment of indium to be 6.40 ± 0.20 percent nuclear magnetons. This value does not depend on any assumptions with regard to the nature of the interaction between the nuclear spin and the electron configuration. Zero moment peaks arising from the metastable $^2P_{3/2}$ state, lying 2212.6 wave numbers above the $^2P_{1/2}$, were found. The intensity of these peaks is in good agreement with what is expected from quantum statistics. Their exact location will permit an evaluation of the nuclear quadrupole moment.

47. On the Magnetic Moments of Neon and Argon. J. M. B. Kellogg and Norman F. Ramsey, *Columbia University*.—It is generally assumed that the nuclear spins of the isotopes having even atomic weights and even atomic numbers are zero. For elements of this type where the spin is not known from band spectra, the possibility remains that the spin is not zero but that the magnetic moment is very small. With an atomic beam apparatus capable of detecting a magnetic moment of the order of 0.05 nuclear magnetons which is half as large as the smallest nonzero nuclear moment hitherto reported, the elements neon and argon have been investigated for the presence of a magnetic moment. Deflection of the atoms was produced in an inhomogeneous magnetic field of length 48 cm and maximum gradient 110,000 gauss/cm. The diminution in intensity at the center of the undeflected beam was determined quantitatively with a Stern-Pirani detector. Helium, spin zero, showed no change in intensity. The weakening of the beam in the cases of neon and argon could be accounted for by the diamagnetic moments of these elements. Thus, if neon and argon have a magnetic moment, it is less than 0.05 nuclear magnetons.

48. *Tabulation and Study of the Energy Levels of the Asymmetrical Rotator.[1] Enos E. Witmer, *University of Pennsylvania*.—In a previous abstract[2] the author stated that there is a very close correspondence between the *doublet* energy levels of the asymmetrical rotator according to quantum mechanics and the energy levels according to the old quantum theory and gave the formulas which link the two theories. Therefore a usable formula for $\tau_c(s; n_2/J)$ is of value to the spectroscopists. The following formula for the epicycloidal motions, which is derived rigorously, is rapidly convergent over a very large part of the domain of τ_c. Let $y=(1-s)^{\frac{1}{2}}(1-n_2/J)$. Then

$$\tau_c\left(s; \frac{n_2}{J}\right) = 2y - \frac{1}{2}\left(\frac{2-s}{1-s}\right)y^2 - \frac{1}{2^5}\left(\frac{s}{1-s}\right)^2 \frac{y^3}{(1-y)^2}(4-3y) - \frac{1}{2^6}\left(\frac{s}{1-s}\right)^3 \frac{y^4}{(1-y)^3}(5-3y)$$

$$-\frac{1}{2^{13}}\left(\frac{s}{1-s}\right)^4\frac{y^5}{(1-y)^6}[528-1264y$$
$$+984y^2-243y^3] \text{ etc.}$$

* To be read by title.
[1] With the support of a grant from the Penrose Fund of the American Philosophical Society.
[2] E. E. Witmer, Phys. Rev. **51**, 1001 (1937).

49. The Experimental Verification of the Quantum Mechanical Dispersion Theory by Reflections and Diffuse Scattering of X-Rays from Zinc. W. A. BRUCE AND G. E. M. JAUNCEY, *Washington University, St. Louis, Mo.*—Experimental values of Δf are obtained by correcting ΔF for thermal vibrations, since

$$\Delta f=(F_{\lambda=.71}-F_{\lambda=1.54})e^{M(K,\psi)}, \qquad K\equiv(\sin\phi/2)/\lambda$$

where $$M(K,\psi)=(a\cos^2\psi+b\sin^2\psi)K^2$$

and is determined from diffuse scattering experiments. $F_{\lambda=0.71}$ is taken from Miller,[1] while $F_{\lambda=1.54}$ is taken from Wollan and Harvey,[2] and Brindley.[3] The reflection experiments and the diffuse scattering experiments were all done at approximately the same temperature. The values of a and b as obtained from our diffuse experiments[4] are 2.27 and 0.64A^2. An average of Δf obtained by using Miller and Brindley's F values and values of a and b determined by diffuse scattering gives $\Delta f_{\text{ave}}=2.35$. Hönl,[5] in a quantum-mechanical treatment of the dispersion theory, gives a value of Δf (for $\lambda=.71$A and $\lambda=1.54$A) of 2.36. M may be obtained by other means. Δfs obtained with these other Ms are also averaged and compared.

[1] R. D. Miller, Phys. Rev. **51**, 959 (1937).
[2] E. O. Wollan, G. G. Harvey, Phys. Rev. **51**, 1054 (1937).
[3] G. W. Brindley, Phil. Mag. **21**, 790 (1936).
[4] G. E. M. Jauncey and W. A. Bruce, Phys. Rev. **51**, 1067 (1937).
[5] H. Hönl, Zeits. f. Physik **84**, 1 (1933).

50. Position of the Center of the Compton Modified Band. G. E. M. JAUNCEY, *Washington University, St. Louis, Missouri.*—Several experimenters[1] have found the center of the Compton modified band to be shifted slightly from its position as given by Compton's simple theory. Jauncey's theory[2] of the profile of the modified band is based on the assumption that the scattered photons which give rise to the band may be treated as having bounced off free electrons having the same distribution of speeds as the actual electrons in the scattering substance. Later, Jauncey[3] showed that to a first approximation, if the component velocity distribution function of the atomic electrons is $f(u)$, the profile of the Compton band is given by $f(Ax)$, where $A=c/\sin\frac{1}{2}\phi$, $x=(\lambda_C-\lambda')/\lambda_C$, and λ' and λ_C are respectively the wave-lengths of the actually scattered and the "Compton" scattered x-rays. To a higher degree of approximation it is now shown that the profile is given by $(1-2bx)\cdot f(Ax(1+bx))$, where $b=(1+\text{cosec}^2\frac{1}{2}\phi)/2$. This profile is not symmetrical about $x=0$ even though $f(u)$ is symmetrical about $u=0$. A Maxwell distribution with a most probable speed of 25 volts gives a shift of 0.23 X.U. for Mo $K\alpha$ rays at $\phi=180°$.

[1] Ross and Kirkpatrick, Phys. Rev. **46**, 668 (1934). Kirkpatrick, Ross and Ritland, Phys. Rev. **50**, 928 (1936). DuMond and Kirkpatrick, Phys. Rev. **52**, 419 (1937).
[2] Jauncey, Phil. Mag. **49**, 427 (1925); Phys. Rev. **25**, 314 and 723 (1925).
[3] Jauncey, Phys. Rev. **46**, 668 (1934).

51. A Theory of the X-Ray Absorption Edges and Their Fine Structure in Ionic Compounds. ROLF LANDSHOFF, *University of Minnesota.*—It is assumed that the act of absorption lifts the electron into the unoccupied outer shell of a nearby cation, to the nearest for the edge and to those farther away for the short wave satellites. The older theory pictured the electron as jumping into one of the traveling states. Its main disadvantage is, that the removal of an electron from the emitting ion gives rise to an electric field in the neighborhood of this ion, and therefore to a polarization energy which should be considered in the energy balance, but which spoils the good numerical agreement. The present theory restores this agreement. The occurrence of discrete localized levels below the continuum of traveling states has already been stated by Slater[1] and v. Hippel[2] in the theory of the ultraviolet absorption of ionic crystals. From the experiments of Brewington[3] this seems to be even more distinct in the case of the x-ray absorption with a more pronounced line structure near the edge.

[1] Slater and Shockley, Phys. Rev. **50**, 705 (1936).
[2] v. Hippel, Zeits. f. Physik **101**, 680 (1936).
[3] Brewington, Phys. Rev. **46**, 861 (1934).

52. The Use of Intensifying Screens in X-Ray Diffraction Work. CARL GAMERTSFELDER AND NEWELL S. GINGRICH, *University of Missouri.*—The photographic method of investigating x-ray diffraction by liquids has given reliable relative intensity measurements, but it has the disadvantage that long exposure times are required. A Fluorazure intensifying screen has been used in an attempt to decrease this exposure time, and an investigation is being made to determine the reliability of intensity measurements using a film in conjunction with an intensifying screen. Diffraction patterns of liquid potassium with Mo $K\alpha$ radiation have been obtained with and without an intensifying screen and microphotometer curves have been obtained from them. The relation between blackening and intensity for the film alone does not hold when an intensifying screen is used. In order to obtain the relation between x-ray intensity and blackening of the film, the Mo $K\alpha$ and Cu $K\alpha$ lines, reflected from a calcite crystal, have been recorded on films with and without intensifying screens, and through various filters of known materials and thicknesses. These experiments show that the intensifying factor, using Cu $K\alpha$, varies from about 1.2 at a film blackening of 0.12 to about 2 at 0.46, and the intensifying factor using Mo $K\alpha$ varies from about 5 at a film blackening of 0.14 to about 12 at 0.52. There is no indication of an increase in line width with the screen, and there has been no difficulty with afterglow.

53. The Determination of the Characteristic Temperature of MgO from X-Ray Measurements. H. S. RIBNER AND E. O. WOLLAN, *Washington University.*—The characteristic temperature Θ of a simple crystal can be determined from measurements of the ratio of the intensities of a regularly reflected x-ray line at two different temperatures, at various values of $\sin\theta/\lambda$. We have made such measurements for MgO at room temperature and at the

temperature of liquid air by a photographic method and have analyzed the results by a procedure which does not require a knowledge of the absolute ratio of the intensities at the two temperatures. The value of Θ which we obtain in this way is equal to $721°\pm21°$K. This corresponds to a root mean square amplitude of thermal vibration of the atoms of 0.069A at room temperature. The characteristic temperature has also been obtained by comparing the experimental scattering factor for MgO at room temperature with the theoretical scattering factor for the atom at rest and the result is found to show satisfactory agreement with the above mentioned value. A value for Θ can also be calculated from specific heat data, and the relation between the value so obtained and that obtained by x-ray measurements will be discussed.

54. The Effect of Lattice Enlargement upon Our Ideas of Order *versus* Disorder in Crystals, Including Mix-Crystals. F. C. BLAKE, *Ohio State University.*—In 1918 Professor Max von Laue, in discussing mix-crystals, stated the two alternative views of such crystals for certain ternary compounds: (a) random distribution of two of the three atoms involved; (b) a great enlargement of the unit cell with an ordered arrangement of the two atoms that normally would substitute for each other in (a). No one seems adequately to have studied the possibilities of view (b), since, in general, "superlattice" lines tend to appear due to the difference in scattering power of the two substitutional atoms for first and higher order reflections. By enlarging the lattice to a definite but finite size it is possible to determine an "ordered" arrangement that is the exact equivalent of the random distribution (a). Details of this arrangement for one type of cubic crystals will be given. This means, of course, that all superlattice lines are absent.

55. Electric Impedance of Single Arbacia Eggs. KENNETH S. COLE AND HOWARD J. CURTIS, *College of Physicians and Surgeons, Columbia University.*—The end of a two or three mm thin-walled glass tube is heated until it closes down to a capillary about 50μ in diameter and 200μ long. The capillary end of the tube is partially immersed in sea water, and when an egg, 75μ in diameter, is dropped in the upper open end, it settles to the top of the capillary. The water level in the tube is then raised until the egg is pushed into the middle of the capillary. Measurements are made between electrodes placed in the tube and in the outside solution. The low frequency resistance of a 48μ tube rose from 24,000 ohms when filled with sea water to 840,000 ohms with an unfertilized egg in place. This increase might be due to a membrane resistance of 13 ohms cm² but this value is no more than a lower limit since a layer of sea water 0.2μ thick between the egg and the glass would produce the same result. Assuming the membrane to be nonconducting, the observed low frequency capacities and the higher frequency data give average membrane capacities of 0.8μf/cm² for the unfertilized, and 2.8μf/cm² for the fertilized eggs. These results are in agreement with those obtained from suspensions, and the technique may be used for several problems which are not otherwise possible.

56. A Three-Component Accelerometer. J. E. SHRADER, *Drexel Institute of Technology.*—A type of accelerometer has been devised which measures the three components of acceleration simultaneously and records them on the same photographic film. The distinctive features of this accelerometer are: (1) The method of securing great sensitivity by large magnification of the motions of the pendulums. (2) The employment of special damping devices by means of which the pendulums become practically dead beat. (3) The disposition of the pendulums and the optical system whereby the records of all three components are recorded on the same photographic films. Proper damping which is a very important feature of an accelerometer is secured by the use of hollow discs or diaphragms by means of which energy of vibration is dissipated by forcing air into and out of the hollow chamber through a small opening. It is found that optimum damping is secured by a certain size opening which is determined by trial. By the use of air as a damping fluid the instrument can be operated in any position and damping does not vary markedly with temperature.

57. A Mechanical Harmonic Synthesizer-Analyzer. S. LEROY BROWN, *University of Texas.*—A machine is described which has thirty harmonic elements (fifteen sine components and fifteen cosine components) that operate simultaneously. The driving mechanism is a train of twenty intermeshing spur gears that are high grade but selected from commercial stock. These gears drive fifteen shafts with rotational ratios ranging from one to fifteen. A Scotch cross head is operated from each end of each shaft with the pin of each cross head set in quadrature with the pin of the cross head at the other end of the respective shaft. The sum of the thirty sinusoidal movements is communicated to a tracer point (pencil) by means of pulleys and a continuous fusee chronometer chain, and the curve is traced on a drawing board that is driven uniformly past the pencil point. Analysis is accomplished by setting the amplitudes of the thirty elements to correspond to the values of thirty of thirty-two equispaced ordinates from a wave-length of the curve to be analyzed. Thirty components (fifteen sine and fifteen cosine components) of the curve being analyzed are then determined from the values of thirty of thirty-two equispaced ordinates of a wave-length from a single trace produced by the machine.

58. *Photoelectric Geiger-Müller Counters with Caesium Cathodes. GORDON L. LOCHER, *Bartol Research Foundation of the Franklin Institute.*—Several photoelectric counters with cathodes of thin caesium hydride on silver and on hydrogen-soaked platinum have been made. The caesium surface is prepared by bombardment of caesium azide with H^+ ions or with electrons; the metal thus liberated is distilled on to the cathode and lightly bombarded with H^+ ions. Glass envelopes of Pyrex and Nonex are used. The counter gas is hydrogen at 2 to 6 cm pressure, purified by: passage through subliming magnesium and two cold traps, storage in a flask heavily lined with evaporated barium, and conduction to the counter through two cold traps and another barium flask. The counters have a narrower

"voltage plateau" than ordinary counters used with the same coupling resistance. At room temperature, the spontaneous rate, due to thermionic emission, is usually high. These tubes have thresholds (by filters) of about 8000A, and have sensitivities greatly exceeding those of any other photoelectric counters that the writer has produced. One type has a cathode that can be cooled with CO_2 ice or liquid air without refrigerating the entire tube. Work done so far shows that it is entirely feasible to use photoelectric surfaces with low work-functions in counters. The quantum efficiencies of the surfaces have not been determined, and can certainly be improved. Some stellar photometric measurements made with one of these tubes, by Dr. O. Mohler, of the Cook Observatory, indicate that the over-all sensitivity of the tube (used as a counter) is of the order of that of a good photo-cell and pliotron arrangement. The oldest caesium counters retained were made in June and in Sept. 1937.

* Read by title.

59. A New Geiger Counter. T. G. How and K. Lark-Horovitz,[1] *Purdue University.*—Following the suggestion of Geiger of the possibility to use an inverted counter: tube inside, wire outside, different forms of counters have been investigated which allow the direct introduction of the sample into the counter. The final form adopted consists of three wires inside the cathode cylinder held at the usual potential difference in respect to the cylinder. Argon-air mixtures of pressure from 4 cm to 8 cm are being used. The sensitivity of the counter is comparable with that of an ordinary counter. The counters have been tested using potassium and rubidium salt crystals.[2]

[1] I am indebted to the American Academy of Arts and Sciences for funds supporting this work.
[2] The counters will be exhibited in operation at the Science exhibit of the A. A. A. S. during the meeting.

60. Effects of Fringing Flux in Large Magnets. J. D. Howe and I. Walerstein, *Purdue University.*—The magnet constructed for the Purdue cyclotron has tapered pole pieces shaped according to an equation suggested by Bethe to reduce the fringing flux in the space outside the pole gap. In this design the flux density at the pole face is the same as it is near the yoke, and the product of its value and the maximum radius of curvature of the accelerated particles is about 15 percent higher than it would be for cylindrical pole pieces. To minimize the loss due to fringing flux the energizing coils are placed some distance from the yoke. The ampere interaction of the current in the coils with the fringing flux is found to produce a force causing a repulsion of the coils away from the air gap. Complete mapping of the magnetic field in the neighborhood of the pole pieces shows that for an energizing current of 160 amperes in each coil the field in the air gap between the pole pieces is 16,050 gauss, and the horizontal component of the field in the neighborhood of the coils has an average value of 750 gauss. The resulting force tending to "float" the upper coil is 3.4 tons.

61. High Frequency Systems for the Cyclotron, J. R. Dunning and H. L. Anderson, *Columbia University.*—Improved methods have been developed for feeding high frequency energy to the accelerating electrodes of the cyclotron (or any electrodes having appreciable capacitance). By using, in place of the usual coil, a short-circuited section of a transmission line having approximately equal inductive reactance, the resonant circuit thus formed with the electrode capacitance may be made to have a much higher Q value than has been hitherto attained. Both parallel wire and concentric lines may be used, but in general any method employing parallel wire lines may be improved electrically and mechanically by using concentric lines. In the concentric line system adopted here the advantages are: (1) much higher accelerating voltages; (2) higher efficiency; (3) higher frequencies; (4) shielding; (5) elimination of insulators; (6) energy fed into the system at low potential; (7) ease of adjustment; (8) water lines introduced at ground potential. Power from the oscillator is fed capacitatively to a nonresonant low impedance coaxial line which in turn feeds the resonant loaded quarter-wave line electrode system. The oscillator is frequency stabilized by a high Q concentric line directly exciting the grids, and operates with an efficiency of about 50 percent at 20 mC. Virtually all of the power output is delivered to the electrodes. For the cyclotron this means a considerable increase in energy and intensity of the ion beam.

62. Some Observations of Magnetic Viscosity in Iron. C. W. Heaps, *Rice Institute.*—Measurements of magnetic viscosity in iron wires have been made, using a ballistic galvanometer and fine wires, so that effects due to eddy currents are negligible. When the current in the magnetizing solenoid is cut off the flux in the iron specimen may continue to change appreciably for as long as a minute after the field is removed. By adjusting resistances and condensers the time required to remove the magnetizing field may be varied. It is found that the mode of decay of the magnetizing field influences very decidedly the magnitude of the viscosity. Under certain conditions of nonoscillatory decay magnetic viscosity will not appear at all. A cathode-ray oscillograph has been used in estimating rates of removal of the magnetic field and in detecting oscillations. Under certain conditions magnetic viscosity can be observed even though a reverse current is produced in the solenoid by an oscillation at break.

63. A Few Related Experiments with Fast Neutrons. M. L. Pool, *Ohio State University.*—The angular distribution of the fast neutrons produced from the deuteron bombardment of lithium was measured by the radioactivity induced in a number of substances placed symmetrically about the neutron source. The cyclotron at the University of Michigan was used to produce 6.3 Mev deuterons. The intensity variation of the radioactive samples of silver indicated a very distinct forward throw of the neutrons. A similar conclusion can be drawn from the radioactivity induced in Al, Sn, In, Pt and Au. With decreasing bombarding voltage of the incident deuterons on lithium, the change of intensities of the fast neutron reactions was compared with the change of the slow neutron reactions. The intensity of the radioactivity in

Ag (24.5 min.), Cu (10.0 min.) and Sc (4.0 hr.) decreased much more rapidly than did the activity in Dy (2.5 hr.), Cu (12.8 hr.) or Al (14.8 hr.). A number of elements were bombarded with deuterons for the purpose of finding other sources of fast neutrons. Cu, Sc, Ag and Al were used as detectors. Under fast neutron bombardment several nuclei were found to eject a proton, two neutrons and an alpha-particle. The branching ratios for these nuclei have been calculated from the observed intensities of the induced radioactivities.

64. Preliminary Experiments with a Cosmic-Ray Telescope. W. H. PICKERING, *California Institute of Technology.*—An attempt to discover astronomical influences on the cosmic radiation is in progress. For this purpose a Geiger counter telescope having very large counters has been mounted on a polar axis. The instrument is arranged so that, in addition to the usual right ascension and declination axes, the plane of the counters can be rotated around an axis lying in that plane, parallel to the direction in which the telescope is pointing. The counters are spaced so that the solid angle over which at least half the counter area is effective is about $5°\times15°$. With the counters oriented so that their axes were parallel to the Milky Way, observations have been taken at two declinations, $+20°$ and $-25°$. A series of points spaced one hour apart in right ascension give the intensity of the radiation in two bands around the sky. The results to date indicate that if astronomical bodies in these regions affect the radiation, their effect must be very small, or else the earth's magnetic field so distorts the paths of the rays that it cannot be found at the earth's surface.

AUTHOR INDEX TO ABSTRACTS OF INDIANAPOLIS MEETING

Allen, James S., Robert O. Haxby and John H. Williams—No. 18
Alvarez, Luis W.—No. 21
Anderson, H. L.—see Dunning, J. R.
Astin, A. V.—see Curtiss, L. F.

Barnes, S. W.—see DuBridge, L. A.
Beams, J. W. and C. Skarstrom—No. 26
Bell, M. E., E. A. Coomes and W. B. Nottingham—No. 30
Blake, F. C.—No. 54
Bowen, I. S., R. A. Millikan and H. V. Neher—No. 32
Bramley, Arthur—No. 8
Brown, B. W.—see Curtiss, L. F.
Brown, S. Leroy—No. 57
Bruce, W. A. and G. E. M. Jauncey—No. 49
Bruch-Willstätter, M. and H. Sponer—No. 12
Buck, J. H.—see DuBridge, L. A.

Cameron, Donald M.—see Sears, William C.
Carlson, J. F.—No. 38
Cleveland, Forrest F. and M. J. Murray—No. 43
Colby, W. F.—see Spees, A. H.
Cole, Kenneth S. and Howard J. Curtis—No. 55
Coomes, E. A.—see Bell, M. E.
Copeland, Paul L.—No. 29
Curtis, Howard J.—see Cole, Kenneth S.
Curtiss, L. F., A. V. Astin, S. A. Korff, L. L. Stockmann and B. W. Brown—No. 39

Dart, F. E. and Eugene Guth—No. 25
Devaney, T. Edwin—see Pietenpol, W. B.
Dodson, H.—see Nielsen, J. Rud
DuBridge, L. A., S. W. Barnes, E. O. Wiig, J. H. Buck and C. V. Strain—No. 23
Dunning, J. R. and H. L. Anderson—No. 61
Dwyer, Robert J.—No. 10

Focke, Alfred B.—No. 13
Fryer, Oscar G.—No. 14

Gamertsfelder, Carl and Newell S. Gingrich—No. 52
Germer, L. H. and K. H. Storks—No. 3
Gingrich, Newell S.—see Gamertsfelder, Carl
Gold, Otto—see Guth, Eugene
Good, Wilfred M.—No. 5
Gorham, John E.—No. 45
Goudsmit, S.—see Spees, A. H.
Green, J. B.—see Maxwell, H. N.
—— **and R. A. Loring**—No. 42
Guth, Eugene—see Dart, F. E.
—— see Haas, Arthur E.
—— **and Otto Gold**—No. 1

Haas, Arthur E. and Eugene Guth—No. 9
Harkins, William D. and John G. Kirkwood—No. 2
Haxby, Robert O.—see Allen, James S.
Heaps, C. W.—No. 62
Hire, Chas.—No. 15
How, T. G. and K. Lark-Horovitz—No. 59
Howard, R. A.—No. 11
Howe, J. D. and I. Walerstein—No. 60

James, Hubert M.—see Johnson, Vivian A.
Jauncey, G. E. M.—see Bruce, W. A.
—— No. 50
Johnson, Thomas H.—No. 36
Johnson, Vivian A. and Hubert M. James—No. 28

Kellogg, J. M. B. and Norman F. Ramsey—No. 47
Kirkwood, John G.—see Harkins, William D.
Koch, W. R.—No. 16
Korff, S. A.—see Curtiss, L. F.

Landshoff, Rolf—No. 51
Lark-Horovitz, K.—see How, T. G.

Locher, Gordon L.—No. 58
Loring, R. A.—see Green, J. B.
Luyet, Basile J.—No. 7

Maxwell, H. N. and J. B. Green—No. 41
Millikan, R. A.—see Bowen, I. S.
Millman, S., I. I. Rabi and J. R. Zacharias—No. 46
Montgomery, C. G. and D. D. Montgomery—No. 35
Montgomery, D. D.—see Montgomery, C. G.
Murray, M. J.—see Cleveland, Forrest F.
Myers, R. D.—No. 19

Neher, H. V.—see Bowen, I. S.
—— see Pickering, W. H.
—— No. 33
Nielsen, Harald H.—see Sears, William C.
Nielsen, J. Rud, N. E. Ward and H. Dodson—No. 44
Nordheim, L. W.—No. 37
Nottingham, W. B.—see Bell, M. E.
—— No. 31

Pickering, W. H.—No. 64
—— **and H. V. Neher**—No. 34
Pietenpol, W. B. and T. Edwin Devaney—No. 17
Pool, M. L.—No. 22, 63
Powell, Wilson M.—No. 27

Rabi, I. I.—see Millman, S.
Ramsey, Norman F.—see Kellogg, J. M. B.
Ribner, H. S. and E. O. Wollan—No. 53

Sears, William C., Donald M. Cameron and Harald H. Nielsen—No. 40
Shrader, J. E.—No. 56
Skarstrom, C.—see Beams, J. W.
Spees, A. H., W. F. Colby and S. Goudsmit—No. 20
Sponer, H.—see Bruch-Willstätter, M.
Stewart, G. W.—No. 6
Stockmann, L. L.—see Curtiss, L. F.
Storks, K. H.—see Germer, L. H.
Strain, C. V.—see DuBridge, L. A.
Stranathan, J. D.—No. 4

Thornton, R. L.—No. 24

Walerstein, I.—see Howe, J. D.
Ward, N. E.—see Nielsen, J. Rud
Wiig, E, O.—see DuBridge, L. A.
Williams, John H.—see Allen, James S.
Witmer, Enos E.—No. 48
Wollan, E. O.—see Ribner, H. S.

Zacharias, J. R—see Millman S.